

Controlled Power Point Tracking for Grid Connected and Autonomous Operation of PMSG based Wind Energy Conversion System

Shubham Khandelwal

A Dissertation Submitted to
Indian Institute of Technology Hyderabad
In Partial Fulfillment of the Requirements for
The Degree of Master of Technology



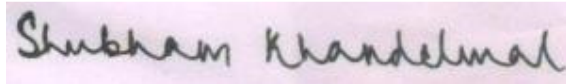
भारतीय प्रौद्योगिकी संस्थान हैदराबाद
Indian Institute of Technology Hyderabad

Department of Electrical Engineering

June, 2014

Declaration

I declare that this written submission represents my ideas in my own words and where others' ideas or words have been included, I have adequately cited and referenced the original sources. I also declare that I have adhered to all principles of academic honesty and integrity and have not misrepresented or fabricated or falsified any idea/data/fact/source in my submission. I understand that any violation of the above will be a cause for disciplinary action by the Institute and can also evoke penal action from the sources that have thus not been properly cited, or from whom proper permission has not been taken when needed.



(Signature)

_____Shubham Khandelwal_____

-----EE12M1034-----

(Roll No)

Approval Sheet

This thesis entitled – Controlled Power Point Tracking for Grid Connected and Autonomous Operation of PMSG based Wind Energy Conversion System – by – Shubham Khandelwal – is approved for the degree of Master of Technology from IIT Hyderabad.



-Dr. Pradeep Yemula, Electrical Department -
Internal Examiner



-Dr. Phanindra Jampana, Chemical department-
External Examiner



-Dr. Ketan P. Detroja-
Adviser



-Dr. Ravikumar Bhimasingu, Electrical Department-
Chairman

Abstract

With continuous depletion of conventional sources of energy, Wind Energy Conversion Systems (WECS) are turning out to be one of the major players with immense potential to meet the future energy demands. It is one of the most preferable source, as it can be installed onshore as well as offshore. But with the increasing penetration of wind energy into power system, wind energy conversion systems (WECSs) should be able to control the power flow for limited as well as maximum power point tracking. Apart from tracking desired power, there are some other issues which needs to be addressed for stable and reliable operation of WECS in grid connected as well as islanded mode.

In the grid connected mode synchronization of the system to the grid and maintenance of dc-link voltage in absence of ESS are the main control requirements apart from controlled power extraction from the wind turbine. Unlike the grid connected mode, where most of the system level dynamics are imposed by the grid and hence load voltage magnitude an frequency are dictated by the grid itself, in the autonomous operation of WECS the load voltage magnitude and frequency control comes in as additional control requirements other than controlled power extraction from Wind Turbine. However the usage of batteries in the system is unavoidable due to stability and reliability issues.

In contrast to the traditional pitch angle control, this work focusses on field oriented speed control of permanent magnet synchronous generator (PMSG) for controlling the active power flow based on the wind turbine characteristics. A back to back AC/DC/AC topology is implemented for interfacing the WECS to the distribution network with various power electronic interfaces providing the necessary control over the power flow. By maintaining the dc-link voltage constant and by deploying PLL, power balance and grid

synchronization are attained respectively in grid connected operation of WECS.

For the standalone operation of WECS, however the ideology for controlled power extraction from WECS remains same but the load voltage magnitude and frequency control are attained by carrying out the analysis and design exercise in synchronously rotating reference frame so that linear control techniques can be employed easily and sinusoidal command following problem gets transformed to an equivalent dc command tracking thus yielding desired performance with zero steady state error. The motive behind using batteries in the system is to facilitate transient stability and enhance reliability. Proper decoupling and feed forward techniques have been deployed to eliminate cross-coupling and mitigate the effect of load side disturbances.

Simulations are carried out under varying load demand as well as changing weather conditions to demonstrate the applicability and effectiveness of the proposed control strategies for grid connected as well as standalone WECSs.

Overall, the project work involves study, design, modelling and simulation of grid connected as well as standalone Wind Energy Conversion System.

Nomenclature:

Abbreviations:

MPP	: Wind Power System
VSWPS	: Variable Speed Wind Power System
CSWPS	: Constant Speed Wind Power System
WECS	: Wind energy conversion system
MPPT	: Maximum power point tracking
MPP	: Maximum power point
LPPT	: Limited power point tracking
LPP	: Limited power point
PLL	: Phase Locked Loop
AC	: Alternating current
DC	: Direct current
MPC	: Model Predictive Control
VSI	: Voltage source inverter
CSI	: Current source inverter
PV	: Photovoltaic
WEC	: Wind energy conversion
PCC	: Point of common coupling
PSF	: Power signal feedback
DG	: Distributed Generation
WT	: Wind Turbine
SCM	: Speed Control Mode
PCM	: Power Control Mode

HAWT	: Horizontal Axis Wind Turbine
VAWT	: Vertical Axis Wind Turbine
TSR	: Tip Speed Ratio
SRRF	: Synchronously Rotating Reference Frame
SRF	: Stationary Reference Frame
PWM	: Pulse Width Modulation
SSE	: Steady State Error
HCS	: Hill Climb Search
ESS	: Energy Storage System
TV	: Time Varying

Symbols:

v_w	: wind speed
A	: area swept by the blades
ρ	: air density
λ	: tip speed ratio
λ_{opt}	: optimum tip speed ratio
β	: pitch angle
R	: blade radius
A	: axial interference factor
ω_t	: turbine angular speed
T_t	: turbine torque
ω_t	: optimum turbine angular speed
C_{pref}	: power coefficient reference
C_{pmax}	: maximum power coefficient
P_{ref}	: power reference
P_{max} point	: maximum power that can be extracted from the turbine
P_{load}	: electrical power delivered to load from the turbine
P_{avail}	: power available from wind
v_{sabc}	: 3 phase load voltages
i_{Labc}	: 3 phase load currents
V_{ll}	: line to line grid voltage
C_{dc}	: Capacitance at dc link
J_T	: turbine moment of inertia

J_G	: generator moment of inertia
w_e	: electrical rotating speed of the generator
w_{gref}	: speed reference for generator
w_g	: actual speed of the generator
Φ_m	: permanent magnet flux
w_g	: actual speed of the generator
T_e	: electromagnetic torque of the generator
V_{dcref}	: dc-link voltage reference
V_{dc}	: actual dc-link voltage
m	: modulation index
L	: filter inductance
C_f	: filter capacitance
\vec{v}_t	: inverter terminal end voltage space phasor
\vec{v}_s	: load voltage space phasor
\vec{i}	: current space phasor
\hat{v}_{sn}	: nominal peak value of line to neutral voltage
v_{tabc}	: inverter terminal end phase voltages
i_{Ld}	: d axis load current component
i_{Lq}	: q axis load current component
P_s	: active power available at PCC
Q_s	: reactive power available at PCC
v_{sq}	: d axis load voltage component
v_{sq}	: q axis load voltage component
m_d	: d component of modulation index
m_q	: q component of modulation index
i_d	: d axis current component
i_q	: q axis current component

ω	: angular frequency of load voltage
P_v	: proportional gain for voltage control scheme
I_v	: integral gain for voltage control scheme
P_i	: proportional gain for current control scheme
I_i	: integral gain for current control scheme
K	: gain for frequency controller
u_d	: control input for d axis current control
u_q	: control input for q axis current control
$G_d(s)$: plant for d axis current control scheme
$G_q(s)$: plant for q axis current control scheme
$l(s)$: loop gain
τ	: time constant for current control scheme
f_s	: switching frequency of the inverter
ξ	: damping ratio
Δi	: current ripple

Table of Contents

1 Introduction	1
1.1 WECS: An Overview	3
1.2 Motivation	4
1.3 Scope of Work.....	5
1.4 Outline of chapters.....	6
2 Literature Review.....	8
2.1 Brief review on Wind Turbines	8
2.1.1 Brief review on classification and Design of Wind Turbines.....	9
2.1.2 Terminologies related to Wind Turbine systems	12
2.2 Brief review on configurations of WECSs	13
2.3 Reference Frame Theory and Sinusoidal Command Tracking	18
2.3.1 Reference Frame Theory.....	19
2.3.2 Sinusoidal Command Tracking in various Reference Frames	20
2.4 Brief review on basic and advanced control techniques for WECSs.....	22
2.4.1 Multivariable Control by using Classical Control Techniques	22
2.4.2 Modern Control Techniques.....	24
2.5 MPPT by Machine Side Control of WECSs	27
2.6 Grid Side Control for WECSs	33
2.6.1 DC-Link Voltage Control.....	37
2.6.2 Importance of PLL in grid connected operation of WECS	39
2.7 Load Side Control for WECSs.....	42
2.8 Filter Design	42
2.10 Conclusion.....	44
3 Principle of Operation, Modelling and Control of Wind Power Systems	45
3.1 Aerodynamics of Wind Turbines	45
3.2 Modelling of Wind Turbines.....	48

2.9.1 System Description	49
3.3 Control of Wind Power Systems	50
3.3.1 Pitch Angle Control.....	51
3.3.2 Controlling the Electrical Power Output from Wind Turbine	51
3.3.2.1 MPPT from VSWPS	52
3.3.2.2 LPPT from VSWPS	54
3.4 Conclusion.....	55
4 Controlled Power Point Tracking for grid-connected operation of WECS	56
4.1 Wind power configuration	56
4.1.1 System description.....	56
4.1.2 System modeling	58
4.1.3 Control structure	60
4.2 Simulation and Results	69
4.3 Conclusion.....	73
5 Controlled Power Point Tracking for Autonomous operation of WECS	74
5.1 Wind power configuration	74
5.1.1 System description.....	74
5.1.2 System modeling	75
5.1.3 Control structure	76
5.1.4 Filter Design	84
5.2 Simulation and Results	86
5.3 Conclusion.....	91
6 Stability Analysis for Grid Side Converter in grid connected WECS	92
6.1 Mathematical Analysis.....	92
6.2 Conclusion.....	95
7 Conclusion	96
References	99

List of Figures:

	Page no.
Figure 2.1: Major Components of Wind Turbine.	9
Figure 2.2: Design for HAWTs.	10
Figure 2.3: Design for VAWTs.	12
Figure 2.4: Air Foil cross-section.	13
Figure 2.5: Constant Speed Wind Turbines.	15
Figure 2.6: Asynchronous Machine based WECS.	17
Figure 2.7: DFIG based WECS.	17
Figure 2.8: PMSG based WECS.	18
Figure 2.9: Direct-Drive PMSG based WECS.	18
Figure 2.10: Arbitrary Rotating Reference Frame.	20
Figure 2.11: Simplified Block Diagram of half-bridge converter	21
Figure 2.12: Feedback Control Structure	23
Figure 2.13: Feed forward Control Structure	23
Figure 2.14: Control Architecture for LQR based controller	25
Figure 2.15: Block Diagram of MPC	25
Figure 2.16: TSR Control based MPPT Controller	29
Figure 2.17: PSF Control based MPPT Controller	30
Figure 2.18: Path view of HCS Control	30

Figure 2.19: P&O Flow Diagram	31
Figure 2.20: Two different modes of Machine Side Converter outer loop control	32
Figure 2.21: PMSG based WECS with intermediate boost converter stage	33
Figure 2.22: General structure for SRRF control strategy	35
Figure 2.23: General structure for stationary reference frame control strategy	35
Figure 2.24: General structure for natural reference frame control strategy	35
Figure 2.25: Conventional DC-Link Voltage Controller	38
Figure 2.26: Energy based DC-Link Voltage Controller	39
Figure 2.27: Inverter Terminal end interfaced to the grid	40
Figure 2.28: $\alpha\beta$ and dq coordinate system	40
Figure 3.1: Control Volume of a Wind Turbine	46
Figure 3.2: Power (P_t) vs Turbine angular speed (ω_t) for different wind speeds.	50
Figure 3.3: Variation of C_p with λ for different pitch angle (β) values.	51
Figure 3.4: Variation of MPP with turbine angular speed for different speeds.	53
Figure 3.5: Variation of Turbine Torque with turbine angular speed for different wind speeds.	54
Figure 3.6: Variation of C_p with λ for $\beta=0$.	55
Figure 4.1: WECS configuration	57
Figure 4.2: Wind Mill coupled to generator	60
Figure 4.3: Block Diagram representation of the overall control system	60
Figure 4.4: Schematic Representation of the overall control system architecture	61
Figure 4.5: Block Diagram Representation of Machine Side Control	62
Figure 4.6: Proposed LPPT Controller	63

Figure 4.7: Variation of Power with turbine angular speed for different wind speeds	64
Figure 4.8: Speed Control of PMSG	64
Figure 4.9: PWM signals from Hysteresis Control Scheme	65
Figure 4.10: Schematic of Hysteresis Control Scheme	65
Figure 4.11: Block Diagram Representation of Grid Side Control	66
Figure 4.12: Power Flow at DC-Link	67
Figure 4.13: DC-Link Voltage Control Scheme	68
Figure 4.14: Reference Angle sensing by using PLL	68
Figure 4.15: Response to step change in load demand	70
Figure 4.16: Operation under insufficient power condition	72
Figure 4.17: Operation under sudden climatic change condition	73
Figure 5.1: A schematic representation of system	75
Figure 5.2: Block Diagram representation of the overall control system	77
Figure 5.3: Schematic representation of the overall control system architecture	77
Figure 5.4: Block Diagram representation of Load Side Control	78
Figure 5.5: Voltage/Frequency Control Scheme	79
Figure 5.6: Current Control Scheme	81
Figure 5.7: d-axis closed loop current controller	83
Figure 5.8: q-axis closed loop current controller	83
Figure 5.9: Single phase LC filter	85
Figure 5.10: Response to step change in load demand	87
Figure 5.11: Operation under insufficient power condition	89
Figure 5.12: Operation under sudden climatic change condition	90
Figure 6.1: Three phase structure for connection between inverter terminal and grid.	92

List of Tables:

	Page no.
Table 2.1: Commonly used reference frames	19
Table 2.2: Different types of Filters and their characteristics	43
Table 3.1: Wind Turbine Model Coefficients	49
Table 3.2: Wind Turbine parameters	50
Table 4.1: WECS Parameters	57
Table 4.2: Wind Turbine and Generator Specifications	58
Table 4.3: LPPT controller parameters	66
Table 4.4: DC link voltage and hysteresis controller parameters	69
Table 5.1: Filter Parameters	75
Table 5.2: Controller Parameters for Voltage/Frequency Scheme	80
Table 5.3: Controller Parameters for Current Control Scheme	84
Table 5.4: Filter Design Considerations	85

Chapter 1

Introduction

Major portion of the electric power in the world is produced using conventional sources of energy like coal, petroleum, natural gas etc., which are non-renewable. But the continuous depletion of the conventional energy resources and the continuously increasing energy demand has drawn the focus towards the use of renewable sources of energy like wind, solar, tidal, bio-fuels, fuel cell etc. Alternative/ renewable sources are going to play a vital role in reducing the energy deficit for re-emerging nations. Installed capacity of various renewable sources of energy such as solar, wind, tidal etc. is increasing rapidly and steadily. Harnessing power from renewable sources of energy is one of the cleanest and most sustainable ways to generate electricity, as, they do not cause toxic pollution and global warming. In this regard Wind Energy is one such source, which has immense potential which can be deployed to meet the future energy demands. Wind farms have capability to produce large amounts of power (typically of the order of MW-GW's of power). Wind energy is the most preferred renewable energy source around coastal regions and it can be installed onshore or offshore [1].

Due to fluctuating voltage levels and/or frequency, the power generated from the wind cannot be directly used for commercial and household applications. Therefore, proper and efficient control techniques are required to make the energy available from the wind usable. As it comes to power conditioning, the power electronic interfaces like ac-dc converters (rectifiers), dc-dc converters (choppers) and dc-ac converters (inverters) effectively comes into picture and provides necessary control over the entities of interest(Voltage, Frequency, Current). As many power electronic interfaces we have in the system, the system becomes more and more flexible and can provide

control over multiple quantities. However, each converter has its own efficiency and therefore processing the power again and again incur large losses and is usually avoided. Therefore profound control strategies are required wherein we can attain control over multiple electrical quantities of our interest with minimum power conditioning stages (power interfaces). Various linear as well as non-linear control techniques like PI control, PR control, sliding mode control, hysteresis control, fuzzy logic control etc. have been implemented for these power electronic converters. Recent advancements in power electronic devices and their control techniques have made the energy production by wind more accessible and cheaper. Systems generating suitable AC or DC form from wind energy are called wind energy conversion systems (WECSs). These WECS are interfaced to local loads through a microgrid.

Based on the mode of operation the Wind energy conversion systems (WECSs) can be broadly classified into Grid connected and Standalone WECSs. While in the grid connected mode the WECS as a micro source meets the power demand by the load as well as it has an active link for sharing power with the grid, on the contrary the Standalone WECSs operate in islanded mode meeting the load demand in isolation from the grid. Each mode of operation has its own challenges and proper control techniques are required to address them. Grid-connected WECSs are more reliable than standalone systems as power can be extracted or dumped into the grid depending on load demand. However, there are many offshore islands in the world where grid integration is very difficult and the power exigency is met either by diesel generators or by energy storage devices like batteries. But transportation of fuel, installation and maintenance of batteries incur large costs. With the advent of WECS, wind energy has become a promising alternative. Hence standalone WECSs needs equivalent attention as the grid connected WECSs get, since in remote areas and islands they can provide a clean, efficient and feasible solution in meeting the power exigency. These systems are not reliable because their output depends on the environmental conditions i.e. the wind speed and therefore, Energy storage devices like batteries are necessary with the standalone systems to have reliable operation.

Most of the present WECSs use maximum power point tracking control strategies to extract maximum power available from wind. A large number of maximum power point control strategies have been proposed in the literature e.g. tip speed ratio control, power signal feedback control, pitch/stall control etc. [2,3]. All these control strategies try to extract maximum power all the time. However, for a standalone

distribution generation system, there may be situations when WECSs are not supposed to generate maximum power [4]. Even in the grid connected mode an active power control from WECSs can be utmost help for enhancing power system reliability. A recent report by National Renewable Energy Laboratory [5] states that active power control from WECSs can be extremely beneficial in many situations where minimum thermal generation levels and transmission constraints needs to be met. However, this capability has been ignored because wind power(along with other renewable resources) has a free fuel source , and therefore system operators have historically attempted to use as much wind generation as possible at all times. Generally, tracking maximum power from WECSs all the time requires high capacity energy storage systems to maintain power balance in the system. To minimize the need of high capacity batteries/dumping loads, limited power point (LPP) control techniques should be implemented. This battery requirement for grid connected WECSs can be eliminated by deploying proper control techniques, however in the islanded mode there should be some reserve capacity in the system in order to ensure stable and reliable operation of the microgrid. Limited power point control techniques generate power based on load demand (or a reference value), i.e. when wind energy is sufficient to satisfy the load requirements the system operates at a limited power point, and the system operates at maximum power points (MPP) under insufficient energy conditions. Thus in both the cases excessive power, which was required to be dumped into batteries or dummy loads earlier, is never generated and hence grid dependency is also reduced [6].

1.1 WECS: An Overview

A Wind Turbine converts kinetic energy in mechanical domain into electrical energy with the help of Wind Mill coupled to the generator. Based on the type of machine (synchronous or asynchronous) it is coupled to, there can be various configurations of WECSs possible. Usually a gear-box is used in the drive train for speed magnification. Although direct-drive WECSs [7,8] have also been in use. Wind power plants with ratings from few kilowatts to gigawatts have been installed across the world.

A typical grid connected or standalone WECS has two power conditioning stages. The first stage consists of a power electronic interface i.e. a controlled rectifier and

the second stage consists of another power conditioning unit i.e. an inverter and therefore the power undergoes transformation from uncontrolled AC to controlled DC and DC to controlled AC. The inverter can be VSI or CSI. There can be an intermediate stage also which can be a DC-DC boost converter to boost the inverter end's dc voltage, however this is usually avoided due to efficiency requirement. The task of tracking maximum power is done by the first power conversion stage while the task of maintain power balance in the system and controlling the load side electrical quantities like voltage, current and frequency is done in the second power conditioning stage and hence is handled by the inverter.

A large number of maximum power point control strategies have been proposed in the literature e.g. tip speed ratio control, power signal feedback control, pitch/stall control etc. While WECS is widely recognized, controlled power extraction has thus far not received significant attention and, thus only maximum power point tracking (MPPT) is used in WECS [8]. Although MPPT control has now been quite a matured concept in WECSs, Limited power point tracking technique has still not received enough attention and is mostly overlooked. Extracting maximum power all the time makes the system vulnerable to sudden climatic changes and can cause problems such as DC link voltage collapse or sudden reduction in power output [9]. Some limited power point tracking techniques based on sliding mode control [10] and fuzzy logic control [11] have been proposed. These techniques rely on energy storage systems such as batteries. However there has been some works done on limited power point tracking control for Photovoltaic [12] and Wind Energy Conversion Systems [1] operating in grid connected mode where battery requirement for the system has been eliminated but tracking limited power from standalone WECSs while minimizing the usage of batteries in the system has not received much attention.

Although in the grid connected mode of operation of WECSs wherein there is an active link between the grid and the DG unit, the requirement for battery in the system can be completely eliminated. However in the islanded mode of operation of WECSs, since there is no active link between the grid and the micro source, having support from an energy storage not only facilitates transient stability but is essential for reliability.

1.2 Motivation

Most of the efforts have been made to implement MPP control from WECSs. However as was discussed in the previous section that providing active power control in the system in the grid connected mode can be useful for grid reliability and can respect various transmission constraints. In the standalone mode due to absence of active link between the micro source and the grid, having control over power is not only useful but also essential. However for the grid connected mode the battery requirement for the system can be eliminated but for standalone systems it is unavoidable due to stability and reliability aspects of the system which is one of the utmost requirements which needs to be met for standalone systems. As WECS is a high inertia system with sluggish transient response, it is necessary to incorporate energy storage systems (ESS) (such as batteries), which possess fast energy dynamics at the dc link. Having reserve capacity facilitate stable and reliable operation of the system in standalone mode [12].

Some of the main reasons why batteries should be minimized or eliminated are: i) initial investment of batteries is very high and including batteries would result in higher capital cost of renewable energy system. ii) Maintenance cost of the batteries is also high as life of batteries is much less compared to other renewable energy system components. And iii) used batteries have a significant impact on environment and cost of safely discarding these batteries is considerable [6]. In spite of these disadvantages, due to lack of proper control strategies, batteries are invariably connected at DC link of SPVECS and WECS in order to keep DC link voltage constant. Thus there is a need to develop control strategies for grid-connected as well as standalone WECSs by which can extract any desired power from the system while eliminating or minimizing the use of batteries in the system.

During this thesis research, the main focus was on proposing control architecture for grid-connected and standalone WECS from which we can extract limited as well as maximum power from the system in face of climatic change conditions while eliminating the usage of batteries in grid connected operation and minimizing it for standalone systems. Elimination/minimization of batteries from such systems will reduce the cost of whole system and also minimize the issues related to batteries like constant maintenance, control of battery charging and discharging, over voltages etc.. Scope of the work is outlined in the next section.

1.3 Scope of work

Wind energy being an abundant and clean energy source has immense potential in meeting the future energy demand. However due to lack of efficient, flexible and cost effective solutions it's usage has been limited to only MPP Control with large ESS support. It is important to decrease the overall cost and at the same time improve reliability of these systems. Intelligent control schemes are needed to meet the stringent standards and for efficient utilization of various components [13]. With respect to these issues main objectives of this research are

- Analysis, design and control of grid-connected, three-phase, two-stage WECS with LPPT controller for controlled power point tracking.
- Analysis, design and control of standalone, three-phase, two-stage WECS with LPPT controller for controlled power point tracking.
- Highlighting the advantages of using the proposed LPPT control techniques over the MPPT control techniques by eliminating/minimizing the requirement of energy storage system.
- Stability Analysis for grid side system of grid connected WECS.
- Simulation for grid-connected and standalone, three phase, two stage WECS.

1.4 Outline of chapters

This chapter gives an introduction and general features of WECS. It also specifies the objectives of this project work in precise and orientation of the thesis.

Chapter 2: This chapter covers the literature survey on various configuration of WECSs, machine side, grid side and load side control for grid connected and standalone WECSs, Importance of PLL and filter design.

Chapter 3: This chapter deals with the aerodynamics, modelling and system overview of Wind turbine.

Chapter 4: This Chapter deals with the implementation of limited power point tracking controller for grid connected WECSs.

Chapter 5: This Chapter deals with the implementation of limited power point tracking controller for standalone WECSs.

Chapter 6: This chapter deals with the stability analysis for grid side control of grid connected WECSs.

Chapter 7: This Chapter deals with the final conclusions on the basis of this study. Suggestions for future work are also given at the end of the thesis.

Chapter 2

Literature Review

A brief introduction, highlighting main focus of the thesis was given in the previous chapter. This chapter consists of a brief literature survey, which covers the design of WT, various configurations of the wind energy conversion systems (WECSs), Machine Side and the Grid Side Control for WECSs, Maximum Power Point Tracking (MPPT) techniques, the importance of PLL and the filter design.

2.1 Brief review on Wind Turbines

A WT is a revolving machine which converts the kinetic energy from the wind into mechanical energy. The mechanical energy is then converted to electricity that is then send either to the loads or to the power grid. The turbine components responsible for these energy conversions are the rotor and the generator. The rotor is the area of the turbine that consists of the hub as well as the blades. As wind strikes the turbine's blades as well as the hub rotates due to aerodynamic forces. This rotation is then sent through the transmission system to the machine coupled to the turbine for mechanical to electrical conversion. The transmission system consists of the main bearing, high speed shaft, gearbox and the low speed shaft. Based on the gearbox ratio the generator speed gets amplified to the levels necessary for efficient electricity production. Also there are systems where the generator is directly coupled to the turbine rotor and hence the maintenance requirements are reduced. These are known as direct-drive systems. The main components of a WT are the gearbox, generator, rotor, hub, low speed shaft, high speed shaft and the main bearing. Figure 2.1 gives a pictorial representation of the assembly of WT system components. The structure which houses the components is called the nacelle [14].

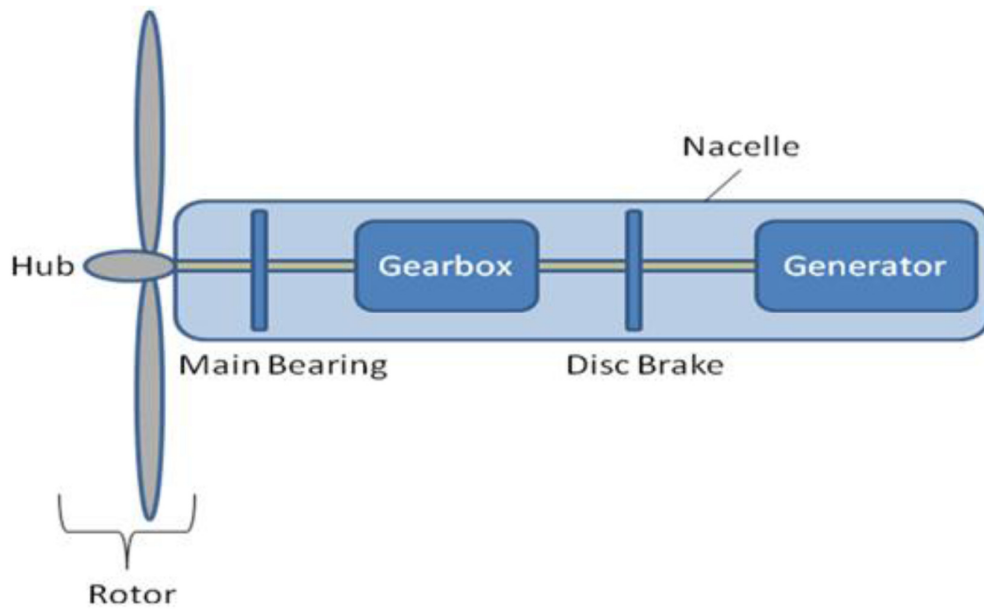


Figure 2.1: Major Components of Wind Turbine [14]

2.1.1 Brief review on Classification and Design of Wind Turbines

Wind Turbines (WT) are classified into two general types:

1. Horizontal Axis Wind Turbines (HAWTs)
2. Vertical Axis Wind Turbines (VAWTs)

A HAWT has its blades rotating on an axis parallel to the ground. On the contrary a VAWT has its blades rotating on an axis perpendicular to the ground [15].

1. Horizontal Axis Wind Turbines

This is the most common WT design. In addition to being parallel to the ground, the axis to the rotation is parallel to the wind flow. Some machines are designed to operate in an upwind mode, with the blades upwind of the tower. In this case a tail vane is used to keep the blades facing into the wind. Other design operate in a downwind mode so that the wind passes the tower before striking the blades. Without a tail vane the machine rotor naturally tracks the wind in a downwind mode. Some very large WT use a motor-driven mechanism that turns the machine in response to a wind direction sensor mounted on the tower. Based on the construction these can

be classified as single blade HAWT, two blade HAWT and three blade HAWT. While the single blade HAWTs are rarely used due to the tower shadow effects, needs counter weights on the other side of the blade, the two blade HAWTs on the other hand requires very complex design due to the requirement of sustaining wind shocks, it is less stable. The three blade HAWTs are the most commonly used HAWT structures as they have high strength to withstand heavy wind storms, less affect due to tower shadow and produces high output. A pictorial representation of single, two, three blade HAWTs is shown in figure 2.2.



(a) One Blade

(b) Two Blade

(c)

Three Blade

Figure 2.2: Designs for HAWTs [16]

Advantages:

It offers the flexibility to adjust the pitch of the blades to catch the wind at just the right angle to collect the maximum amount of wind energy.

The HAWTs inherently tall tower base enables unobstructed access to stronger winds, significantly increasing the blade speed collection and resulting in higher power output.

HAWT have blades that are designed perpendicular to the wind direction. The efficient design increases the wind power throughout the entire rotation. In contrast, VAWTs require airfoil surfaces to backtrack against the wind for part of the cycle in a less efficient manner [17].

Drawbacks:

The propellers on HAWT designs make more noise as the wind speed increase.

Cannot be installed in turbulent wind conditions because the flow of wind must be smooth to make the HAWT efficient.

Structurally less stable and cannot withstand extreme weather conditions.

2. Vertical Axis Wind Turbines

Although the VAWTs have existed for centuries but at present their use has almost been ceased. The main reason for this is that they do not take advantage of the higher wind speeds at higher elevations above the ground. The basic vertical axis designs comprises of Darrieus which has curved blades and efficiency of 35%, the Giromill which has straight blades and efficiency of 35% and the Savonius, which uses scoops to catch the wind and has an efficiency of about 30% [15]. These VAWT designs have been shown in figure 2.3.

Advantages:

The generator and the gearbox can be placed near to ground making maintenance easier and lower the construction cost.

It does not need to be pointed towards the wind to be effective. In other words it can be used on the sites with high variable wind direction.

They are quiet, efficient, economical and perfect for residential energy production, especially in urban environments.

Drawbacks:

As they are mounted closer to the ground hence less wind speed is available to harness which means less productivity of electricity.

They are very difficult to erect on towers which means they are installed on base such as ground or building.

Inefficiency of dragging each blade back through the wind.



(a) Darrieus

(b) Giromill

(c) Savonius

VAWTs [16]

Figure 2.3: Designs for

2.1.2 Terminologies related to WT systems [18]

- **Angle of attack**

The amount of surface area available for the incoming wind is key to increasing the aerodynamic forces on the rotor blades. The angle at which the blade is adjusted is referred to as the angle of attack. The angle is measured with respect to the relative wind direction and the chord line of the blade.

- Pitch Angle

The angle between the chord and the plane of rotation is called the pitch angle.

- Cut-in Speed

Cut-in Speed is the minimum wind speed at which the blades will turn and generate usable power.

- Rated Speed

The rated Speed is the wind speed at which the turbines will generate its designated rated power. At wind speeds between cut-in and rated, the power output from a turbine increases as the wind speed increases.

- Cut-out Speed

At very high wind speeds, most WT cease power generation and shut down. The wind speed at which shut down occurs is called the cut-out speed.

- Tip Speed Ratio (TSR)

It is the ratio of the rotating blade tip speed to the speed of the free stream wind.

Figure 2.4 gives a pictorial view indicating some of these quantities.

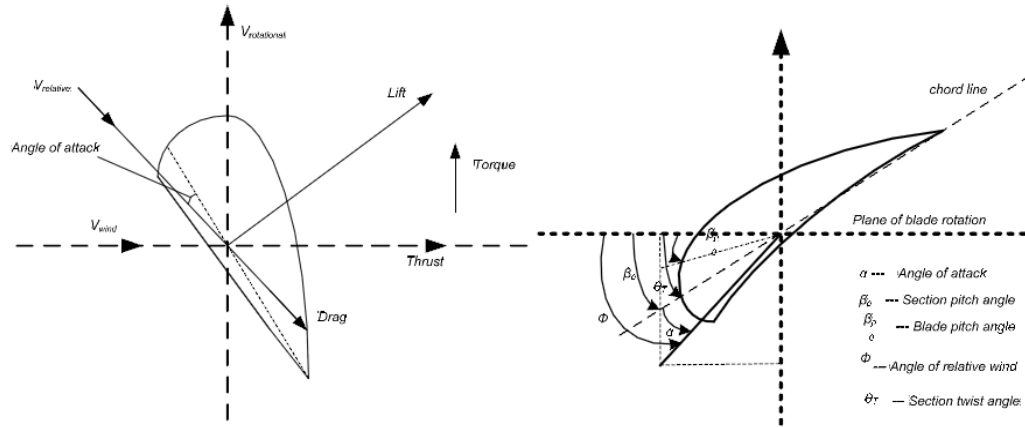


Figure 2.4: Air Foil cross-section [19]

2.2 Brief review on Configurations of WECSs

A wind energy conversion system (WECS) converts the kinetic energy of wind speed into electrical energy with the help of wind turbines (wind mills coupled with generators). Wind mill convert the kinetic energy of the wind into mechanical energy. Windmills are coupled to synchronous/asynchronous generators through a drive train. The generators convert the mechanical energy of wind mill to electrical energy (AC form). Electrical energy obtained from the generators is converted into suitable AC or DC form depending on the requirement at consumer side. A typical grid-connected or standalone WECS consists of two stages. First stage is the controlled/uncontrolled converter which operates the wind turbine at maximum power points (when using controlled converter) and converts the AC output of the generator into suitable DC form. Second stage is essentially a VSI or CSI which interfaces the wind system to grid or the load. A DC/DC boost converter intermediate stage can also be there. DC/DC boost converter is connected between first and second stage. It is used to boost up the voltage for VSI's DC end voltage [6].

Based on the blade pitching and speed control of machine WECSs can be broadly listed under the following [14]:

1. Fixed Speed Fixed Pitch (FSFP)

It is the configuration where it is impossible to improve performance with active control. In this design the turbine generator is directly coupled to the power grid causing the generator speed to lock to the power line frequency and fix the rotational speed. These turbines are regulated using passive stall methods at high wind speeds. The gearbox ratio selection becomes important for this passive control because this ensures that the rated power is not exceeded.

2. Fixed Speed Variable Pitch (FSVP)

This configuration operates at a fixed pitch angle below the rated wind speed and continuously adjusts the angle above the rated wind speed. The fixed speed operation implies a maximum output power at one wind speed only. Both feather and stall pitch control methods can be deployed in this configurations to limit power. But the problems associated with feathering which takes a significant amount of control design while stalling which increases unwanted amount of thrust forces makes this configuration less implementable in real world.

3. Variable Speed Fixed Pitch (VSFP)

This configuration continuously adjusts the rotor speed relative to wind speed through power electronics controlling the speed of the generator. In this type of control the generator and the drive train are free to rotate independent of the grid frequency.

4. Variable Speed Variable Pitch (VSVP)

This configuration is a derivation of VSFP and FPVS. Operating below the wind speed VSFP are used to maximize the energy capture and increase the power quality. Operating above the rated wind speed, FSVP permit efficient power regulation at the rated power.

Based on the speed control and fixed pitch operation discussed above, the wind power systems can be broadly classified into constant-speed and variable-speed systems [6,20,21,22]:

1. Constant Speed Wind Power System

A wind power system is composed of a wind turbine that is mechanically coupled via gearbox to an asynchronous generator. A squirrel cage induction generator is directly coupled to the grid and hence the machine synchronous frequency is dictated by the grid itself. The rotor speed of an asynchronous machine is typically within 3-8% of the synchronous speed and is thus fairly constant. Since the machine operates in generating mode, therefore, the rotor speed is slightly higher than the synchronous speed. Now since the asynchronous machine requires reactive power, therefore a shunt compensating capacitor bank is installed at the machine grid interface so as to maintain the voltage profile and thereby ensuring stable operation. The schematic of constant-speed operation of wind power system is depicted in Figure 2.5. They operate with very little variation in turbine rotor speed, and employ squirrel-cage induction machines directly coupled to the grid. Advantages and disadvantages of fixed speed wind turbines:

Advantages:

- Relatively Robust
- Reliable

Disadvantages:

- Energy capture from the wind is sub optimal
- Reactive power compensation is required

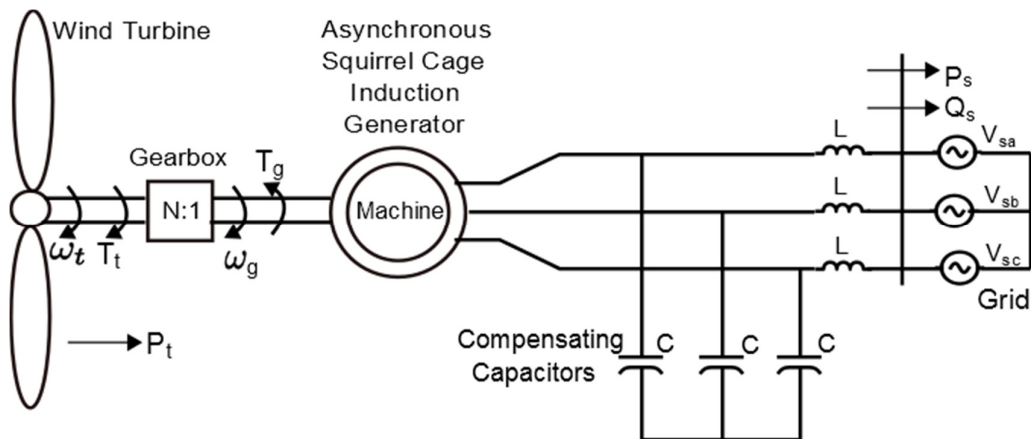


Figure 2.5: Constant Speed Wind Turbines

2. Variable Speed Wind Power Systems

Based on the machine and configuration of the system, variable speed wind power systems can attain following topologies:

- Based on asynchronous machine and power electronic converter.

The power flow, machine frequency and the rotor speed are controlled by the power electronic interface. The schematic of asynchronous machine based WECS is shown in Figure 2.6.

- Based on Doubly-fed asynchronous machine and reduced rating power electronic converter.

The power electronic converter not only adjusts the excitation frequency of the rotor circuit but also permits a bi-directional power exchange between the machine rotor circuit and the grid. The schematic of Doubly-fed induction generator based WECS is shown in Figure 2.7.

Some advantages and disadvantages of asynchronous machine based VSWPS are:

Advantages:

- Reduced converter cost
- Improved efficiency due to reduced losses in the power electronic converter
- Control may be applied to the lower cost due to reduced converter power rating

Disadvantages:

- Increased control complexity due to increased number of switches in converters
- Increased capital cost and need for periodic slip ring maintenance

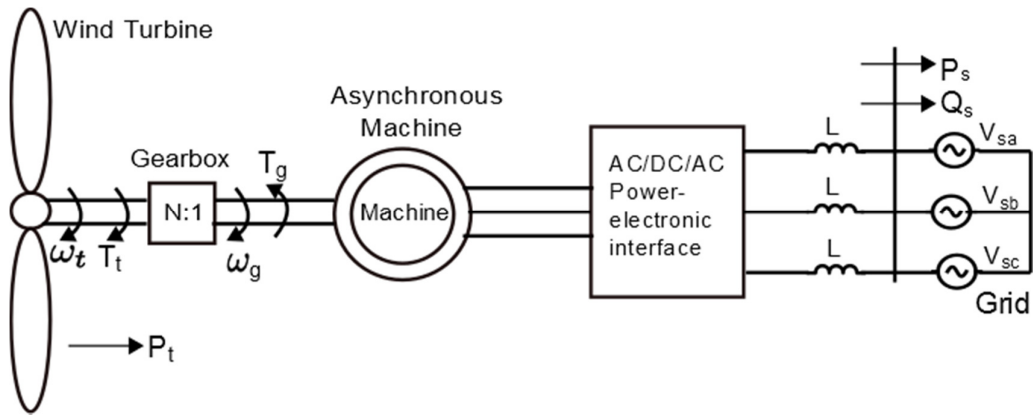


Figure 2 .6: Asynchronous Machine based WECS

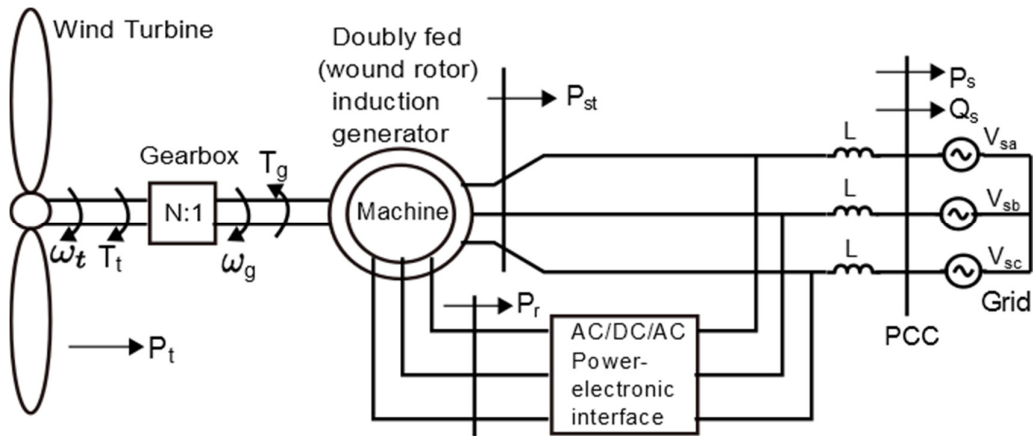


Figure 2 .7: DFIG based WECS

- Based on PMSG and power electronic converter.

The synchronous generator can have a wound rotor or can be excited using permanent magnets. The power electronic converter system adjusts the frequency of stator circuit excitation to permit a variable rotor speed.

- Based on gearless driven synchronous machine and power electronic converter.

By using a low speed and high pole synchronous generator we can eliminate the requirement for gearbox in a direct driven synchronous machine based WECS.

Schematic of PMSG based WECSs is shown in Figure 2.8 and 2.9.

Some advantages and disadvantages of PMSG based VSWPS are:

Advantages:

- Flexibility in design allows for smaller and lighter designs
- Lower maintenance cost and lower losses
- Low noise and installation cost in case of direct-drive PMSG based WECSs.

Disadvantages:

- High Initial cost due to high price of magnets used.

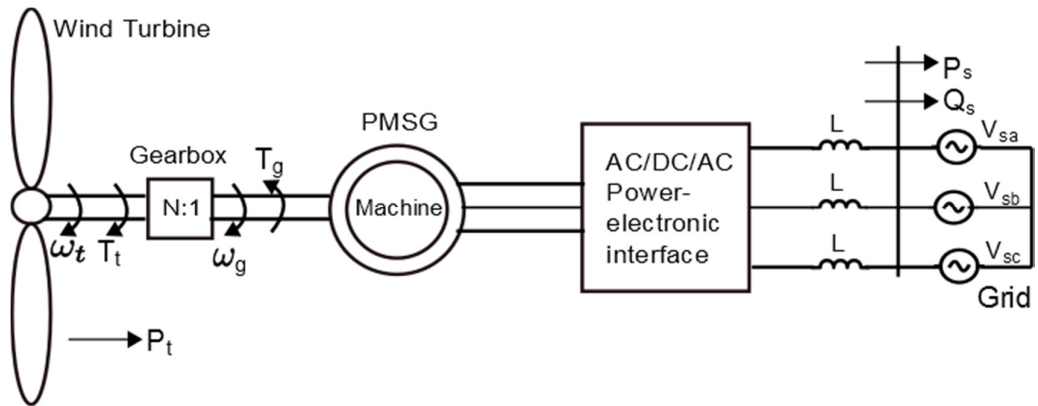


Figure 2.8: PMSG based WECS

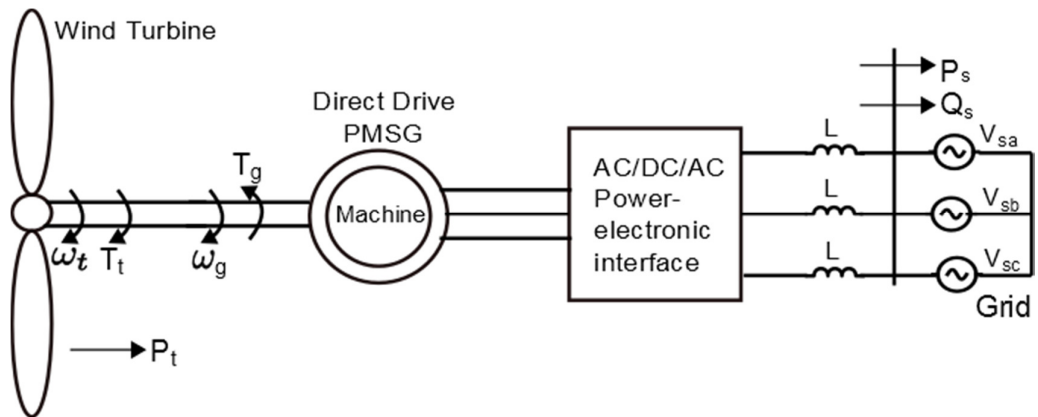


Figure 2.9: Direct-Drive PMSG based WECS

2.3 Reference Frame Theory and Sinusoidal Command Tracking

This section explains the usage of reference frame theory in simplifying the design and control problem and the problems faced by using PI control in abc domain for Sinusoidal command following which is one of the most important requirements in VSC control.

2.3.1 Reference Frame Theory

With the advent of reference frame theory the analysis and design procedure for electric machines was simplified to a great extent. It was appreciated how a simple change of variables can reduce the complexity of the differential equations [23]. A single transformation can transform the real variables from any given frame to any desired frame. This general transformation refers machine variables to a frame of reference that rotates at an arbitrary angular speed. All known real transformations can be obtained from this transformation by simply assigning the speed of rotation of the reference frame.

Table 2.1: Commonly used reference frames

Reference Frame	Reference Frame Speed	Notation used for variables
Natural Reference Frame (NRF)/ abc frame	Synchronous Speed (ω)	f_a, f_b, f_c
Stationary Reference Frame (SRF)/ $\alpha\beta$ frame	Zero	f_α, f_β, f_o
Synchronously Rotating Reference Frame (SRRF)/ dq frame	Synchronous Speed (ω)	f_d, f_q, f_o
Arbitrary Reference Frame (ARF)	Arbitrary Speed (ω_a)	f_{da}, f_{qa}, f_{oa}

Transformation between Reference Frames

Often it is desired to relate variables in one reference frame to the variables in other reference frame or transform variables from one reference frame to other reference frame so as to simplify the analysis and design procedure for the system. By using the matrix given by equation it is possible to express variables specified in any arbitrary frame x to other arbitrary frame y . The individual reference frames have been shown in figure.

$${}^x K^y = \begin{pmatrix} \cos(\theta_y - \theta_x) & -\sin(\theta_y - \theta_x) & 0 \\ \sin(\theta_y - \theta_x) & \cos(\theta_y - \theta_x) & 0 \\ 0 & 0 & 1 \end{pmatrix} \quad (2.1)$$

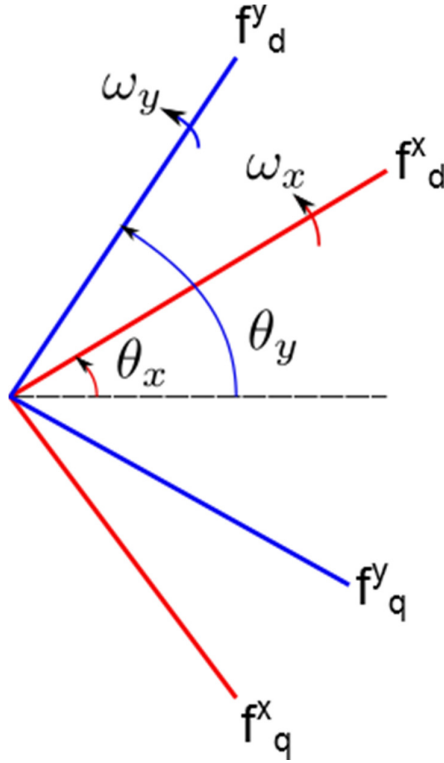


Figure 2.10: Arbitrary Rotating Reference Frames

2.3.2 Sinusoidal command tracking

The half-bridge converter which is employed as a basic building block of three phase VSC systems have a typical requirement of following sinusoidal commands. Hence simultaneous control of three half-bridge converters is the main control requirement from the three phase VSC control unit. The easiest option which one can think of deploying in the VSC control is that of a PI controller. But the basic control theory says that a PI controller can only yield a zero SSE for dc commands. Hence there can be two possible solutions for the problem at hand when the control design exercise is carried out in natural (abc) or stationary reference frame ($\alpha\beta$) [21,24]. These are:

1. The loop gain very large at ac system frequency by inclusion of complex conjugate (unstable) poles of Laplace Transform of command signal. This class of controllers which is based on providing infinite gain at the resonance (target) frequency so as to have zero SSE is known as stationary frame generalized integrator or proportional resonant (PR) controller.
2. Alternatively, the compensator design should be carried out in such a way that the bandwidth of the closed loop system is adequately larger than the frequency of the command signal but even after that the tracking will not be perfect and will yield a steady state error (SSE) which is ineluctable.

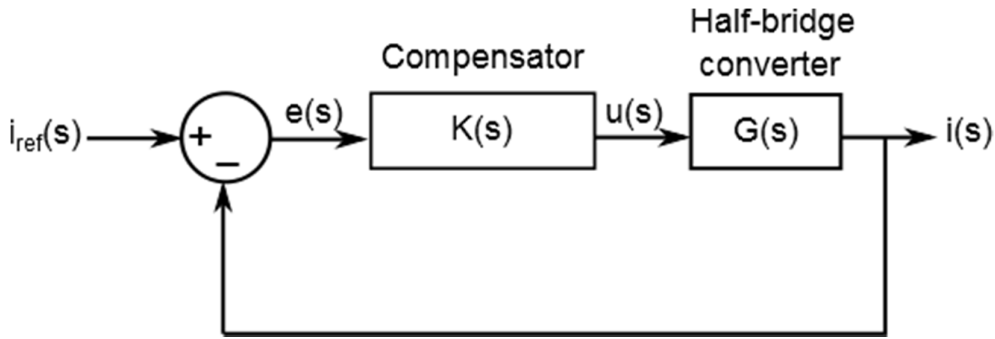


Figure 2.11: Simplified Block Diagram of half-bridge converter

The following illustration clarifies the above discussion. Figure 2.11 shows a simple closed loop control block diagram for the half-bridge converter.

The overall transfer function of the closed loop system can be written as:

$$\frac{i}{i_{ref}}(s) = \frac{l(s)}{1+l(s)}$$

where, the loop gain, $l(s) = K(s)G(s)$

The frequency response of the closed loop system can be written as:

$$G_c(s)|_{s=j\omega} = \frac{l(j\omega)}{1+l(j\omega)} \quad (2.2)$$

The same can be expressed in polar coordinates as

$$G_c(j\omega) = |G_c(j\omega)| e^{i\theta} \quad (2.3)$$

Where, $|G_c(j\omega)|$ and θ are the magnitude and the phase angle of $G_c(j\omega)$ respectively. Equation (2.3) which expresses the frequency response of the closed loop system suggests that the steady state response of a closed loop system to a sinusoidal command is scaled by $|G_c(j\omega)|$ and phase shifted by θ . In order to have perfect tracking, $|G_c(j\omega)|$ should be made equal to unity and θ should be forced to zero all the time. As seen from (2.2) that this condition can only be satisfied if the loop gain $l(s)$ is made infinity at the frequency of the command signal. The way to achieve this is to include the unstable poles of the Laplace Transform of the command in the compensator itself. This not only ensures sinusoidal command tracking with zero SSE but also eliminates all disturbances of the same type in the steady state. This is known as internal model principle.

2.4 Brief review on basic and advanced control techniques for WECSs

The basic and advanced control techniques forms the basic building block of the control strategies which are deployed for the control of grid connected and standalone WECSs. Some of them are:

2.4.1 Multivariable Control by using Classical Control Techniques:

In this approach the multivariable interactions are reduced either by doing Relative Gain Array analysis and selecting the best pairing or having cross coupling controllers in order to minimize the interaction terms or by designing a decoupler for the system. But in all these approaches the basic idea is to minimize the loop interactions.

Feedback and Feed forward Control Structures

For a feedback configuration the controller responds very fast to the SP changes. Although the feedback control takes care of parameter variation and disturbance rejection, but if there is a load disturbance or any other external disturbance acting on the plant, then the controller will only get intelligent about it once we feed the affected output response back to it so that indirectly it gets knowledgeable about the disturbances acting on the system. But takes a bit of time to complete the feedback cycle and making the controller intelligent about the disturbance so that accordingly

it can take the corrective action. The delay introduced because of the feedback action makes the system response sluggish to disturbance rejection. Figure 2.12 and 2.13 shows the structures for feedback and feed forward controls respectively.

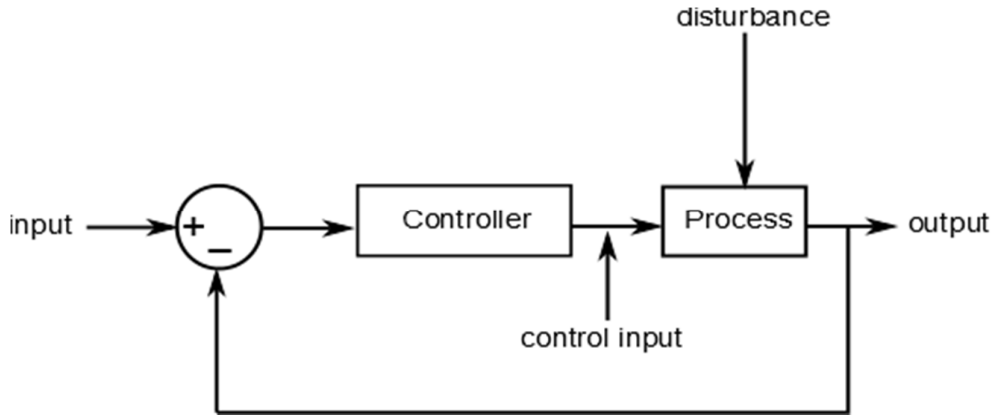


Figure 2.12: Feedback Control Structure

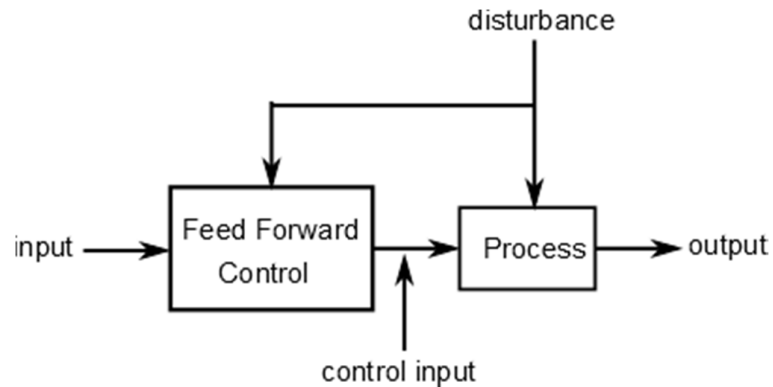


Figure 2.13: Feed forward Control Structure

So we move on to another control structure i.e. feed forward control. With known disturbance dynamics feed forward control solves the aforementioned problem by directly conveying the information about the disturbances acting on the plant to the controller and thereby speeding up the corrective action taking process. Hence feed forward control measures the load disturbance and takes predictive action even before it affects output and thereby it provides an effective means of cancelling the effects of disturbance on the system output. But since it's an open loop control, therefore,

the efficacy of control depends to a large extent on the accuracy to which the process model is available [25,26].

But we need a control structure that not only speed up the response but also improves the performance of the overall system. Therefore, we integrate the feedback which essentially puts the system in closed loop along with feed forward control which makes the controller directly intelligent about the disturbance, so that we can enjoy the fruitful advantages of feedback as well as feed forward control thereby improving the dynamic response of the system.

Feed forward control can be used to [27]:

1. Decouple the dynamics of two mutually coupled quantities.
2. Mitigate the effect of disturbance on the output variable.

2.4.2 Modern Control Techniques:

Unlike the Classical multivariable control techniques where we attempt to reduce the need to consider interaction terms in the design exercise or to transform the problem into an equivalent problem where interaction effects are zero or small enough to be neglected, modern control techniques considers the interacting multivariable system as a single unit and yields multivariable controller design directly without the need to eliminate interaction [28]. Some techniques based on state space approach (LQR and MPC) have been discussed in the following text:

1. Linear Quadratic Regulator

WECS interfaced to grid with linear quadratic regulator (LQR) based techniques has been implemented in [29]. Due to multivariable nature of the WECS, LQR based control technique has been implemented. State space model of the whole system is obtained in synchronous reference frame (dq). Using dq frame state space model and a user defined cost function, the LQR algorithm returns a constant control matrix K that minimizes the cost function by using $u = -Kx$ control law where u is the control input and x is the states (i_d, i_q) . LQR controller decides the switching signal for VSI. Control architecture of this system is shown in Figure 2.14

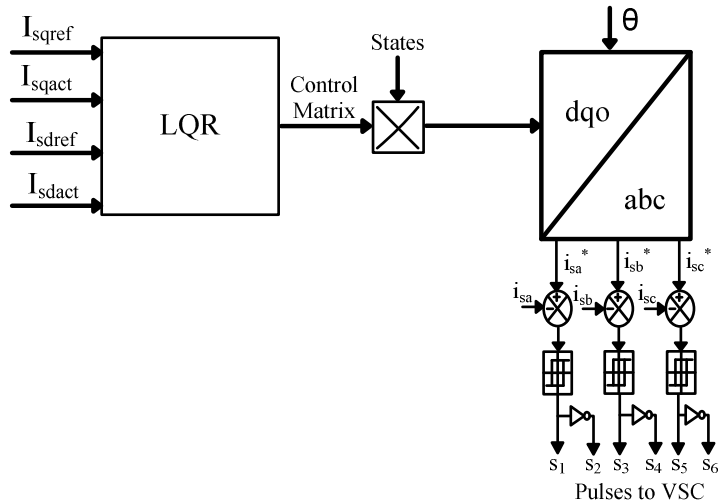


Figure 2.14: Control architecture for LQR based controller [6]

2. Model Predictive Control

It's a model based control technique widely used in multivariable control and is based on on-line use of dynamic model. It's a class of control strategies based on explicit use of process model to generate the predicted values of output at future time instants, which are then used to compute a sequence of control moves that optimize the future behavior of the plant [30]. Figure shows a block diagrammatic representation of MPC.

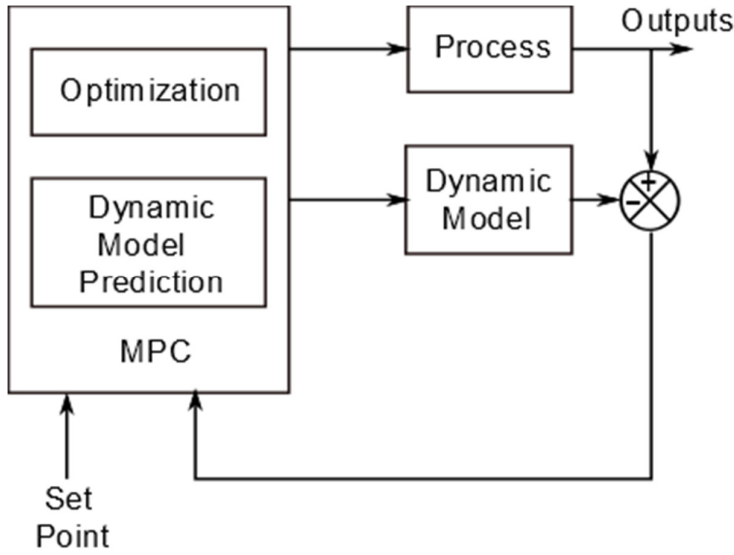


Figure 2.15: Block Diagram of MPC

Given a model for the plant dynamics, possible consequences of the current input moves on the future plant behavior can be forecasted on-line and can be used while deciding the control move. MPC refers to a class of computer control algorithms that utilize an explicit process model to predict the future response of the plant. At each control interval an MPC algorithm attempts to optimize future plant behavior by computing a sequence of future manipulated variables adjustment. The first input in the optimal sequence is then sent to the plant and the entire calculation is repeated at subsequent control intervals [31]. A block diagrammatic representation of MPC scheme is shown in figure 2.15. Equation (2.4) shows the general form of objective function which is aimed at minimizing the error between the predicted output and the set-point while minimizing the control effort.

$$J = \sum_{j=N1}^{N2} [[\hat{y}(k+j|k) - r(k+j)]^T Q(k+j) [\hat{y}(k+j|k) - r(k+j)] + \sum_{j=N1}^{N3} [u(k+j)^T R(k+j) u(k+j)] \quad (2.4)$$

where, J is a quadratic function with $u(k+j)$ the future inputs, the first quadratic term includes the error between the future values of reference output $r(k+j)$ and predicted outputs $\hat{y}(k+j|k)$, $R(k+j)$ and $Q(k+j)$ are weighing matrices used to adjust the error and the inputs respectively. $N2-N1$ is the prediction horizon and $N3$ is the control horizon [32].

MPC is commonly used at the supervisory level in the control hierarchy as it is easy to take optimality considerations into account and at the same time meet various constraints. The primary control objective is usually to manipulate the operating points of various DG units talking to each other in a MG framework to generate enough energy to satisfy the load demand. The other control objectives will be minimization of cost and inclusion of various constraints, for example :

Bounds on manipulated variables ($u^L < u(k+j|k) < u^H$)

This is to put an upper and lower bound on the individual capacities of DG units like wind and photovoltaic systems.

$$P_{w,ref} < P_{w,max}$$

$$P_{pv,ref} < P_{pv,max}$$

Where $P_{pv,ref}$ and $P_{w,ref}$ are the reference power set points for photovoltaic and wind energy system respectively while $P_{pv,max}$ and $P_{w,max}$ are the rated capacities of photovoltaic and wind energy system respectively.

Bounds on rate change of manipulated variables ($\Delta u^L < u(k+j|k) < \Delta u^H$)

This is to reduce peak value of surge currents. Including hard constraints in MPC optimization problem to restrict the maximum increasing rates of generated power of the subsystems.

$$P_{w,ref}(k+1) - P_{w,ref}(k) < dP_{w,max}$$

$$P_{pv,ref}(k+1) - P_{pv,ref}(k) < dP_{pv,max}$$

MPC as a master controller at the supervisory level is implemented in [33-36] wherein the optimality considerations have been taken into account while respecting various constraints which are to be met in a MG operation.

2.5 MPPT by Machine Side Control for WECSs

The entire power conditioning scheme for MPPT from WECSs is usually composed of 2 stages (uncontrolled AC-DC and DC-controlled AC). The first stage is referred to as Machine Side Control and the second stage is referred to as Grid Side Control for Grid connected operation of WECSs and Load Side Control for autonomous operation of WECSs. PMSGs are now being used instead of Induction Generators because of improved efficiency, low cost, reliability, modularity, absence of excitation current and high power factor [1,8,37-40].

Control objectives and structure of Machine Side Controller

The main objective of Machine Side Controller is to extract maximum power from the turbine. Broadly speaking, the power extracted from the turbine can only be varied by either controlling the pitch angle or by varying the TSR. MPPT control algorithms are used to extract the maximum electrical power from WECSs. These maximum power points are the system operating points at which we get the maximum power output from the system. Implementation of MPPT result in 40% more efficient systems than the systems operating without the maximum point algorithms.

So, any MPPT Controller either focusses on operating the turbine on MPP obtained by MPP algorithm by varying the speed of the machine or by tracking maximum power by varying the pitch angle. The maximum power extraction from a WT depends upon the accuracy with which the maximum power points are tracked in face of wind speed variations. Some of the most popularly used MPPT algorithms have been discussed in the present section. These are:

1. Tip Speed Ratio Control

The TSR Control method regulates the rotational speed of the generator in order to maintain TSR to an optimum value at which the power extracted is maximum [21,37,41]. This method requires both the wind speed and the turbine speed to be measured or estimated in addition to requiring the knowledge of optimum TSR of the turbine in order for the system to be able to track maximum power all the time. Based on the knowledge of wind speed and TSR, optimum value of speed reference is generated as given by equation (2.5)

$$w_{gref} = \frac{\lambda_{opt} v_w}{R} \quad (2.5)$$

Where λ_{opt} is the optimum TSR, R is the radius of the blade and v_w is the wind speed. Although the wind speed measurement and estimation itself is a challenging task. Wind speed estimation based TSR Control is proposed in [42]. A PI controller simply controls the speed of the generator to the optimal value as calculated from equation(2.5). A schematic of TSR Control is shown in figure 2.16.

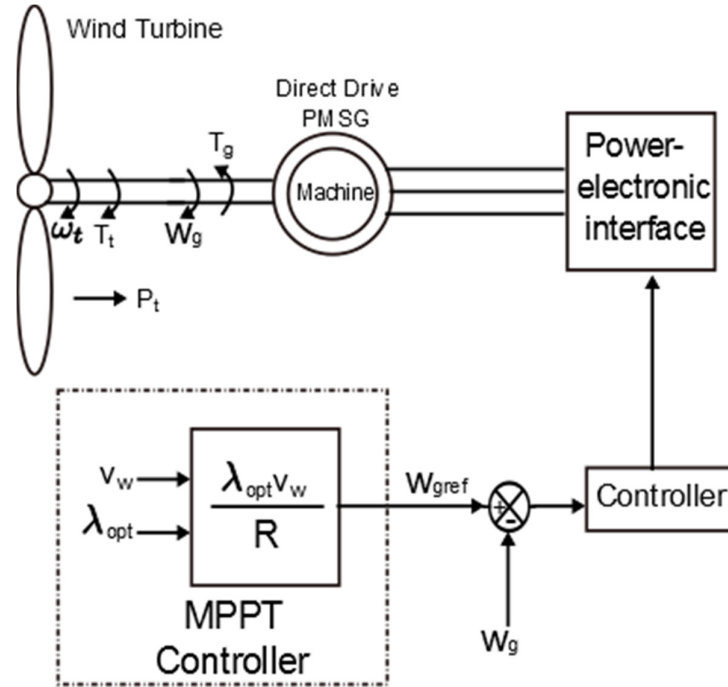


Figure 2.16: TSR Control based MPPT

Controller

2. Power Signal Feedback Control

With the knowledge of WT maximum power curve it is possible to track the maximum power by following the maximum power curve which is nothing but a cubic function of the generator speed [38,41] as given by equation (2.6). A schematic of PSF Control is shown in figure 2.17.

$$P_{max} = K_{opt} W_g^3 \quad (2.6)$$

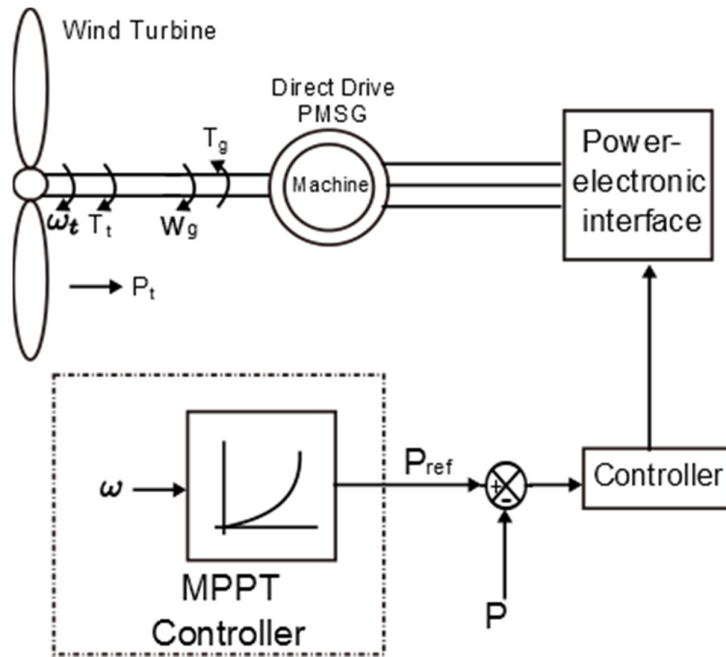


Figure 2.17: PSF Control based MPPT

Controller

3. Hill Climb Search Control (P&O Control)

The HCS algorithm continuously searches for the peak power of the wind turbine. The relation between power and speed is used and a continuous search process is activated which moves along the turbine characteristics in order to find the maxima. This maxima is nothing but the point of operation which will yield maximum power extraction from the turbine. Figure 2.18 shows the path view of HCS Control while Figure 2.19 shows the HCS algorithm.

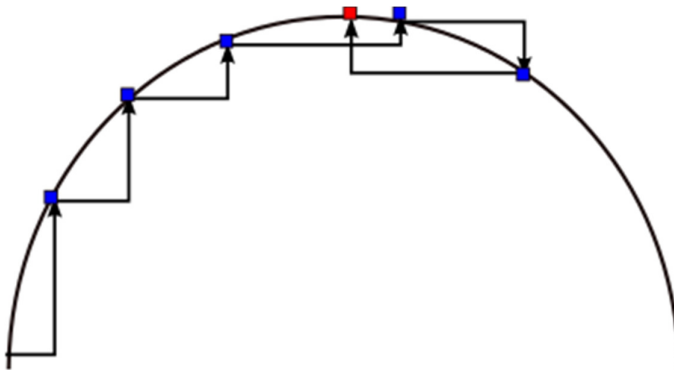


Figure 2.18: Path view of HCS

Control

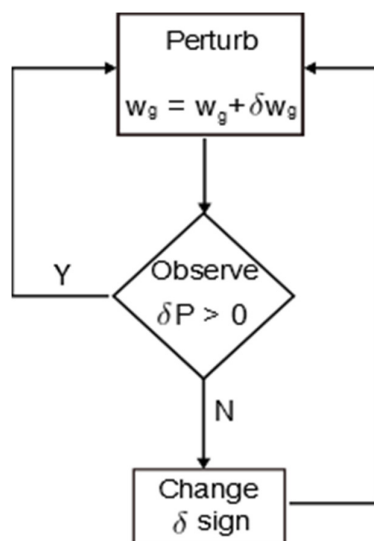


Figure 2.19: P&O Flowdiagram

4. Pitch Angle Control

The pitch angle control mechanism rotates the blade about their axis and hence manipulates the angle of attack which makes the wind to see different airfoil area than what it was seeing previously. Hence, the lift force on the blade gets changes, thereby changing the turbine characteristics itself. By this way Maximum power extraction from the turbine is ensured in face of wind speed variations.

5. Optimal Current Given (OCG) MPPT Control

This control strategy combines the PSF and HCS control techniques. Instead of using power signal feedback it employs current signal feedback and controls the speed of PMSG by using vector control. However, K_{opt} as mentioned in equation (2.6) is calculated using HCS algorithm. There is an improvement in the response speed and the accuracy of the system as compared to PSF and HCS methods [39].

TSR Control and PSF Control are the most commonly used MPPT methods. Hence, either by regulating the rotor speed or by adjusting the active power MPPT can be

attained. The former termed Speed Control Mode (SCM) employs a speed controller to regulate the rotor while the latter termed as Power Control Mode (PCM) uses an active power controller to optimize the power. They are fundamentally equivalent, but since they use different controllers at the outer control loop of the Machine Side Converter (MSC) controller, the time dependence of the control system differs depending on whether SCM or PCM is used. In case of constant wind speed the two control mechanisms yield almost the same results whereas when the wind speed fluctuations were increased in magnitude, differences appeared between them and it was concluded that SCM is preferable than PCM in terms of power coefficient and hence yields a slightly higher power output thereby increasing the efficiency of the system. [42] Forth brings a comparison study between SCM and PCM. A schematic diagram of the two control modes is shown in Figure 2.20.

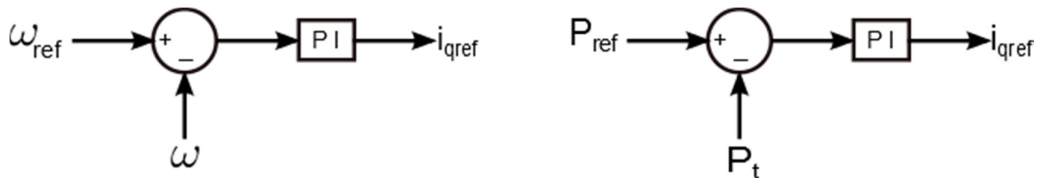


Figure 2.20: Two different modes of Machine Side Converter outer loop control

There has been many other MPPT Control structures proposed in literature, like Limit Cycle based MPPT Control for small size WT PMSG system with diode bridge rectifier [43] in which an intermediary boost converter stage is used to control the power flow. In [44] a 3 stage power conversion control strategy has been proposed wherein an uncontrolled rectifier converts ac-dc, a boost converter is dedicated to track maximum power from the turbine based on the P&O MPPT algorithm and thereafter a VSI converts dc-ac thereby transferring maximum power to the grid. Schematic of such scheme is shown in figure 2.21. Fuzzy Logic based MPPT Controller [45] in which one fuzzy logic controller is used for speed control of Squirrel Cage Induction Generator by FOC strategy while the other is dedicated for controlling the excitation. A non-linear Sliding Mode Based Control Strategy for extracting maximum power from the turbine based on the optimum TSR [45]. A

variable step MPPT algorithm to get fast and stable maximum power point tracking by mountain climb method has been proposed in [46].

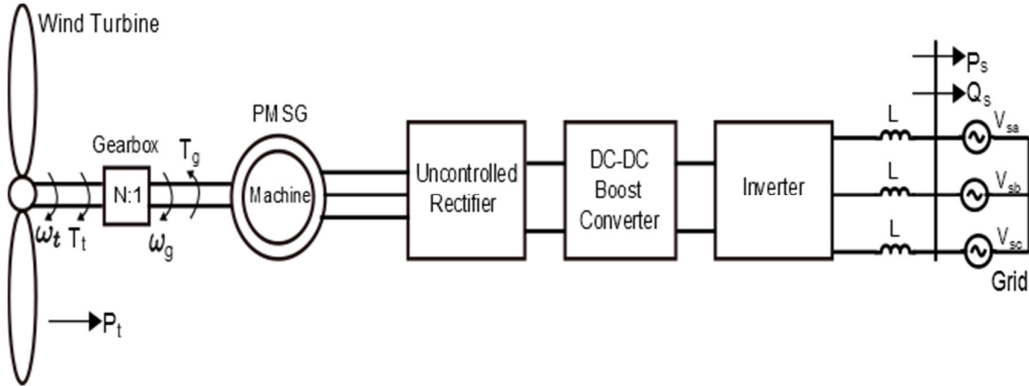


Figure 2.21: PMSG based WECS with intermediate boost converter stage

Although the MPPT Control for WECS is quite a matured area and a considerable amount of work has been done in this regard, but LPPT Control has been ignored and very little work has been done on controlled power point tracking from WECS. [2] Projects the necessity of active power control in grid connected WECS. In [8] a real power control strategy based on Direct Torque Control has been reported.

2.6 Grid Side Control for WECSs

The WECS is interfaced to the grid by grid side converter, hence transferring the power available at the dc-link to the grid requires DC-controlled AC transformation. The Grid Side Control is dedicated for the same.

Control objectives for Grid side Controller for grid connected operation of WECSs:

- Control of Active Power supplied to the grid.
- Control of reactive power transferred between WECS and grid.
- Control of dc-link voltage in the absence of ESS (like batteries).
- Ensure high quality of injected power.
- Grid Synchronization.

Control Structures for Grid Connected WECSs

The grid side converter control consists mainly of two independent cascaded loops. The first one consists of a fast inner current control loop which regulates the grid current and an outer voltage control loop which regulates the dc-link voltage. The other one consists of an outer reactive power regulation loop cascaded with inner current control loop which controls the reactive power injection to the grid [47]. The current loop is responsible for current protection and power quality issues while the dc-link voltage controller is dedicated for balancing the power flow in the system. However [48] considers inner power loop instead of current loop cascaded with outer voltage control loop in which the current injected into the grid is indirectly controlled. There are also some control strategies which have been reported [49], which instead of outer voltage control loop employs a power control loop cascaded with an inner current control loop. Although the control structure for outer voltage control loop and outer power control loop with inner current control loop conceptually remains same, the only difference is in the way of generating current reference [50]. However, outer voltage and inner current cascaded loop control structure is the most commonly deployed control strategy for Grid Connected DPGS due to its excellent dynamic performance. Based on the type of reference frame adopted the controller design process for outer voltage and inner current control structure for Grid Connected DPGS can be listed under the following heads:

- Natural Frame Control

The control design in abc frame requires three different controllers for each phase of grid current. Normally, abc control is a structure where non-linear controllers like hysteresis or dead beat are preferred due to their high dynamics. But the high signal processing requirement possess restriction on its usage. A possible implementation of abc control is shown in figure 2.22. The control signal obtained from the dc-link voltage loop sets the current command. The abc current references obtained from the dq to abc transformation block are compared with the actual currents and the error signals are given to the individual current controllers which sets the desired modulation signals for the PWM strategy. If in case hysteresis or dead beat controllers are deployed instead of PI controllers then the controller outputs directly gives the switching states for the switches.

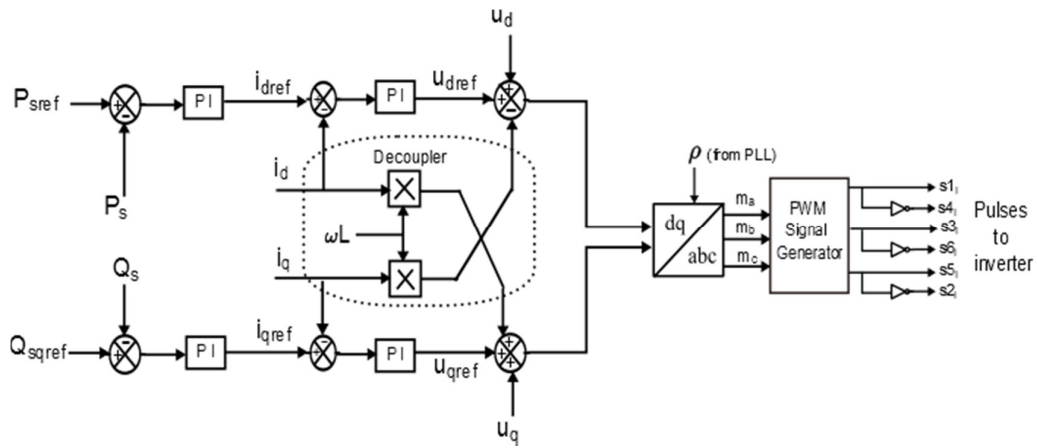


Figure 2.22: General structure for SRRF control strategy

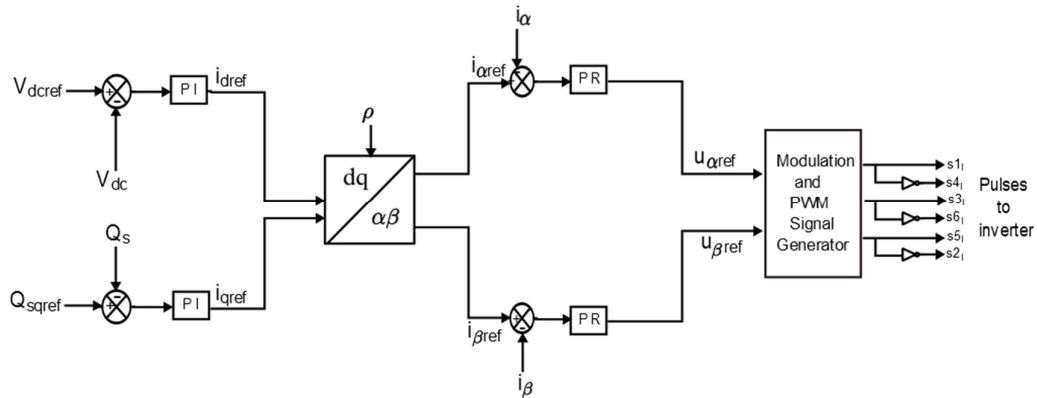


Figure 2.23: General structure for stationary reference frame control strategy

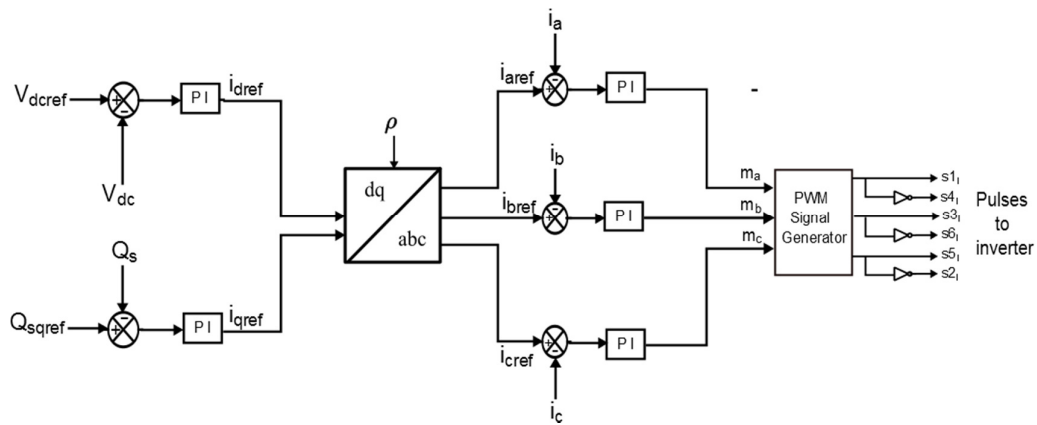


Figure 2.24: General structure for natural reference frame control strategy

Both PI as well as PR controllers can be used in natural frame control. [51] Discusses the control in abc frame by using PI controllers in which the control matrix is given by equation(2.7). While the usage of PR controllers wherein the controller is already in stationary frame and hence there is no dependency between the components is discussed in [52]. Equation (2.8) describes the control structure for the PR controller in abc frame.

$$\mathbf{G}_{PI}^{abc}(s) = \frac{2}{3} \begin{pmatrix} K_p + \frac{K_i s}{s^2 + \omega^2} & -\frac{K_p}{2} - \frac{K_i s + \sqrt{3}K_i \omega_0}{2(s^2 + \omega_0^2)} & -\frac{K_p}{2} - \frac{K_i s + \sqrt{3}K_i \omega_0}{2(s^2 + \omega_0^2)} \\ -\frac{K_p}{2} - \frac{K_i s + \sqrt{3}K_i \omega_0}{2(s^2 + \omega_0^2)} & K_p + \frac{K_i s}{s^2 + \omega^2} & -\frac{K_p}{2} - \frac{K_i s + \sqrt{3}K_i \omega_0}{2(s^2 + \omega_0^2)} \\ -\frac{K_p}{2} - \frac{K_i s + \sqrt{3}K_i \omega_0}{2(s^2 + \omega_0^2)} & -\frac{K_p}{2} - \frac{K_i s + \sqrt{3}K_i \omega_0}{2(s^2 + \omega_0^2)} & K_p + \frac{K_i s}{s^2 + \omega^2} \end{pmatrix} \quad (2.7)$$

$$\mathbf{G}_{PR}^{\alpha\beta}(s) = \begin{pmatrix} K_p + \frac{K_i s}{s^2 + \omega^2} & 0 & 0 \\ a_{21} & K_p + \frac{K_i s}{s^2 + \omega^2} & 0 \\ 0 & 0 & K_p + \frac{K_i s}{s^2 + \omega^2} \end{pmatrix} \quad (2.8)$$

- SRF Control

The SRF Control overcomes the deficiency of getting zero SSE for sinusoidal command tracking by employing PR controllers instead of PI. A considerable amount of work has been done in this regard and has been discussed in [53,54]. The controller matrix for the PR controller is given by equation (2.9).

$$\mathbf{G}_{PR}^{\alpha\beta}(s) = \begin{pmatrix} K_p + \frac{K_i s}{s^2 + \omega^2} & 0 \\ 0 & K_p + \frac{K_i s}{s^2 + \omega^2} \end{pmatrix} \quad (2.9)$$

Where, ω is the resonance frequency of the controller, K_p is the proportional gain and K_i is the integral gain of the controller. The characteristics of this controller is that it achieves a very high gain value around the resonance frequency and thereby enabling perfect sinusoidal tracking with zero SSE. The high dynamic characteristics

obtained by deploying PR controller have been discussed in [52]. A schematic of SRF Control is shown in figure 2.23.

- SRRF Control

In SRRF Control the design and analysis exercise is carried out in dq frame which rotates synchronously with the grid voltage. In dq frame however the control variables becomes dc quantities and hence the control task simply boils down to tracking of dc TIV commands. A schematic of SRRF Control is shown in figure 2.24. We can also achieve unity power factor by setting the reactive power reference to zero or according to the requirement we can set the reactive power reference. Since the commands are dc quantities therefore a PI controller can itself suffice to yield satisfactory performance with zero SSE. The control structure for SRRF Control is given by equation(2.10).

$$\mathbf{G}_{PR}^{dq}(s) = \begin{pmatrix} K_p + \frac{K_i}{s} & 0 \\ 0 & K_p + \frac{K_i}{s} \end{pmatrix} \quad (2.10)$$

Where, K_p and K_i are the proportional and integral gains of the controller respectively. The expressions for the active and reactive power delivered to the ac system are given by equation (2.11) and(2.12) respectively.

$$P_s = \frac{3}{2}(v_{sd}i_d + v_{sq}i_q) \quad (2.11)$$

$$Q_s = \frac{3}{2}(-v_{sd}i_q + v_{sq}i_d) \quad (2.12)$$

If v_{sq} is made zero then the active and the reactive powers can be independently controlled by i_d and i_q respectively [55]. Hence independent control of active and reactive power is attained in SRRF Control by deploying a PLL whose task is to force v_{sq} to zero. PLL is also responsible for extracting the phase angle of the grid voltages and hence synchronizes the DG system with the grid. Also the performance of the PI controller can be improved by including cross coupling feed and voltage forward terms.

2.6.1 DC-link voltage Control

The proper operation of VSI requires variation of dc-link voltage within prescribed limits. The dc-link voltage is directly affected by any load change. The sudden removal of load would result in an increase in the dc-link voltage above the reference value whereas a sudden increase in load would result in decrease in dc-link voltage below its reference value.

Due to transient on the load side, the dc bus voltage is significantly affected. In order to regulate the dc-link voltage closed loop controllers are used. The Proportional-Integral-Derivative (PID) control provides a generic and efficient solution to many control problems. The control signal issued from PID dc-link voltage controller is given by equation(2.13).

$$u = K_p (V_{dcref} - V_{dc}) + K_i \int (V_{dcref} - V_{dc}) dt + K_d \frac{d}{dt} (V_{dcref} - V_{dc}) \quad (2.13)$$

where, K_p, K_i, K_d are proportional, integral and derivative gains of PID controller respectively. While the proportional term enhances the transient performance the integral term on the other hand improvises the steady state performance by yielding a zero SSE. The derivative term aids the system stability but however the practitioners have found the derivative term can behave against anticipatory action in case of transport delay. A cumbersome trial and error method to tune its parameters made many practitioners to switch off or even exclude the derivative term [56,57]. So, a PI controller which uses deviation of capacitor voltage from its reference value as its input is used to maintain dc-link voltage to its reference value. There have been Conventional DC-Link Voltage Controller and Energy based DC-Link Voltage Controller proposed in literature.

Conventional DC-link Voltage Controller

The design of PI controller parameters is not a straightforward task for conventional PI control and hence these parameters are chosen by trial and error. The control signal issued by this controller is given as in equation (2.14)

$$i_{dref} = K_p (V_{dcref} - V_{dc}) + K_i \int (V_{dcref} - V_{dc}) dt \quad (2.14)$$

The schematic of Conventional DC-Link Voltage Controller is shown in Figure 2.25

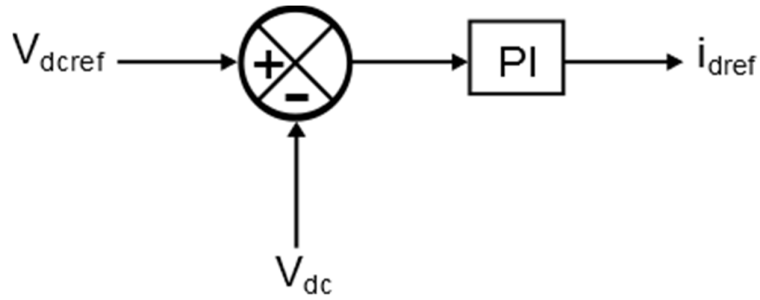


Figure 2.25: Conventional DC-Link Voltage Controller

Energy based DC-Link Voltage Controller

This controller is based on the error obtained by the difference of squared dc-link voltage reference and the actual value. The tuning of this controller is based on energy required by the dc-link capacitor to charge from actual voltage (V_{dc}) to reference voltage (V_{dcref}) and has been discussed in [58]. The control signal issued by this controller is given as in equation (2.15)

$$i_{dref} = K_p (V_{dcref}^2 - V_{dc}^2) + K_i \int (V_{dcref}^2 - V_{dc}^2) dt \quad (2.15)$$

The schematic of Energy based DC-Link Voltage Controller is shown in Figure 2.26

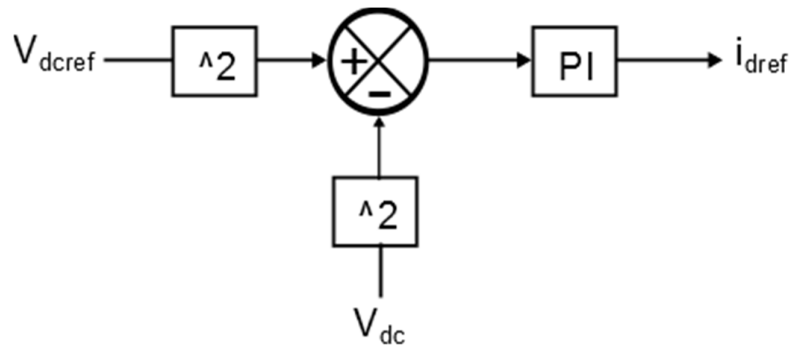


Figure 2.26: Energy based DC-Link Voltage Controller

2.6.2 Importance of PLL in grid connected operation of WECSs

PLL not only synchronizes the DG unit to the grid but also helpful in attaining Unity Power Factor Control. The following illustration clarified the importance of PLL.

Assume the grid to be an infinitely stiff ac source (v_{sabc}) with balanced, sinusoidal and constant frequency voltage waveform which can be expressed by equations(2.16), (2.17) and (2.18) :

$$v_{sa}(t) = \hat{v}_s \cos(\omega_o t + \theta_o) \quad (2.16)$$

$$v_{sb}(t) = \hat{v}_s \cos\left(\omega t + \theta_o - \frac{2\pi}{3}\right) \quad (2.17)$$

$$v_{sc}(t) = \hat{v}_s \cos\left(\omega t + \theta_o - \frac{4\pi}{3}\right) \quad (2.18)$$

where, \hat{v}_s is the peak value of line to neutral voltage, ω_o is the source (grid) frequency and θ_o is the source initial phase angle.

The aforementioned three phase system can be represented by an equivalent space phasor as:

$$\vec{v}_s(t) = \hat{v}_s e^{j(\omega_o t + \theta_o)} \quad (2.19)$$

Figure 2.27 shows the interfacing of inverter output terminal to the grid.

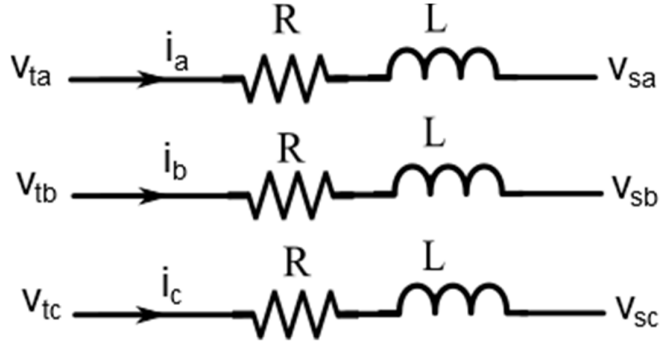


Figure 2.27 Inverter output terminal interfaced to the grid

The dynamics of inductor current is described can be described by the space phasor equation (2.20) as:

$$L \frac{d\vec{i}}{dt} = -R\vec{i} + \vec{v}_i - \vec{v}_s \quad (2.20)$$

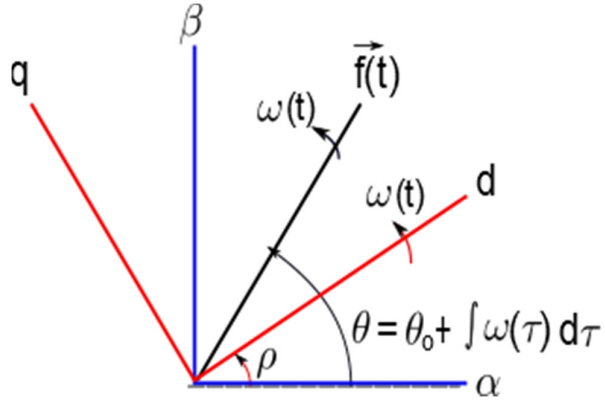


Figure 2.28: $\alpha\beta$ and dq coordinate system

Figure 2.28 shows the pictorial representation of $\alpha\beta$ and dq coordinate system with the adopted convention. From for \vec{v}_s from(2.19) in (2.20) and expressing the obtained expression in dq domain we get(2.21):

$$L \frac{d}{dt} [(i_d + j i_q) e^{j\rho}] = -R(i_d + j i_q) e^{j\rho} + (v_{id} + j v_{iq}) e^{j\rho} - \hat{v}_s e^{j(\omega_s t + \theta_o)} \quad (2.21)$$

(2.21) can be further simplified to obtain (2.22)

$$L \frac{d}{dt} (i_d + j i_q) + j L \rho (i_d + j i_q) = -R(i_d + j i_q) + (v_{id} + j v_{iq}) - \hat{v}_s e^{j(\omega_s t + \theta_o - \rho)} \quad (2.22)$$

Bifurcating the above equation in real and imaginary parts we get:

$$L \frac{d i_d}{dt} = \left(L \frac{d \rho}{dt} \right) i_q - R i_d + v_{id} - \hat{v}_s \cos(\omega_s t + \theta_o - \rho) \quad (2.23)$$

$$L \frac{d i_q}{dt} = \left(L \frac{d \rho}{dt} \right) i_d - R i_q + v_{iq} - \hat{v}_s \sin(\omega_s t + \theta_o - \rho) \quad (2.24)$$

To make the above equations ((2.23)and(2.24)) in standard state space form we introduce a new state equation (2.25)

$$\frac{d \rho}{dt} = \omega(t) \quad (2.25)$$

So, the equations ((2.23)and(2.24)) get simplified to:

$$L \frac{d i_d}{dt} = L \omega(t) i_q - R i_d + v_{id} - \hat{v}_s \cos(\omega_s t + \theta_o - \rho) \quad (2.26)$$

$$L \frac{di_q}{dt} = L\omega(t)i_d - Ri_q + v_{iq} - \hat{v}_s \sin(\omega_o t + \theta_o - \rho) \quad (2.27)$$

Now since the grid is assumed to be an infinitely stiff ac source of constant frequency ω_o , therefore $\omega(t) = \omega_o$ and if we can ensure $\rho(t) = \omega_o(t) + \theta_o$, then (2.26) and (2.27) will get reduced to

$$L \frac{di_d}{dt} = L\omega_o i_q - Ri_d + v_{id} - \hat{v}_s \quad (2.28)$$

$$L \frac{di_q}{dt} = L\omega_o i_d - Ri_q + v_{iq} \quad (2.29)$$

(2.28) and (2.29) describes a second order linear system with i_d and i_q as dc quantities given v_{id} and v_{iq} are also constant quantities in steady state.

So, just by ensuring $\rho(t) = \omega_o(t) + \theta_o$, we have converted a non-linear system into a linear one with all the variables as simple dc time invariant quantities which can be simply controlled by using a PI controller. The mechanism by which we can ensure that $\rho(t)$ remains locked at $\{\omega_o(t) + \theta_o\}$ is PLL.

2.7 Load Side Control for WECSs

Commonly employed system topology for Standalone operation of WECSs is shown in figure 5.1. Unlike the grid-connected mode wherein most of the system level dynamics are governed by the grid due to relatively small size of micro sources, in the standalone mode of operation the system dynamics are dictated by the micro sources themselves, their power regulation control, and to an unusual degree by the network itself [59-61]. Hence the control task for the load side converter is much more complex than the grid side converter. The load side converter control is dedicated for controlling:

- Load/PCC Voltage Magnitude.
- Load/PCC Voltage Frequency.
- Current injected to the load.

Conventional outer voltage and inner current control strategy has been quite popular because of it's excellent dynamic performance. Control of DG unit using the same has been discussed in [61-64]. Contrary to [61-64] wherein feed forward signals are used

to eliminate the cross coupling, [65] presents a multivariable PI control strategy for decoupling the dynamics of d and q axis quantities. In [47] active power/frequency and reactive power/voltage droops are applied in order to determine the active, reactive power production thus downscaling to the VSWTs the conventional control concepts of power plants.

2.8 Filter Design

Most RES are interfaced to the utility or the loads via power electronic interface which performs the task of power conditioning. In this regard, Inverter is almost a necessarily used power electronic converter which interfaces the DG unit with the utility or the load. Inverter output contains high frequency switching harmonics sitting on top of fundamental voltage component (50 Hz). Harmonics in the output voltage are of the order of switching frequency or it's multiple. We need to filter this out before supplying it to load. Hence, this imposes requirement for a filtering stage to be cascaded between the inverter and the load.

As per the IEEE standard the injected current into the grid should not have a THD more than 5%. The standard IEEE 519-1992 entitled IEEE recommended Practices and Requirements for Harmonic Control in Electric Power Systems (RP-519-1992) set harmonic current goals for individual customers and harmonic voltage goals for utility at PCC [66]. According to the Harmonic Standard, 15-20% of the rated current is allowable and the harmonic order greater than 35 should not exceed 0.3% of rated current.

Table 2.2: Different types of Filters and their Characteristics

S. No.	Type of Filter	Order	Attenuation	Resonating Frequency
1.	L	First	-20 dB/decade	----

2.	LC	Second	-40 dB/decade	$f_o = \frac{1}{2\pi\sqrt{LC}}$
3.	LCL	Third	-60 dB/decade	$f_o = \frac{1}{2\pi} \sqrt{\frac{L_1 + L_2}{L_1 L_2 C}}$

A second order low pass filter (LC filter) can be a good candidate to be opted as a filter for autonomous operation of WECSs, as it can offer higher attenuation for the same frequency compared to a first order lag. An LC filter being a second order system possess a characteristic equation of the form $s^2 + 2\xi\omega_n s + \omega_n^2$ and hence it's gain decreases at the rate of 40 dB/decade after the corner frequency. Filter parameters are decided based on the attenuation and bandwidth requirement [67]. But since these are inherently undamped systems, hence they show a large resonant peak at their corner frequency (resonant frequency). Hence, we need to provide active damping in the system so as to improve the system response. So a resistor is included in the filter design which serves as a damper for the suppressing the oscillations [68].

2.10 Conclusion

Based on the extensive literature review on WECSs operating in grid connected as well as islanded mode .Following areas are considered for further investigation,

- Implementation of controlled power point tracking for grid connected WECSs.
- Implementation of controlled power point tracking for standalone WECSs.

Chapter 3

Principle of Operation, Modelling and Control of Wind Power Systems

Various designs of WT, different configurations of WECSs, Machine Side and the Grid Side Control were discussed in previous chapter. This chapter deals with the Aerodynamic Principle on which almost all modern WT works, Modelling of WT, Control of Wind Power Systems encompassing pitch angle control and controlling the electrical power output from WT (LPPT as well as MPPT) is discussed.

3.1 Aerodynamics of Wind Turbines

The function of wind turbine is to extract energy from the air and to produce mechanical energy which later may be transformed into other forms of energy. The following assumptions are made in the derivation of maximum possible output of a wind turbine [69]:

- 1) Blades operates without frictional drag.
- 2) A slipstream i.e. well defined separates the flow passing through the rotor disc from that outside the disc.
- 3) Static pressure in and out of the slip stream far ahead of and behind the rotor are equal to the undisturbed free stream static pressure.
- 4) Thrust loading is uniform over the rotor disc.
- 5) No rotation is imparted to the flow by the disc.

Now applying the laws of momentum theory to the control volume as shown in figure where the upstream and downstream planes are at infinite distance from the plane of rotation of the blades.

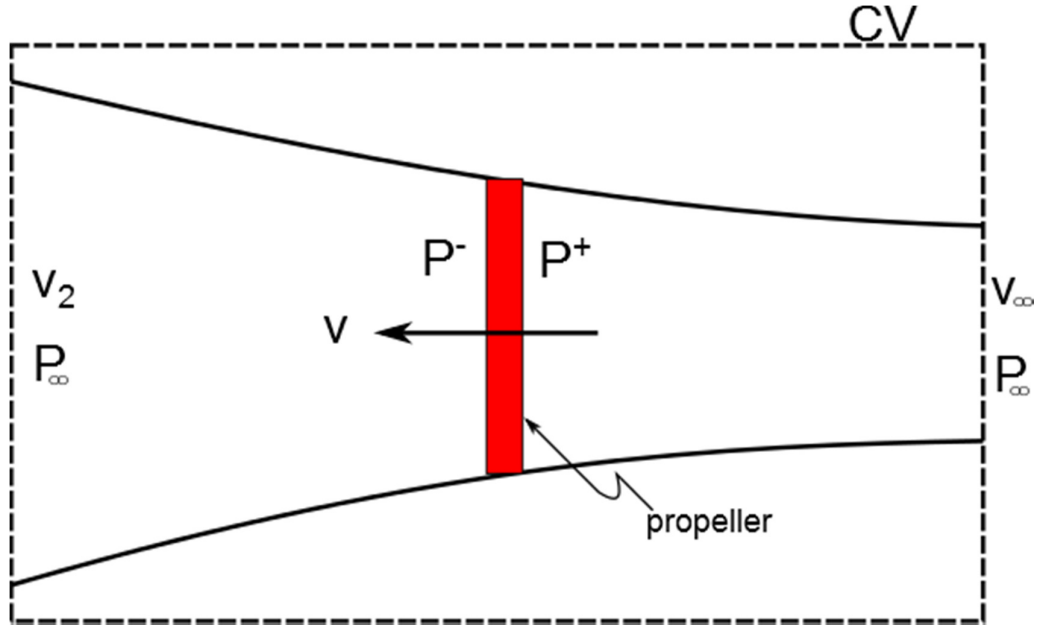


Figure 3.1: Control Volume of a Wind

Turbine

Thrust = momentum flux out – momentum flux in

$$= \rho A v (v_{\infty} - v_2) \quad (3.1)$$

Applying the Bernoulli's law to the control volume considered in figure

$$\frac{1}{2} \rho v_{\infty}^2 + P_{\infty} = \frac{1}{2} \rho v^2 + P^+ \quad (3.2)$$

$$\frac{1}{2} \rho v_2^2 + P_{\infty} = \frac{1}{2} \rho v^2 + P^- \quad (3.3)$$

Solving (3.2) and (3.3) we get

$$P^+ - P^- = \frac{1}{2} \rho (v_{\infty}^2 - v_2^2)$$

Therefore, Thrust (T) will be given by equation

$$T = A(P^+ - P^-) = \frac{1}{2} \rho A (v_\infty^2 - v_2^2) \quad (3.4)$$

Equating (3.1) and (3.4) as shown in (3.5) we get (3.6)

$$\frac{1}{2} \rho A (v_\infty^2 - v_2^2) = \rho A v (v_\infty - v_2) \quad (3.5)$$

$$v = \frac{1}{2} (v_\infty + v_2) \quad (3.6)$$

This result states that the velocity through the turbine is the average of the wind velocity far upstream of the rotor (v_∞) and the wind velocity in the wake (v_2).

Now, we introduce an axial interference factor (a) which relates v , v_∞ and v_2 .

$$v = v_\infty (1 - a) \quad (3.7)$$

Equating (3.6) and (3.7) we get

$$v_2 = v_\infty (1 - 2a) \quad (3.8)$$

Power extracted = Drop in Kinetic Energy of air

$$P = \frac{1}{2} \rho A v (v_\infty^2 - v_2^2) \quad (3.9)$$

Substituting for v_2 from (3.8) in (3.9) and simplifying further we get (3.10)

$$P = \frac{1}{2} \rho A v_\infty^3 (4a - 8a^2 + 4a^3) \quad (3.10)$$

Maximizing P with respect to a and substituting the resultant to zero as shown in equation (3.11) in order to find the maximum power that can be extracted from the turbine we get the value of $a = 1/3$, 1 .

$$\frac{dP}{da} = \frac{d}{da} \left(\frac{1}{2} \rho A v_\infty^3 (4a - 8a^2 + 4a^3) \right) = 0 \quad (3.11)$$

Now since $a=1$ is not feasible because at this value of axial interference factor the speed of wind at rotor plane is 0 thereby the power extracted will be 0. Hence $a=1$ is discarded and at $a=1/3$ we extract the maximum power from the turbine.

Substituting $a=1/3$ in (3.7) we get the relation between v and v_∞ at $a=1/3$ as given by equation (3.12)

$$v = \frac{2}{3}v_\infty \quad (3.12)$$

Now substituting $a=1/3$ in (3.10) we get the expression for maximum power that can be extracted from the turbine as :

$$P_{\max} = \frac{1}{2}\rho Av_\infty^3 \left(\frac{16}{27} \right) \quad (3.13)$$

The available power contained in the wind is given as:

$$P_{\max} = \frac{1}{2}\rho Av_\infty^3 \left(\frac{16}{27} \right) \quad (3.14)$$

Using (3.13) and (3.14) we get:

$$P_{\max} = \left(\frac{16}{27} \right) P_{avail} \quad (3.15)$$

(3.15)Suggests that the maximum power that we can extract from a turbine is $16/27=0.593$ times the power contained in the wind and this is known as the Betz limit given by equation (3.16).

$$C_{pmax} = \frac{P_{\max}}{P_{avail}} = 0.593 \quad (3.16)$$

This brings us in defining a metric which is an indication of the power extracted from the wind turbine from the available power contained in the wind. This is termed as power coefficient or performance coefficient in literature which is a dimensionless quantity and is expressed as ratio of power extracted from the turbine to the available power contained in the wind at any given point of time as given by equation(3.17) :

$$C_p = \frac{P_{ref}}{P_{avail}} \quad (3.17)$$

3.2 Modelling of Wind Turbines

Almost all the modern Wind Turbines work on the Aerodynamics Principle and hence these are lift operated rather than thrust operated.

The wind turbine model is based on the following three general equations [70-73]:

1. The extracted aero dynamical power (3.18)
2. The turbine power coefficient C_p (3.19)
3. The tip speed ratio λ (3.20)

The model has three inputs: the wind speed, the pitch angle and the rotor speed

$$P_t = \frac{1}{2} \rho A v_w^3 C_p \quad (3.18)$$

$$C_p = a_1 \left(\frac{a_2}{\lambda_i} - a_3 \beta - a_4 \right) e^{-\frac{a_5}{\lambda_i}} \quad (3.19)$$

$$\text{where, } \lambda_i = \frac{1}{\frac{1}{\lambda - 0.02\beta} - \frac{0.035}{\beta^3 + 1}}$$

$$\lambda = \frac{\omega_t R}{v_w} \quad (3.20)$$

where P_t is the power extracted by the turbine in Watts, ρ is the air density is equal to $1.225 \text{ kg}/m^3$, A is the area swept by the blade, v_w is the wind speed and C_p is the power coefficient which depends on the tip speed ratio (λ) which is a dimensionless quantity and β is the pitch angle (in degrees), R is radius of the blade, ω_t is the turbine angular speed.

3.2.1 System description

The coefficients a_1 - a_6 which shapes the WT characteristics are listed in Table 3.1 while the WT Parameters are described in Table 3.2 [1]

Table 3.1: Wind turbine Parameters

a_1	a_2	a_3	a_4	a_5
0.5176	116	0.4	5	21

Table 3.2: Wind turbine Parameters

Performance Parameters	
Rated Electrical Power	29 kW
Wind speed cut- in	3 m/sec
Rated wind speed	10 m/sec
Rotor Parameters	
Type of Hub	Fixed Pitch
Rotor Diameter	15 m
Swept Area	177 m ²
Rotor Speed@ rated wind	100 rpm

3.3 Control of Wind Power Systems

As seen from the modelling equation(3.18), that the power extracted from the turbine depends to a large extent on the wind speed. Figure 3.2 shows the variation of power extracted from the turbine vs the turbine angular speed in face of wind speed variations. Since the wind speed is something which is uncertain and varies continuously, so the control of Power extracted from the WT in face of wind speed variations is not an easy task and requires robust control techniques.

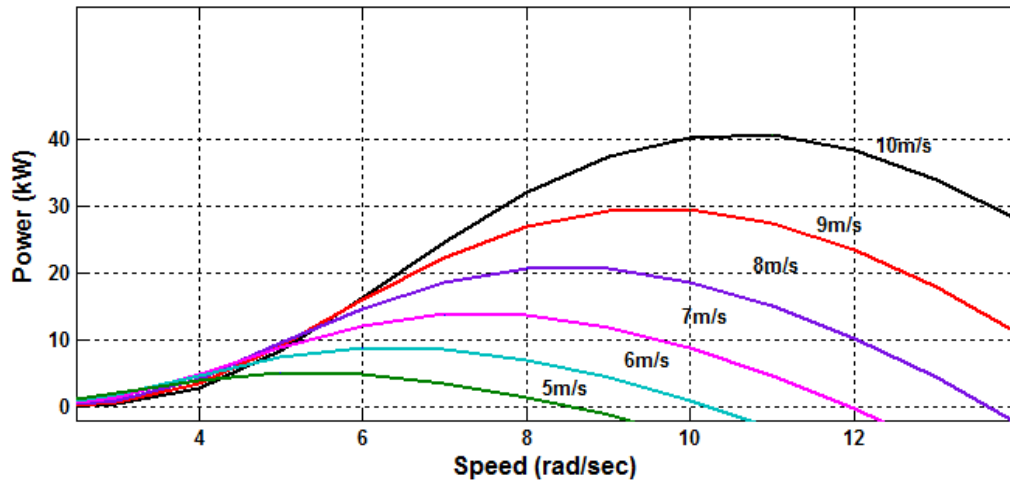


Figure 3.2: Operating under step change in load demand

The most commonly used control techniques for WPS includes:

1. Pitch Angle Control
2. Controlling the Electrical Power Output from the machine by using a power electronic interface.

3.3.1 Pitch Angle Control

The power coefficient which we derived in section 3.1 is a function of angle of attack (α) which is nothing but the angle between the actual blade position and the relative wind direction (w). While the angle of attack itself is a function of the pitch angle (β) which is the angle between the plane of rotation and the chord of the airfoil section.

So, we can adjust the value of power coefficient (C_p) by manipulating the angle of attack (α) which itself can be controlled by varying the pitch angle (β). But controlling the power coefficient means controlling the power extracted from the turbine (P_t).

Therefore, controlling the power extracted from the turbine boils down to the controlling the pitch angle (β), keeping the turbine angular speed (ω) fixed.

The plot of C_p vs λ for different values of pitch angle (β) is shown in figure 3.3.

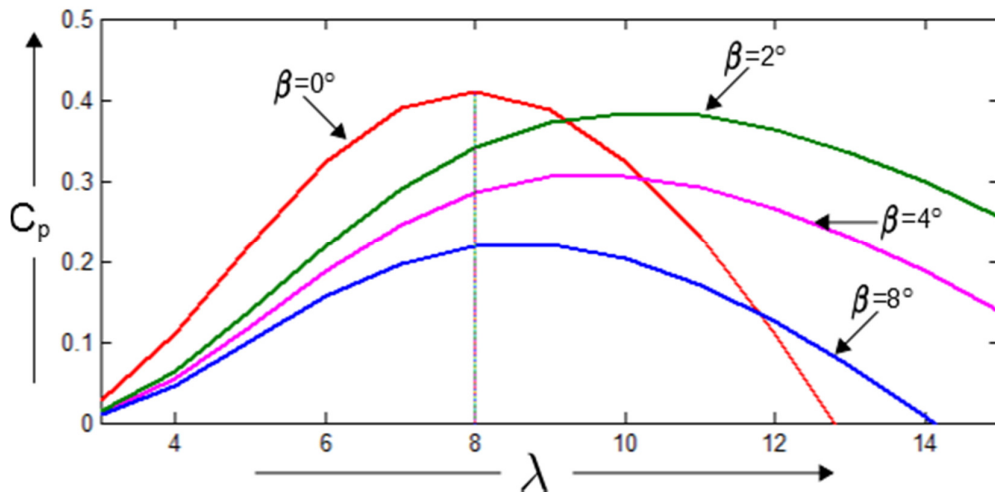


Figure 3.3: Variation of C_p with λ for various pitch angle values

3.3.2 Controlling the Electrical Power Output from the WT

The Electrical power output from the generator which is coupled to the WT is controlled by using a power electronic interface usually a controlled rectifier.

3.3.2.1 MPPT from a VSWPS

The limitation of CSWPS is overcome in VSWPS wherein we can extract maximum power from the turbine which of course is a function of the available power contained in the wind at any given point of time, despite of wind speed variations.

From figure it is clear that if we can manipulate the turbine angular speed, we can ensure that for any given wind speed we will be extracting maximum power that we can from the available power contained in the wind.

Below the rated power the pitch angle (β) is kept fixed at zero since it is clear from figure 3.3 that the peak value of C_p is largest when $\beta=0$. Thus to maximize the turbine power (P_t), the power coefficient ($C_p(\lambda, \beta=0)$) should always freeze at its maximum value ($C_{p\max}$). But in order to get $C_{p\max}$ at any given wind speed we should be able to operate at optimum value of TSR (λ_{opt}) which corresponds to an optimum blade angular speed (ω_{opt}). Therefore we can relate λ_{opt} , ω_{opt} and v_w by the equation.

$$\lambda_{opt} = \frac{R\omega_{opt}}{v_w} \quad (3.21)$$

Substituting for v_w from (3.21) in (3.18) we get equation (3.22) which describes the power extracted from the turbine (P_t) as a function of turbine angular speed (ω_t)

$$P_t = \left(\frac{0.5\rho AR^3 C_{p\max}}{\lambda_{opt}} \right) \omega_{opt}^3 \quad (3.22)$$

$$P_t = K_{opt} \omega_{opt}^3 \quad (3.23)$$

$$\text{where, } K_{opt} = \frac{0.5\rho AR^3 C_{p\max}}{\lambda_{opt}} \quad (3.24)$$

Equation (3.23) suggests that for under constant- λ variable speed operation, the power extracted from the turbine (P_t) varies in proportion to the cube of the turbine angular speed (ω_t^3). Figure 3.4 shows the variation of P_t vs ω_t in constant λ variable speed regime.

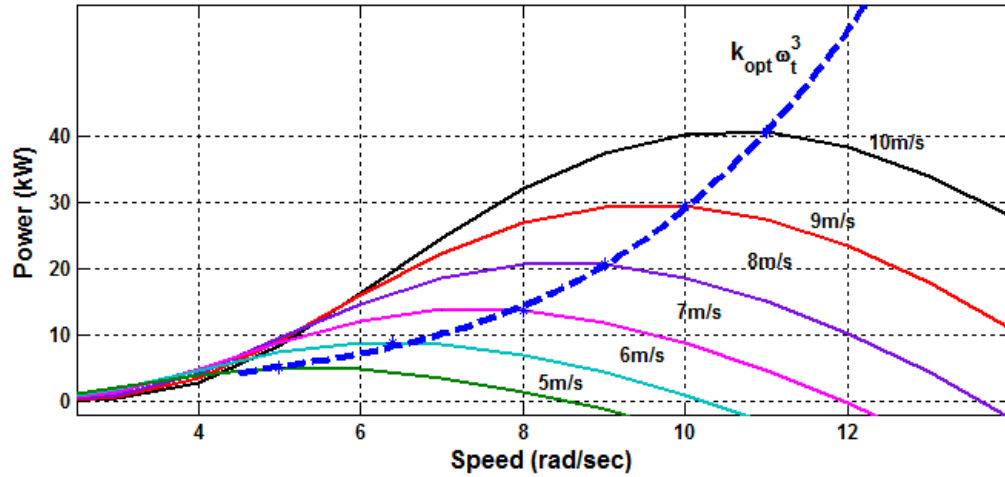


Figure 3.4: Variation of MPP with turbine angular speed for different wind speeds

Based on (3.22) we can write equation (3.25) which describes turbine torque (T_t) as a function of turbine angular speed (ω_t).

$$T_t = \left(\frac{0.5 \rho A R^3 C_{p \max}}{\lambda_{opt}} \right) \omega_{opt}^2 \quad (3.25)$$

$$P_t = K_{opt} \omega_{opt}^3 \quad (3.26)$$

where, K_{opt} is as defined in (3.24)

Equation (3.26) suggests that under constant λ variable speed operation the turbine torque (T_t) is directly proportional to the square of turbine angular speed (ω_t^2). Figure 3.5 shows the variation of T_t vs ω_t in constant λ variable speed regime.

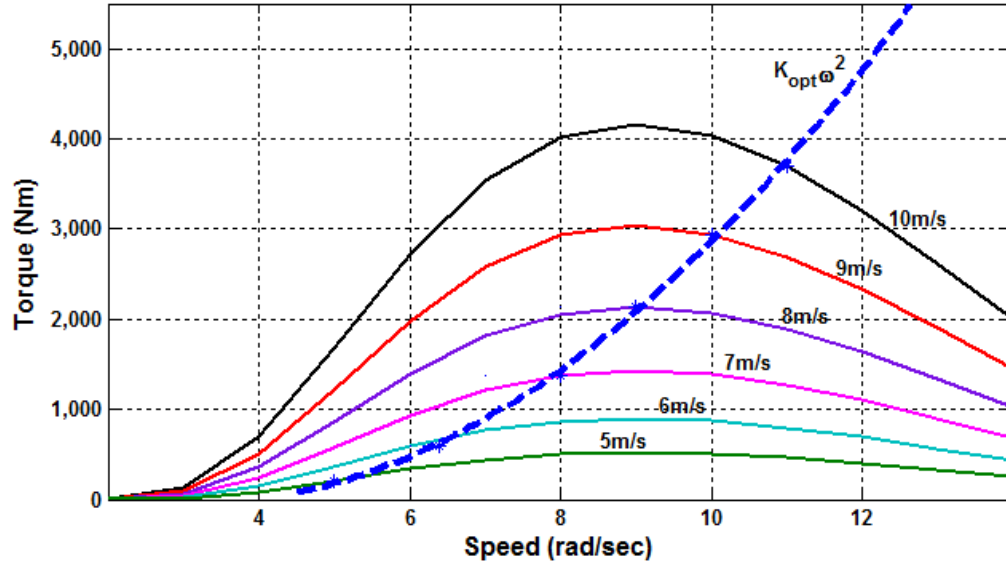


Figure 3.5: Variation of Turbine Torque with turbine angular speed for different wind speeds

3.3.2.2 LPPT from a VSWPS

A basic idea of LPPT technique has been proposed in this section, wherein the motivation was taken from the fact that, based on the turbine angular speed if MPPT is possible by TSR control then we can certainly also extract desired limited power (LPPT) from the turbine if we can operate at the corresponding point on the WT characteristics which can yield desired limited power from the turbine.

The ideology used in LPPT from VSWPS is that if by operating at MPP (λ_{opt}, C_{pmax}) as seen in section 3.3.1.1 we are able to extract maximum out of available turbine power, then we can also extract limited power from the turbine by operating at the corresponding point which can give that much demanded power (P_{ref}). This can be seen from figure 3.6 which shows that based on demanded power if we can fix the point of operation to (λ_{ref}, C_{pref}) then we will be able to extract the demanded power from the turbine.

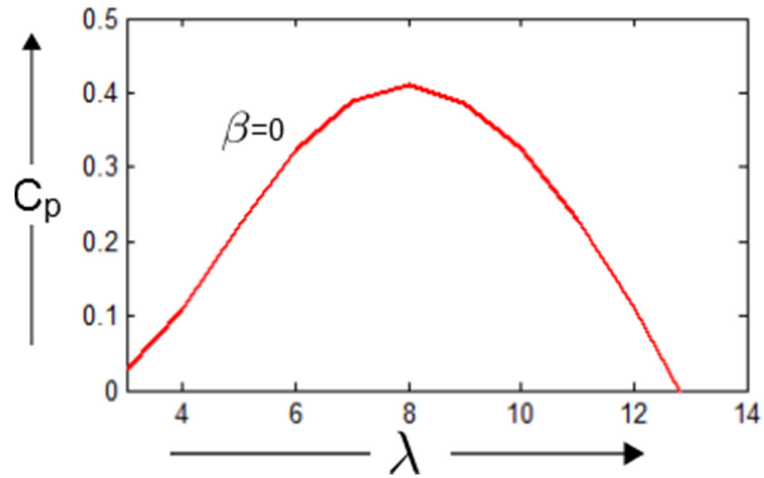


Figure 3.6: Variation of C_p with λ for $\beta=0$

3.4 Conclusion

Power Control from WPS in face of wind speed variations is a challenging task. There has been a lot of work done on MPPT techniques but LPPT has been overlooked and hasn't got enough attention. Based on the same principle on which TSR Control for MPPT has been proposed in the literature, the basic idea for LPPT technique has is thrown in this chapter so that the controller for MPPT and LPPT remains the same. Based on the point of operation which depends on the turbine angular speed we can extract desired power from the turbine.

Chapter 4

Controlled Power Point Tracking For Grid-Connected operation of WECS

As discussed in the Chapter-2, there are various topologies of the wind energy conversion system and turbines. In this chapter a full converter turbine that uses Permanent magnet Synchronous Generator (PMSG) as its generator without the use of battery at DC bus is studied and simulated. In this chapter, we will discuss in detail the wind power energy conversion system configuration, design, proposed control scheme for controlled power point tracking using speed control of permanent magnet synchronous generator (PMSG) in grid connected operation of WECS.

4.1 Wind power configuration

The system description, system modeling and proposed control scheme for limited power point tracking is presented in this section.

4.1.1 System description

In this chapter, a Wind energy conversion system with peak power capacity of 29kW is interfaced with the three phase three wire grid with a shunt connected local load network. A back to back AC/DC/AC topology is implemented for interfacing the WECS (Wind Energy Conversion System) to the distribution network as shown in

Figure 4.1. The First stage consists of a controlled rectifier .The main objective of power balancing is achieved through the vector control technique of this controlled rectifier. The controlled rectifier operates in two operating region i) when WECS output power is sufficient to supply the total load demand ii) when WECS output power is insufficient to supply the load demand and the WECS is at maximum power point. The control technique used for the controlled rectifier to operate in both the regions is speed control of PMSG through vector control. A three-leg two-level voltage source inverter is used for transferring the power from WECS to the point of coupling (PCC) and to meet the reactive power if any. Current source inverter (CSI) can also be used with the proposed control technique and it will not affect the system as both the proposed control technique for Controlled rectifier and the current control of inverter are independent of each other. Three Inductors are used to interface the inverter with the grid. A shunt RC filter is used as a ripple filter to remove high frequency ripple, which are caused due to the high frequency switching of the inverter, from the PCC voltage. The WECS system parameters and Wind Turbine Parameters are given in Table 4.1 & Table 4.2 .

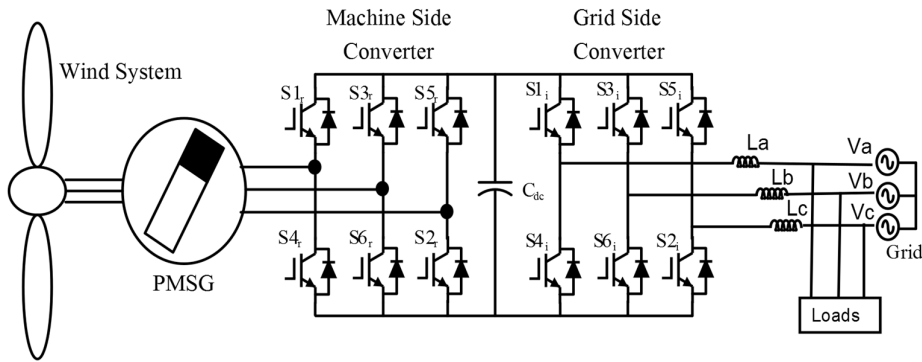


Figure 4.1: WECS System Configuration

Table 4.1: WECS Parameters

C (output capacitance of controlled converter)	6000 μ F
L_{inf} (interfacing inductance)	5 mH
V_{ll} (line to line grid voltage)	400 V

Table 4.2: Wind turbine Parameters

Performance Parameters	
Rated Electrical Power	29 kW
Wind speed cut- in	3 m/sec
Rated wind speed	10 m/sec
Rotor Parameters	
Type of Hub	Fixed Pitch
Rotor Diameter	15 m
Swept Area	177 m ²
Rotor Speed@ rated wind	100 rpm
Generator Parameters	
Type	3 phase/6 pole synchronous
kw @ Rated wind speed	29 kW
Speed RPM nominal	3000 rpm
Transmission Parameters	
Ratio	1 to 30 (rotor to gen speed)

4.1.2 System modeling

A. Modeling of wind turbine with PMSG

The wind turbine model is based on the following equations as was described in Chapter 3, Section 3.2.

1. Equation for the extracted aero dynamical power (4.1)
2. Equation for the turbine power coefficient C_p (4.2)
3. Equation for the tip speed ratio λ (4.3)

The model has three inputs: the wind speed, the pitch angle and the rotor speed

$$P_t = \frac{1}{2} \rho A v_w^3 C_p(\lambda, \beta) \quad (4.1)$$

$$C_p = a_1 \left(\frac{a_2}{\lambda_i} - a_3 \beta - a_4 \right) e^{\frac{-a_5}{\lambda_i}} \quad (4.2)$$

$$\lambda = \frac{\omega_t R}{v_w} \quad (4.3)$$

where ρ is the air density is equal to 1.225 kg/m^3 , A is the area swept by the blade, v_w is the wind speed and C_p is the power coefficient which depends on the tip speed ratio λ and β is the pitch angle, R radius of the blade, ω is the turbine angular velocity. Variation of C_p with respect to the tip speed ratio λ , keeping pitch angle $\beta=0$, is shown Figure 3.6 .

The rotor speed input is connected to the one mass mechanical drive train model computing the turbine rotor swing. The equation is [47] :

$$(J_T + J_G) \frac{dw_g}{dt} = T_T - T_G - Dw_g \quad (4.4)$$

Where J_T and J_G are the turbine and generator moment of inertia, T_T and T_G are the turbine and electromagnetic torque, D is the viscous friction factor and w_g is the generator rotor speed. Figure 4.2 gives a pictorial view of Wind Mill coupled to a generator inside the nacelle.

B. PMSG model

Dynamic modeling of PMSG described in d-q reference system is described as follows [47,74]:

$$\frac{di_q}{dt} = -\frac{r_s}{L} i_q - \omega_e i_d + \frac{\omega_e \Phi_m}{L} - \frac{V_{sq}}{L} \quad (4.5)$$

$$\frac{di_d}{dt} = -\frac{r_s}{L} i_d + \omega_e i_q - \frac{V_{sd}}{L} \quad (4.6)$$

$$\omega_e = p w_g \quad (4.7)$$

The electromagnetic torque is given as :

$$T_e = -\frac{3}{2} p i_q \{ (L_d - L_q) i_d + \varphi_m \} \quad (4.8)$$

For surface mounted PMSGs $L_d = L_q = L_s$ and direct axis current i_d kept zero, (4.8) gets reduced to:

$$T_e = -\frac{3}{2} p \Phi_m i_q \quad (4.9)$$

Where r_s is the stator resistance, L is the inductance of the generator on the d and q axis which are taken to be equal, Φ_m is the permanent magnetic flux and w_e is the electrical rotating speed of the generator defined by equation (4.7) and p_n are the number of pole pairs.

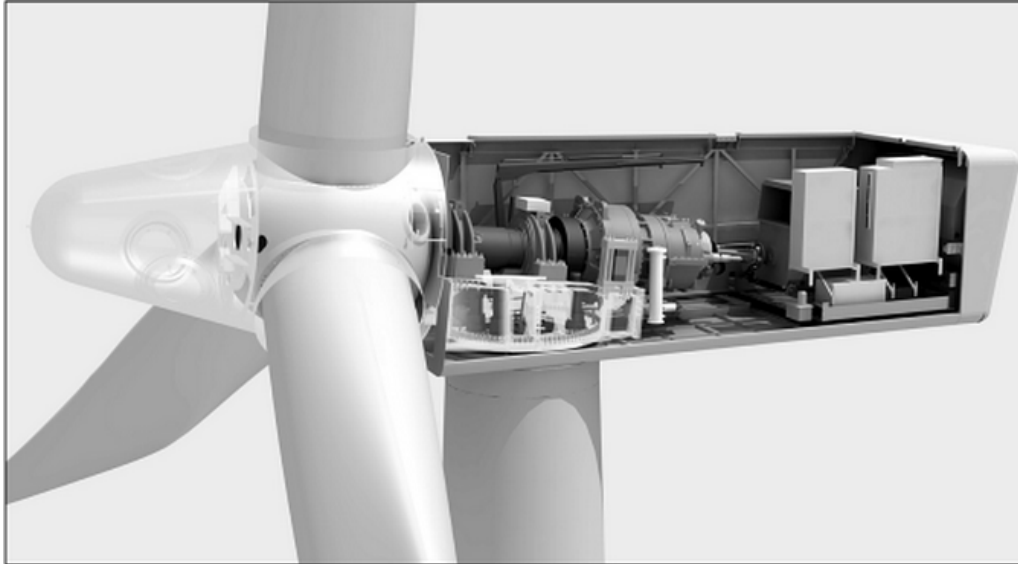


Figure 4.2: Wind Mill coupled to generator [19]

4.1.3 Control structure

The block diagrammatic representation of the proposed control strategy for LPPT as well as MPPT from WECS is shown in figure 4.3.

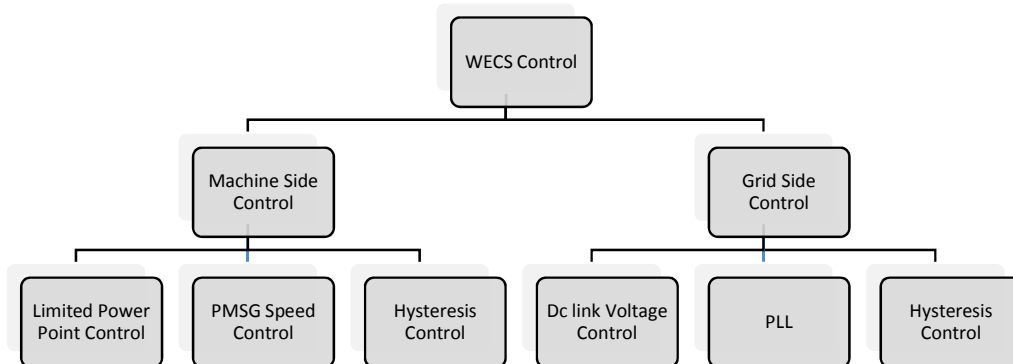


Figure 4.3: Block Diagram Representation of the overall control system

The overall system control has been bifurcated into Machine Side Control and Grid Side Control. While the Machine Side Control comprises of the following control stages:

- i. Limited Power Point Control
- ii. PMSG Speed Control
- iii. Hysteresis Control

The Grid Side Control on the other hand encompasses the following enclosures:

- i. DC link Voltage Control
- ii. Phase Locked Loop (PLL)
- iii. Hysteresis Control

While the Machine Side and the Grid Side Control are independent of each other, each of the sub-heads listed under them as shown in figure talk within well-defined boundaries.

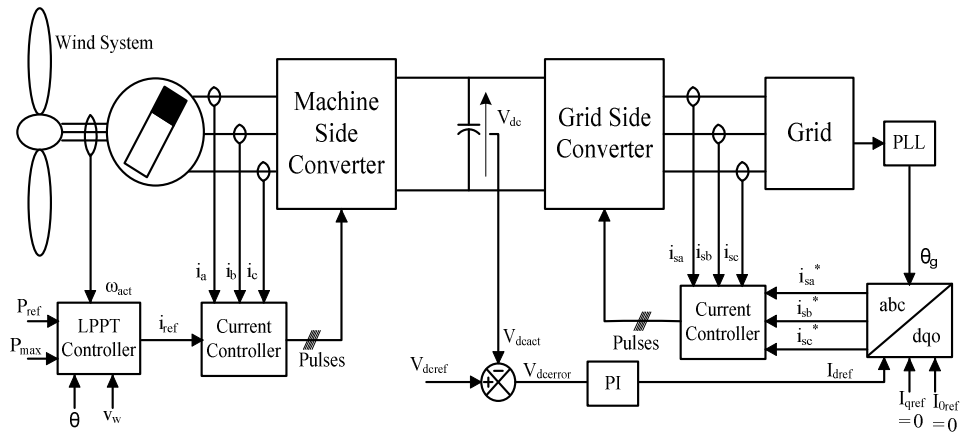


Figure 4.4: Schematic Representation of the Overall control system architecture

Figure 4.4 gives a schematic representation of the overall control system architecture. In this, while the Machine Side Converter is dedicated to extract desired power from

the turbine (P_{ref}), the Grid Side Converter on the other hand is destined to maintain the DC link Voltage at it's reference value (V_{dcref}) and hence attain power balance in the system.

The Machine Side Control and the Grid Side Control are discussed in detail in the subsequent sections.

A. Machine Side Control

This control scheme is dedicated for making the desired power available at the DC link from the turbine. The block diagrammatic representation of the Machine Side Control with various control stages arranged in hierarchical order is shown in Figure 4.5.

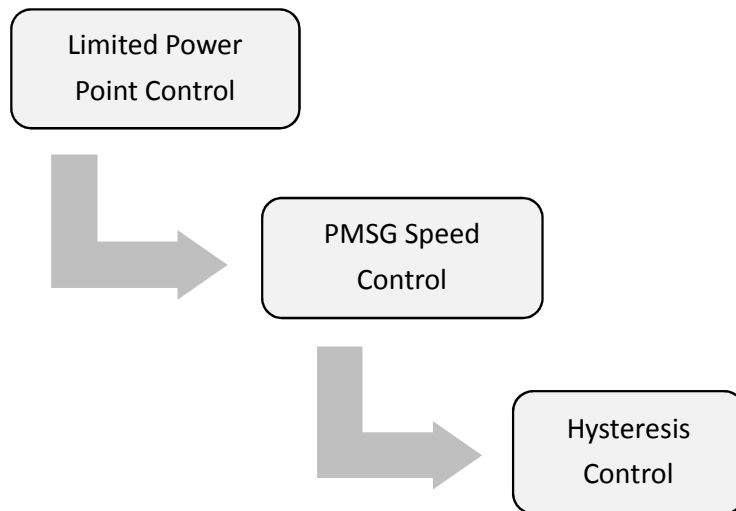


Figure 4.5: Block Diagram Representation of the Machine Side Control

Each of these stages is discussed in detail in the following sub-sections.

- (i) **Limited power point control**

The task of this control stage is to generate speed reference (ω_{ref}) from an equivalent Power reference (P_{ref}). The proposed control technique is based on the characteristics curve between the C_p (power coefficient) and λ (speed tip ratio) for obtaining the required reference speed of the rotor based on the load demand as was discussed in Chapter 3, section. The mathematical relation between P_{ref} (Power Reference/Load Demand) and ω_{ref} (speed of the rotor) required to generate that much Load demand P_{ref} are given by following equation:

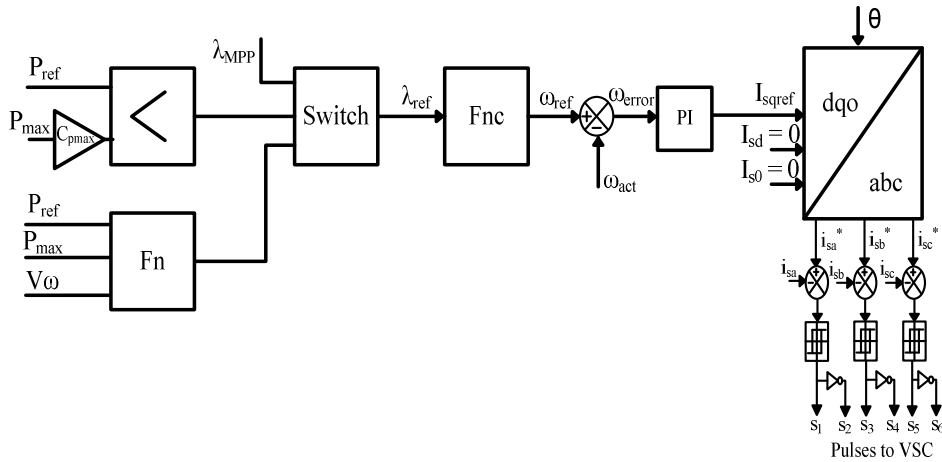
$$C_{pref} = \frac{P_{ref}}{P_{max}} \quad (4.10)$$

$$\text{where, } P_{max} = \frac{1}{2} \rho A v_w^3$$

$$\lambda_{ref} = 12.28 C_p + 2.5 \quad (4.11)$$

$$\omega_{ref} = \frac{\lambda_{ref} v_w}{R} \quad (4.12)$$

Based on the load demand (P_{ref}), power coefficient reference (C_{pref}) for the turbine is generated from equation (4.10). A linear approximation of the curve described by(4.2) has been considered in equation (4.11), so as to simplify the controller design process. An equivalent speed reference (ω_{ref}) for the machine is obtained from equation (4.12) by using the TSR reference (λ_{ref}) which we got from equation(4.11).



* Fn is equation-(4.11)

*Fnc is equation-(4.12)

Figure 4.6: Proposed LPPT controller

The linear approximation of the curve for various wind speeds is shown in figure 4.7.

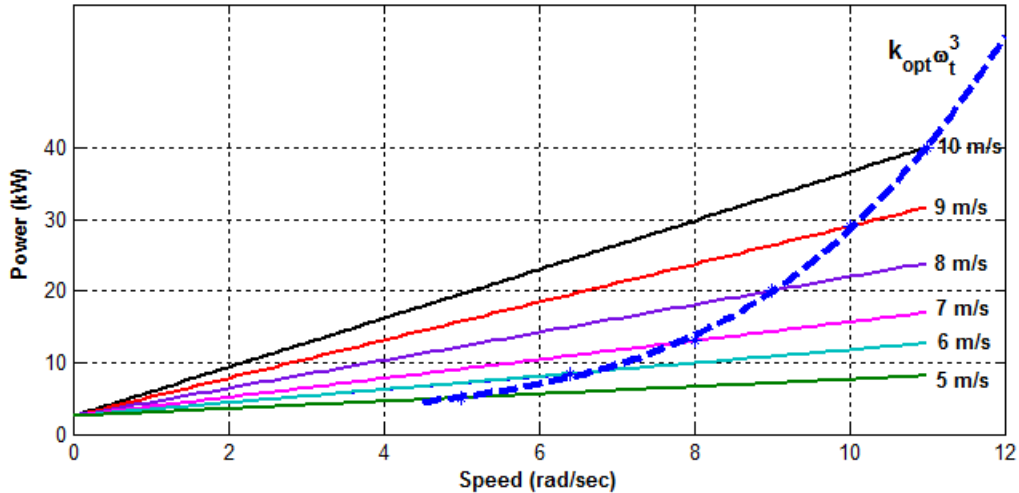


Figure 4.7: Variation of Power with turbine angular speed for different wind speeds

(ii) Speed control of PMSG

Speed Control of PMSG which forms the heart of the Machine Side Control is attained through vector control technique which instead of relying on the steady state relation is based on relation valid for dynamic states. Among the vector control techniques, the most popular one is Field Oriented Control (FOC). In this type of control the motor equations are transformed into a coordinate system that rotates in synchronism with the permanent magnet flux. The FOC uses the shaft speed, obtained by an encoder as outer loop feedback signal and the stator currents as the inner loop feedback signal in the control strategy. An important requirement is that the inner current control loop should possess faster dynamics with respect to input variations than the outer speed control loop. The field oriented Control schematic block is represented in Figure 4.7.

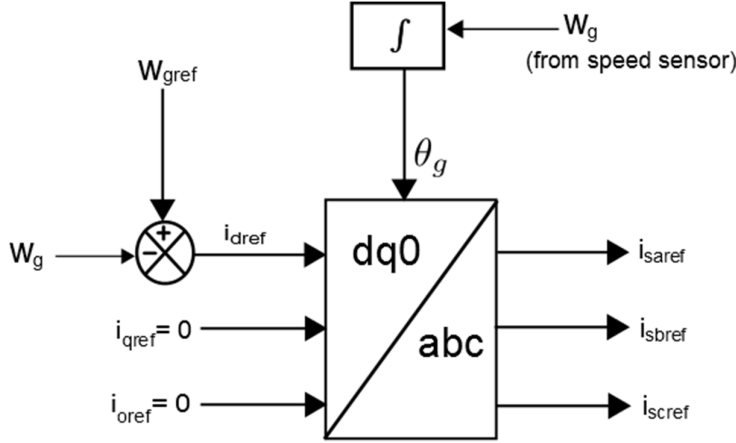


Figure 4.7: PMSG Speed Control

Based on (4.4), the generator rotational speed is governed by the electromagnetic torque and hence the speed control is accomplished by generator torque control. As clear from (4.9), T_e can be directly controlled by q axis current component (i_q). So ultimately the speed control of PMSG boils down to controlling i_q [71].

The rotor speed w_g which is obtained from the speed sensor placed in the feedback loop can then be integrated to obtain rotor position. Knowing the rotor position θ_g the park coordinate transformation is applied to the current references i_{sqref}, i_{sdref} , thus obtaining $i_{saref}, i_{sbref}, i_{scref}$ references in stationary reference frame coordinates.

(iii) Hysteresis Control

Hysteresis current control technique for the Machine Side Converter is dedicated for controlling the power flow through the rectifier circuit. This is one of the easiest implementable control strategies for producing PWM signals. It is nothing but simply on-off control which makes the relay hold either a low state or a high state as shown in figure 4.8. One of the most important advantage of hysteresis control scheme is that it can be used for systems having very fast dynamics.

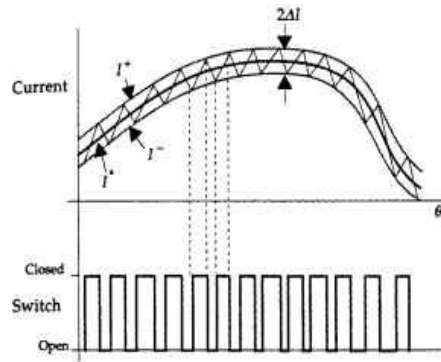


Figure 4.8: PWM signals from Hysteresis control scheme [76]

The reference values thus obtained in stationary reference frame ($i_{saref}, i_{sbref}, i_{scref}$) from the preceding stage are subtracted from the instantaneous values of individual machine phase currents i_{sa}, i_{sb}, i_{sc} and then given to hysteresis controllers operating with a band limit of (-0.1A & 0.1 A) as shown in figure 4.9. The output of the hysteresis control scheme forms the states for the switches which essentially gives the desired PWM signals for the machine side converter by which power balance is attained. The controller parameter are given in Table 4.3

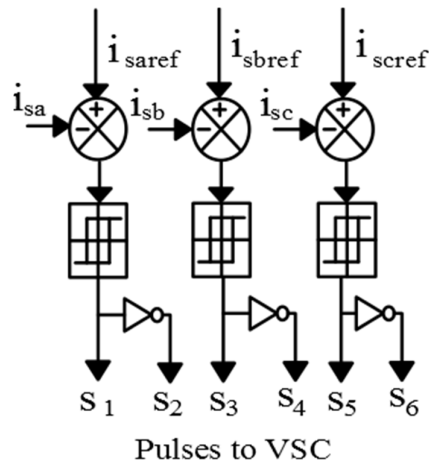


Figure 4.9: Hysteresis control scheme

Table 4.3: LPPT controller parameters

C_{pmax}	0.41
K_p	12
K_i	0.234
Band limit for Hysteresis control	-0.1 to 0.1

B. Grid Side Control

The block diagrammatic representation of the Grid Side Control with various stages arranged in hierarchical order is shown in Figure 4.10 .

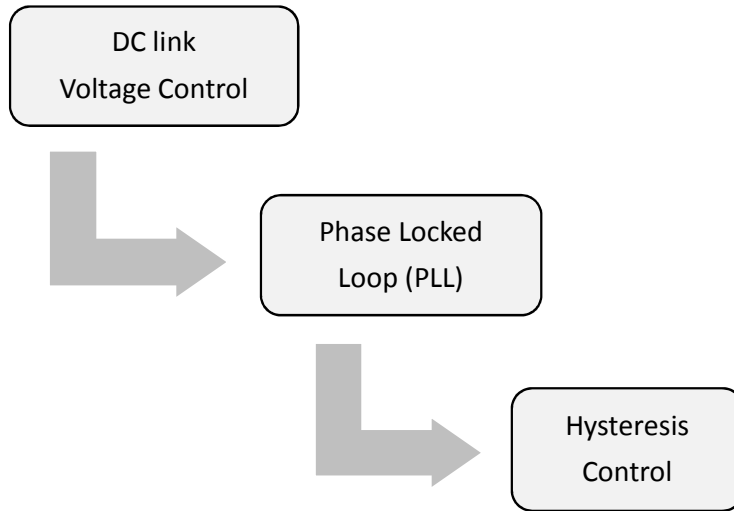


Figure 4.10: Block Diagram Representation of the Grid Side Control

(i) DC Link voltage controller

For satisfactory operation of the inverter, the DC-link voltage should be maintained at a suitable voltage level which is given by the following [46]

$$V_{dc} = \frac{2\sqrt{2}V_{ll}}{\sqrt{3}m} \quad (4.13)$$

where V_{ll} is the line to line voltage of the grid, and m is the modulation index. But due

to the transients on the load side, the dc bus voltage is significantly affected. The sudden removal of load would result in an increase in the dc-link voltage above the reference value whereas a sudden increase in load would result in decrease in dc-link voltage below it's reference value. Therefore, in order to regulate the dc-link voltage closed loop controllers are used. For the system parameters considered in this work, the voltage should be maintained at 700V.

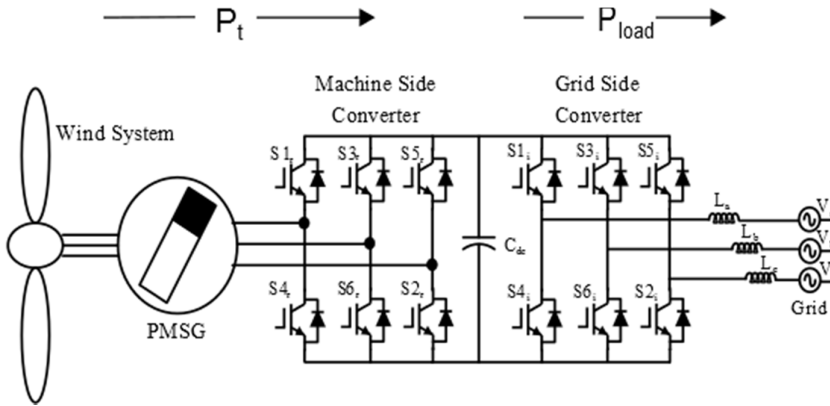


Figure 4.11: Power Flow at DC link

$$C_{dc} \frac{dV_{dc}}{dt} = \frac{P_t}{V_{dc}} - \frac{P_{load}}{V_{dc}} \quad (4.14)$$

As clear from figure 4.11 the dynamics of the DC-Link Voltage is governed by the equation (4.14). It is obvious from(4.14), if we can ensure that V_{dc} is steady $\left(\frac{dV_{dc}}{dt} = 0\right)$ then the power extracted from the turbine will balance the power delivered to the load ($P_t = P_{load}$). On these grounds the control strategy for power balancing via DC link Voltage control is laid.

Reference DC link voltage (V_{dcref}) is compared with actual DC-Link voltage (V_{dc}) and the error signal is given to the PI controller. The output of the PI controller determines current references (I_{dref}) for the VSI which is given by equation(4.15). The conventional DC link Voltage control scheme is shown in figure 4.6. This DC link Voltage control scheme is the heart of inverter control and forms an essential part of the overall control scheme as shown in figure 4.3.

$$I_{dref} = K_p \Delta V_{dc} + K_i \int \Delta V_{dc} dt$$

(4.15)

where, $\Delta V_{dc} = V_{dcref} - V_{dc}$

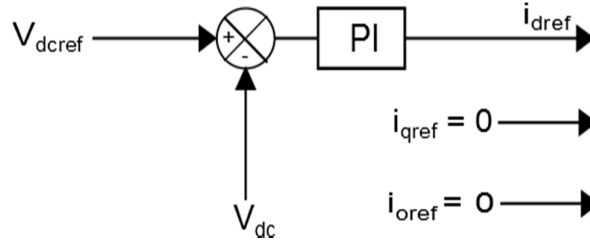


Figure 4.12: Conventional DC link Voltage control scheme

(ii) Phase Locked Loop

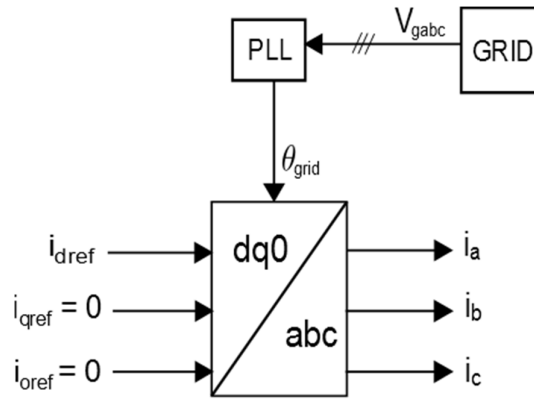


Figure 4.13: Task of PLL

In the grid connected mode of operation of WECS the load voltage magnitude and frequency are dictated by the utility and not the microsource. So, in this regard, load voltage magnitude and frequency control are moot points. But one of the challenging tasks in the grid connected operation of WECS is the synchronization of the DER system with the grid. But since in this work the entire design and analysis exercise is carried out in SRRF (dq frame), with the

help of PLL the complex task of synchronization simply boils down to tracking of dc command signals as shown in figure 4.13. Even we can achieve Unity Power Factor Control by using PLL. The angle of the grid voltage is estimated and provided by the PLL. Using this angle information the final I_{dref} obtained from equation (4.15) along with I_{qref} and I_{oref} set to zero are given to dqo-abc transformation block from which we obtain the current references in abc frame (natural reference frame) using (4.16).

$$(4.16) \quad \begin{bmatrix} I_{saref} \\ I_{sbref} \\ I_{scref} \end{bmatrix} = \frac{3}{2} \begin{bmatrix} \cos(\theta) & \cos(\theta - \frac{2\Pi}{3}) & \cos(\theta + \frac{2\Pi}{3}) \\ \sin(\theta) & \sin(\theta - \frac{2\Pi}{3}) & \sin(\theta + \frac{2\Pi}{3}) \\ \frac{1}{2} & \frac{1}{2} & \frac{1}{2} \end{bmatrix}^{-1} \begin{bmatrix} I_{dref} \\ I_{qref} \\ I_{oref} \end{bmatrix}$$

(iii) Hysteresis Control

Hysteresis current control technique for the Grid Side Converter is used to control the power flow through the inverter. The reference value of currents in natural reference frame ($i_{garef}, i_{gbref}, i_{gcref}$) as obtained from the PLL are subtracted from the instantaneous values of individual phase currents i_{ga}, i_{gb}, i_{gc} and then given to hysteresis controllers operating with a band limit of (-0.1A & 0.1 A). The output of the hysteresis control scheme forms the states for the switches which essentially gives the desired PWM signals for the grid side converter by which power balance is attained.

Table 4.4: DC link voltage and hysteresis controller parameters

K_p	2
K_i	0.1
Band limit for Hysteresis control	-0.1 to 0.1

4.2 Simulation and Results

The proposed wind energy conversion system was designed and modelled in MATLAB Simulink using Simpowersystem blocks. To demonstrate effectiveness and applicability of the proposed control strategy, simulations were carried out for various modes of operation. The simulation cases considered here are chosen to demonstrate the usefulness of the control algorithm under varying load demand as well as varying climate conditions.

Case 1: Sudden change in load demand

First simulations were carried out for variable load demand during power sufficient mode. Initially the WECS system was operating under steady state condition with load demand (P_{ref}) of 10 kW when wind speed is 9 m/sec. At this wind speed the WECS can generate a maximum power (P_{max}) of 29 kW, indicating that the proposed control technique will be operating in power sufficient mode. At time $t=0.5$ sec, a step change from 10 kW to 15 kW in P_{ref} is given. Simulation results pertaining to the power delivered to the load (P_{load}) from the wind turbine, V_{dc} dc link voltage, w_{gref} reference speed of generator in rads/sec, w_g actual speed of the generator, and inverter output current (i_{Labc}) waveforms are shown in Figure 4.14. It can be observed from the waveforms that the proposed controller responds very quickly to the set point changes and hence achieves power balance.

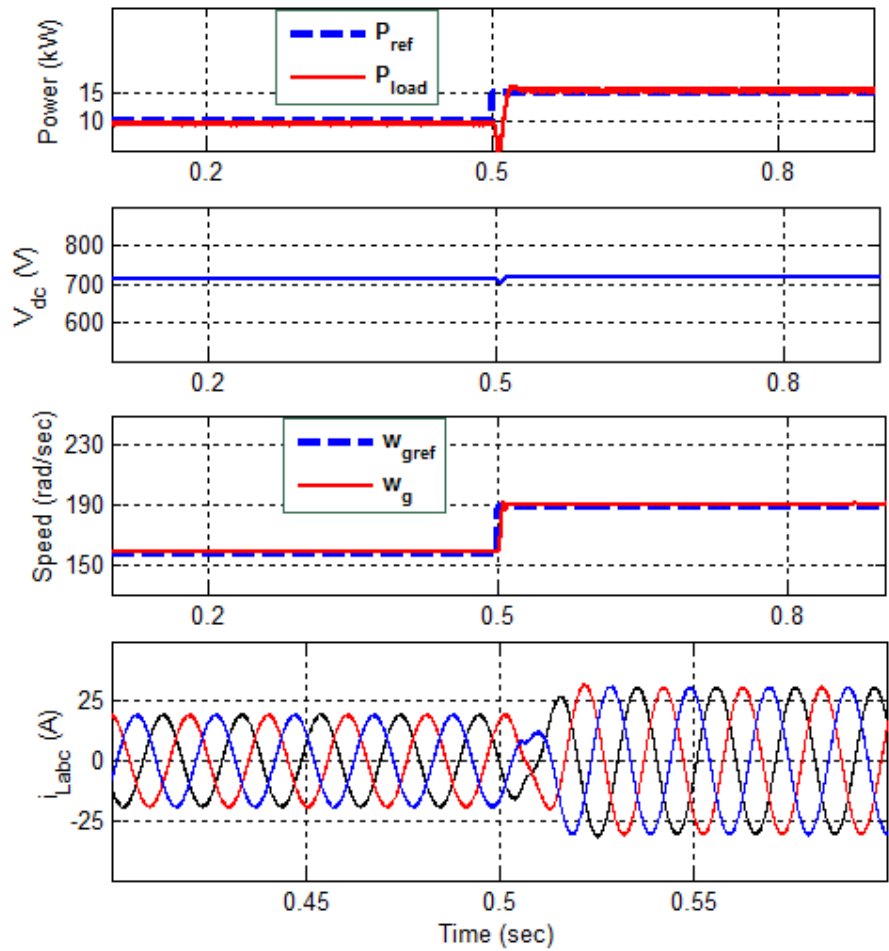


Figure 4.14: Response to a step change in load demand

Case 2: Operation in MPP mode

The system is assumed to be initially operating under steady state condition with load demand (P_{ref}) of 15 kW when wind speed is 9 m/sec .At 0.5 sec P_{ref} was suddenly changed from 15 kW to 35 kW .As stated earlier, for wind speed of 9 m/sec, P_{max} is 29 kw. Thus the purpose of this simulation case is to demonstrate ability of the controller to move from power sufficient mode to power insufficient mode dynamically. Figure 4.15 shows response of the system to sudden increase in load demand and its effect on Power delivered to the load from the WT (P_{load}), dc-link

Voltage (V_{dc}), the generator speed w_g and i_{Labc} . As can be seen the controller successfully switches from power sufficient mode to power insufficient mode and the system starts operating at MPP. As the power demand is more than the maximum that can be delivered from the turbine P_t , the load network will draw remaining 6 kW from the grid. The settling time was found to be about 8ms.

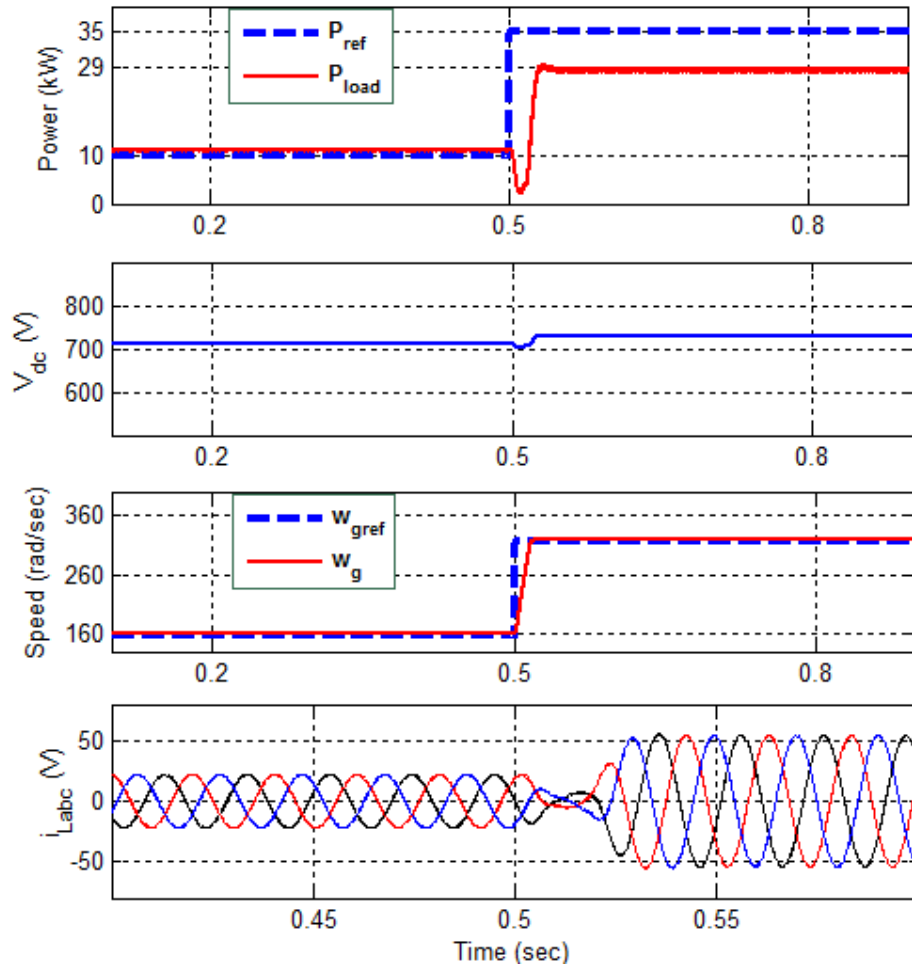


Figure: 4.15: Operation under insufficient power condition

Case 3: Sudden change in climatic conditions

WECS systems often encounter sudden climatic changes, which may sometimes lead to system instability. In this case simulations were carried out to study the effects of varying weather conditions by changing wind speed. The system is initially operating

at $P_{ref}=15$ kW, with wind speed 9 m/sec. At $t=0.5$ sec the wind speed is changed from 9m/sec to 8 m/sec. As can be seen from Figure 4.16, the controller adjusts the speed reference in such a manner so that even in case of wind speed variation we are able to attain power balance in the system.

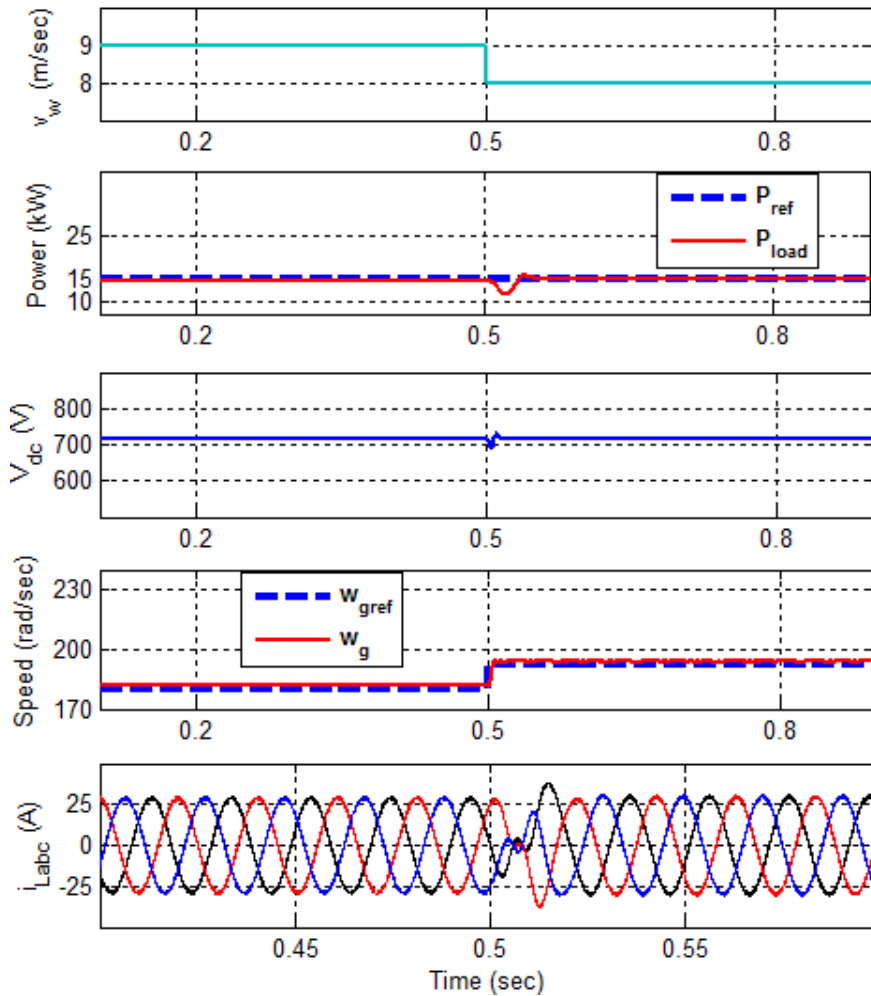


Figure 4.16: Operation under sudden climate change condition

4.3 Conclusion

A power balancing limited power point control strategy is proposed for grid-connected WEC systems. The main advantage of the proposed methodology is that back-up energy storage devices are not required for maintaining power balance and constant

DC line voltage. Elimination of battery banks eliminates its maintenance and cost factor, this will improve overall WECS power economy. The proposed limited power point control algorithm can operate the controlled converter in both the modes i.e. at maximum power point (power insufficient) and limited power point (power sufficient). The performance of the limited power point controller demonstrated its effectiveness and applicability for grid-connected WECS under varying load and weather conditions.

Chapter 5

Controlled Power Point Tracking for Autonomous Operation of WECS

As discussed in the Chapter-2, the various topologies of the WECSs, the control requirements in islanded mode operation of WECS. In this chapter a full converter turbine that uses Permanent magnet Synchronous Generator (PMSG) as its generator with battery at DC bus is studied and simulated. In this chapter, we will discuss in detail the wind power energy conversion system configuration, design, proposed control scheme for controlled power point tracking for standalone WECS using speed control of Permanent Magnet Synchronous Generator (PMSG).

5.1 Wind power configuration

The system description, system modeling and proposed control scheme for controlled power point tracking is presented in this section.

5.1.1 System description

A back to back AC/DC/AC topology is implemented for interfacing WECS having a peak power capacity of 29kW with the turbine and generator parameters as listed in Table 4.2 to the distribution network with battery support of rated capacity 7A-hr and nominal voltage of 1100V at the dc link as shown in Figure 5.1. The first stage consists of a controlled rectifier. The controlled rectifier operates in two regions i) when WECS output power is sufficient to supply the total load demand and, ii) when WECS output power is insufficient to supply the load demand and the WECS is at

maximum power point. The control technique used for the controlled rectifier to operate in both the regions is speed control of PMSG through vector control. A three-leg two-level VSI is used for transferring power from WECS to the point of common coupling (PCC), maintaining the load voltage magnitude, frequency (ω) and to meet the reactive power requirement, if any. The proposed control technique for controlled rectifier and the current control of inverter are independent of each other. A second order low pass LC filter with a damping resistance R has been considered to filter out high frequency switching harmonics sitting on top of fundamental voltage component (50 Hz) from the inverter output. The filter parameters are given in Table 1.

Table 5.1: Filter Parameters

R (Damping resistance)	0.3 Ω
L	1.474 mH
C	429.49 μ F

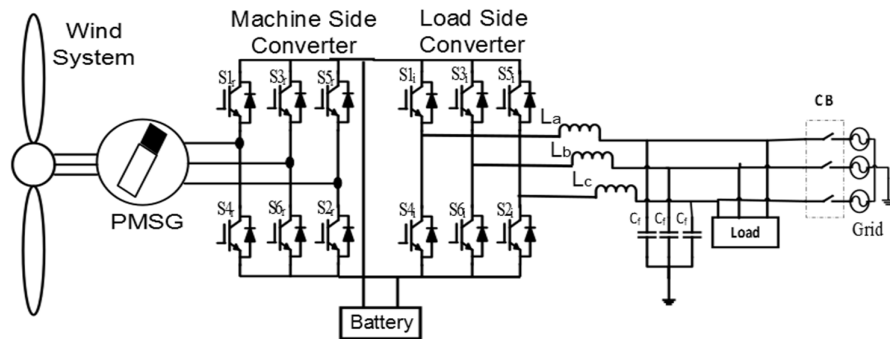


Figure 5.1: A schematic representation of system

5.1.2 System Modelling

A. Modeling of wind turbine with PMSG

The same turbine model as was discussed in Chapter 4, Section 4.1.2(A) has been considered here also.

B. PMSG model

The same Dynamic model as was described for Surface mounted PMSGs in Chapter 4 , Section 4.1.2(B) has been considered in this work of study also.

C. VSC Modelling

The VSC model has been defined in dq frame wherein according to the adopted convention the d axis leads the stationary α axis in anticlockwise direction by an angle ρ [75,21].

The dynamics of PCC/load voltage is described by the space-phasor equation as:

$$C_f \frac{d\vec{v}_s}{dt} = \vec{i} - \vec{i}_L \quad (5.1)$$

Substituting $\vec{v}_s = (v_{sd} + jv_{sq})e^{j\rho}$ in (5.1) and splitting into real and imaginary parts we get:

$$C_f \frac{dv_{sd}}{dt} = (C_f \omega)v_{sq} + i_d - i_{Ld} \quad (5.2)$$

$$C_f \frac{dv_{sq}}{dt} = -(C_f \omega)v_{sd} + i_q - i_{Lq} \quad (5.3)$$

$$\text{where, } \omega = \frac{d\rho}{dt}$$

The dynamics of the inductor current is described by the space-phasor equation as:

$$L \frac{d\vec{i}}{dt} = -R\vec{i} + \vec{v}_t - \vec{v}_s \quad (5.4)$$

Substituting $\vec{i} = (i_d + ji_q)e^{j\rho}$ in (5.4) and splitting into real and imaginary parts we get:

$$L \frac{di_d}{dt} = (L\omega)i_q - Ri_d + v_{td} - v_{sd} \quad (5.5)$$

$$L \frac{di_q}{dt} = -(L\omega)i_d - Ri_q + v_{tq} - v_{sq} \quad (5.6)$$

The following equations represents the VSC model in dq frame:

$$v_{td} = m_d \frac{V_{DC}}{2} \quad (5.7)$$

$$v_{tq} = m_q \frac{V_{DC}}{2} \quad (5.8)$$

5.1.3 Control structure

The block diagrammatic representation of the proposed control strategy for LPPT as well as MPPT from WECS is shown in figure

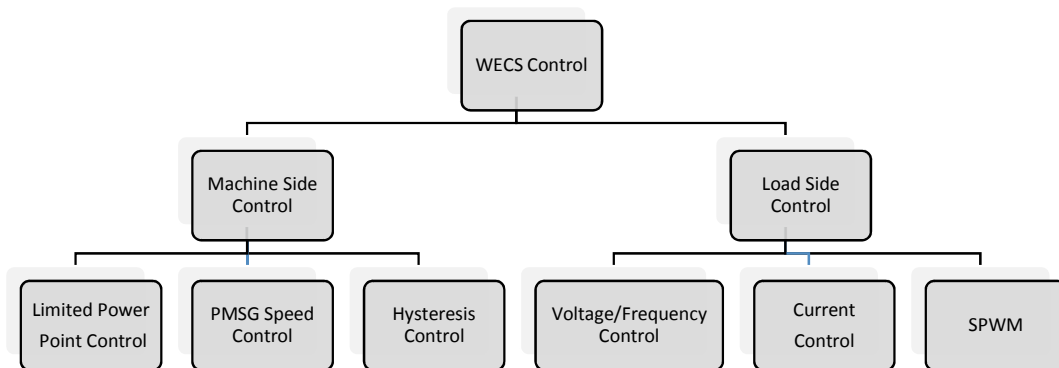


Figure 5.2: Block Diagram Representation of the overall control system

The overall system control has been bifurcated into Machine Side Control and Load Side Control. While the Machine Side Control comprises of the following control stages:

- i. Limited Power Point Control
- ii. PMSG Speed Control
- iii. Hysteresis Control

The Load Side Control on the other hand encompasses the following enclosures:

- i. Voltage/Frequency Control
- ii. Current Control
- iii. Sinusoidal Pulse Width Modulation (SPWM)

While the Machine Side and the Load Side Control are independent of each other, each of the sub-heads listed under them as shown in figure talk within well-defined boundaries.

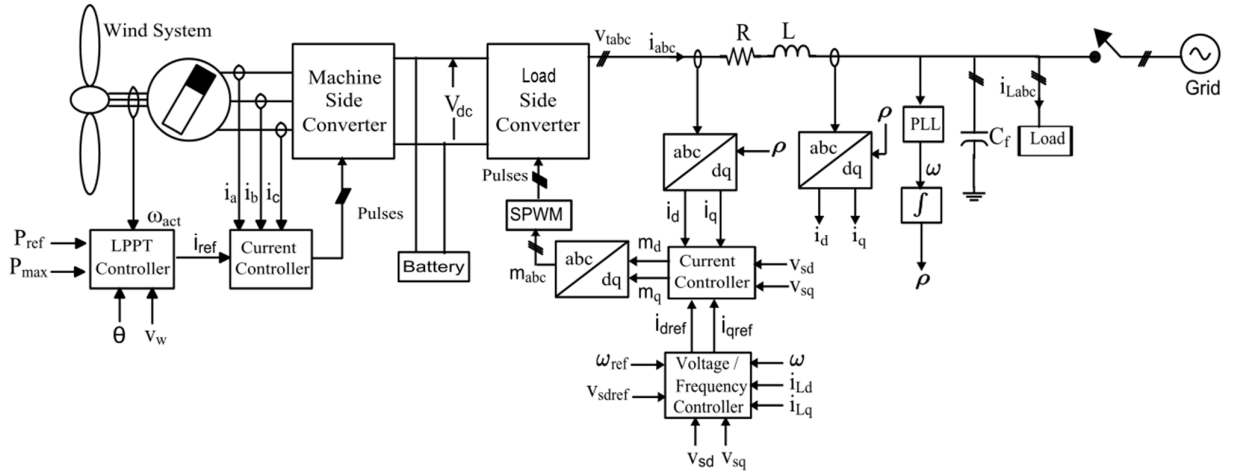


Figure 5.3: Schematic Representation of the Overall control system architecture

Figure 5.3 gives a schematic representation of the overall control system architecture. In this, while the Machine Side Converter is dedicated to extract desired power from the turbine (P_{ref}), the Load Side Converter on the other hand is destined to control the load voltage magnitude, frequency via inner current regulation loop and hence attain power balance in the system while maintaining the desired load voltage profile. The Machine Side Control and the Load Side Control are discussed in detail in the subsequent sections.

A. Machine Side Control

The machine side control for standalone WECS remains same as was described in Chapter 4, Section 4.1.3(A).

B. Load Side Control

The block diagrammatic representation of the Grid Side Control with various stages arranged in hierarchical order is shown in Figure 5.4.

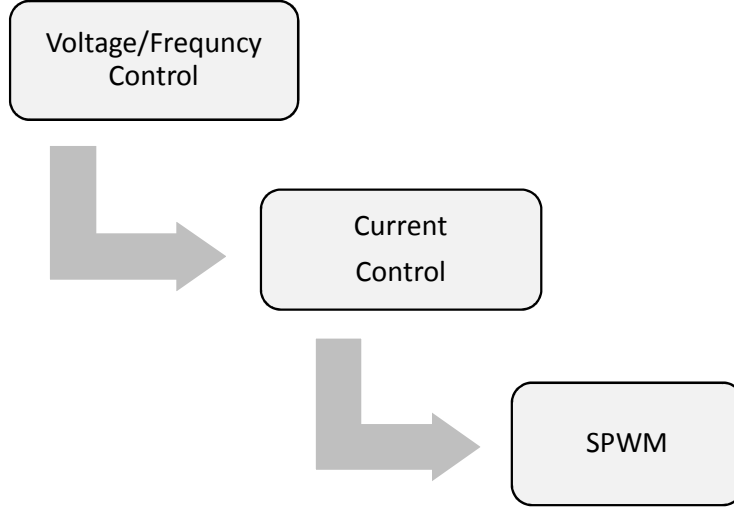


Figure 5.4: Block Diagram Representation of the Load Side Control

(i) Voltage/Frequency control

The Voltage/Frequency regulation is exercised in dq frame. By making the q component of voltage space phasor (\vec{v}_s) i.e. v_{sq} to zero, the regulation of voltage magnitude boils down to control of v_{sd} at its reference value (v_{sdref}) while the control of frequency (ω) at its set point value (ω_{ref}) is attained by forcing v_{sq} to zero. Hence, the amplitude of v_{sabc} i.e. $\sqrt{v_{sd}^2 + v_{sq}^2}$ is predominantly determined by v_{sd} and therefore v_{sdref} is set to \hat{v}_{sn} i.e. the nominal peak value of PCC line-to-neutral voltage which effectively serves as the set point for the amplitude of the DER system terminal voltage while v_{sqref} is issued by another control loop that regulates the frequency (ω) of v_{sabc} . However the control of v_{sd} and v_{sq} is not a straightforward task as [41]:

- a) The open loop control plant (with (i_{dref}, i_{qref}) as inputs and (v_{sd}, v_{sq}) as outputs) is in itself non-linear ,

- b) The dynamics of v_{sd} and v_{sq} are coupled and thus the system represented by the equations ((5.2),(5.3)) is a multi-input multi-output (MIMO) system
- c) The load side dynamics is in general highly inter-coupled, of high dynamic order, non-linear, with uncertain and time-varying parameters.

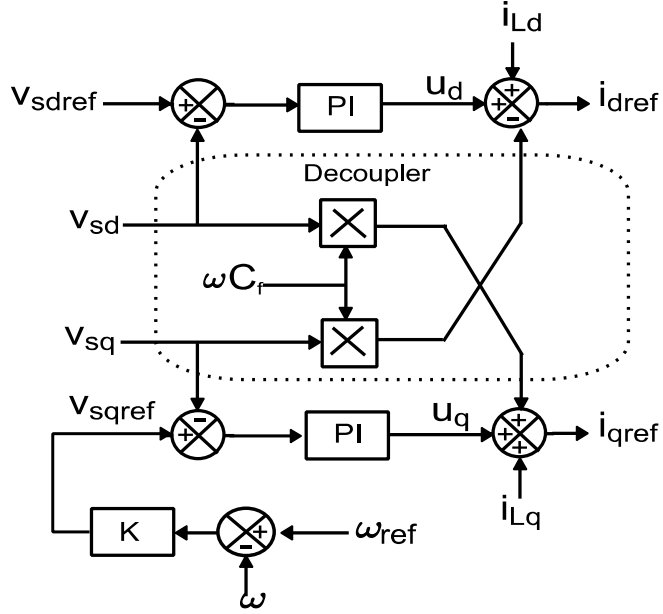


Figure 5.5: Voltage/Frequency

Control Scheme

The aforementioned problems are tackled by cashing on the classical control techniques available at hand thereby enabling us to control v_{sd} and v_{sq} in a linear and independent fashion. This is done in the following manner:

- a) The coupling between v_{sd} and v_{sq} is eliminated by a decoupling feed-forward compensation so as to make the dynamics of v_{sd} and v_{sq} independent of each other.
- b) The measures of i_{Ld} and i_{Lq} are fed as two other feed forward terms in the control process to mitigate the impact of load side dynamics on v_{sd} and v_{sq} .

Therefore the compensated system performs under all load conditions almost the same way as the the uncompensated system would behave under no-load condition [63,64].

Hence the control scheme of fig (4(a)) enables independent control of v_{sd} and v_{sq} by i_{dref} and i_{qref} respectively. The parameters for the voltage controller (P_v, I_v) and frequency controller (K) as obtained by using the MATLAB SISO design tool are given in table 5.2.

Table 5.2: Controller Parameters for Voltage/Frequency Control Scheme

P_v	0.264
I_v	9.633
K	120

(ii) Current Control Scheme

The current control scheme forms the innermost and the most basic block of the DER system control. It's function is to regulate i_d and i_q i.e. the d and the q axis components of VSC ac-side current (i_{abc}) by means of PWM switching strategy.

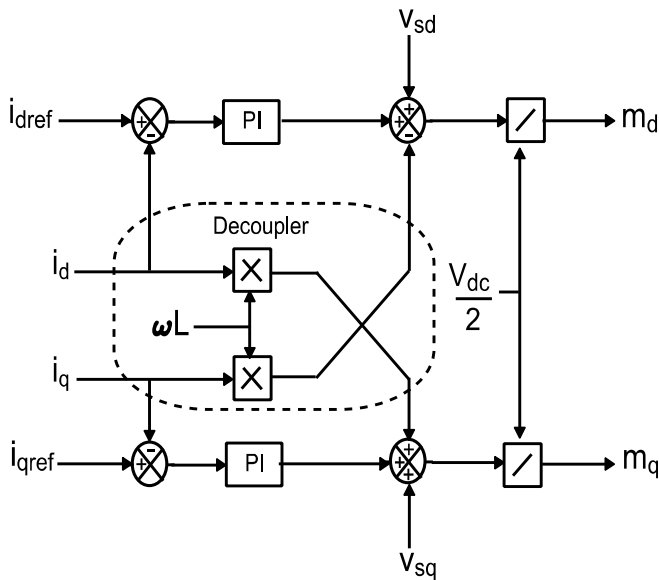


Figure 5.6: Current control scheme

As clear from ((5.5),(5.6)) which describes the dynamics of i_d and i_q with (i_d, i_q) as state variables, (v_{id}, v_{iq}) as control inputs, (v_{sd}, v_{sq}) as disturbance inputs, the dynamics i_d and i_q are coupled. The problem is tackled in a similar fashion as was done in Voltage/Frequency Control. i_d and i_q are decoupled by means of a decoupling feed forward compensation strategy and the impact of the disturbance inputs (v_{sd}, v_{sq}) on the dynamics of i_d and i_q is mitigated by adding another feed forward term in the control loop. Also the control signals issued by the d- and q- axis compensators are divided by the feed forward term $(V_{dc}/2)$ so as to compensate for the converter voltage gain. Hence the modulating signals in dq frame (m_d, m_q) which essentially are the control gears for attaining the desired performance objectives are given as:

$$m_d = \frac{2}{V_{DC}}(u_d - L\omega i_q + v_{sd}) \quad (5.9)$$

$$m_q = \frac{2}{V_{DC}}(u_q + L\omega i_d + v_{sq}) \quad (5.10)$$

Where, u_d and u_q are two new control inputs. Substituting for m_d and m_q in ((5.7),(5.8)) respectively and thereafter substituting the derived values of v_{sd} and v_{sq} in ((5.5),(5.6)), we deduce

$$L \frac{di_d}{dt} = -Ri_d + u_d \quad (5.11)$$

$$L \frac{di_q}{dt} = -Ri_q + u_q \quad (5.12)$$

((5.11),(5.12)) describes two decoupled, first-order, linear systems and hence i_d and i_q can be independently controlled by u_d and u_q respectively [21]. Another important feature of current controller is its inherent capability to limit the DR unit output current [61,65].

Finally m_d and m_q are transformed to m_a, m_b, m_c using the transformation angle as obtained from PLL which serves as inputs to SPWM scheme and generates the desired switching pulses for the inverter. The Laplace Transform of equations (5.11) and

(5.12) gives the plant transfer function for d axis and q axis as described by equations (5.13) and (5.14) respectively.

$$G_d(s) = \frac{i_d}{u_d}(s) = \frac{1}{Ls + R} \quad (5.13)$$

$$G_q(s) = \frac{i_q}{u_q}(s) = \frac{1}{Ls + R} \quad (5.14)$$

Since equations (5.13) and (5.14) describes first order lag with inputs as dc quantities, therefore a PI will suffice to provide satisfactory performance, i.e., fast dynamics and a zero SSE.

Since the plant, the type of set point input as well as the disturbance for the d and q axis systems remains same, the controller parameters for the two systems will be identical. Hence the controller parameters derived for the d axis plant will be same for q axis also.

The closed loop system for the d axis having plant $G_d(s)$ and a PI controller $K_d(s)$ having parameters as (P_I, I_I) is show in figure 5.7. While figure 5.8 gives the closed loop representation for the plant $G_q(s)$ with controller $K_q(s)$ having the controller parameters same as that for the d axis.

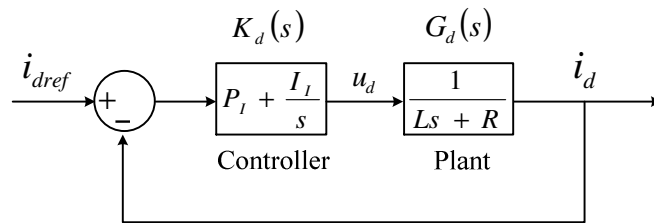


Figure 5.7: d-axis closed loop current controller

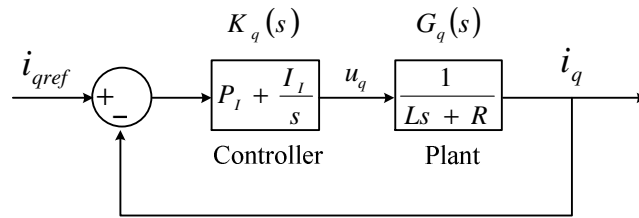


Figure 5.8: q-axis closed loop current controller

The closed loop transfer function for the d axis current controller is given by :

$$\frac{i_d}{i_{dref}}(s) = \frac{l(s)}{1+l(s)} \quad (5.15)$$

where, the loop gain $l(s) = K_d(s)G_d(s)$

$$(5.16)$$

Substituting for $K_d(s) = \frac{sP_I + I_I}{s}$ and the value of $G_d(s)$ from (5.13) in equation (5.16) the loop gain modifies to:

$$l(s) = \frac{P_I}{Ls} \frac{\left(s + \frac{I_I}{P_I}\right)}{\left(s + \frac{R}{L}\right)} \quad (5.17)$$

By cancelling the plant pole ($s = -R/L$) with the controller zero ($s = -I_I/P_I$) the loop gain reduces to:

$$l(s) = \frac{P_I}{Ls} \quad (5.18)$$

Substituting the value of $l(s)$ from (5.18) in equation (5.15) we obtain the closed loop transfer function as:

$$\frac{I_d}{I_{dref}}(s) = \frac{1}{\left(\frac{L}{P_I}\right)s + 1} \quad (5.19)$$

Equation (5.19) describes a first order transfer function which can be written in standard first order lag form as:

$$\frac{I_d}{I_{dref}}(s) = \frac{1}{\tau s + 1} \quad (5.20)$$

$$\text{where, } \tau = \frac{L}{P_I}$$

τ is a design parameter whose value is optimally chosen s.t. it is small enough for achieving fast current-control response but adequately large so as to have smaller closed loop bandwidth ($BW = 1/\tau$) requirement [21]. In this work we have chosen the

switching frequency (f_s) of inverter to be 2000 Hz and BW to be nearly 10 times smaller than $\omega_s = 2\pi f_s$. The controller parameters as obtained from (22) and by using the pole-zero cancellation relation i.e. $R/L = I_l / P_l$ are listed in table 5.3 .

Table 5.3: Controller Parameters for Current Control Scheme

τ	1ms
P_l	1.474
I_l	300

(iii) SPWM

Based on the modulating signal received from the previous stage the SPWM technique compares it with a carrier of frequency (f_s) 2000Hz and generates the desired switching pulses for the inverter.

5.1.4 Filter Design

A second order LC filter with a series resistance has been considered here for filtering the high frequency switching harmonics sitting on top of fundamental voltage component (50 Hz). The resistance serves as an active damping mechanism and helps in suppressing the high frequency oscillations and hence improves the system response. A single phase equivalent of the three phase system shown in figure 5.9 has been considered. Since the system is assumed to be balanced, hence the filter values derived for single phase will be valid for the other phases also.

Consider the phase a after the inverter ac terminal as shown in figure

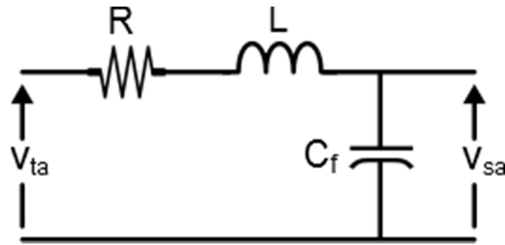


Figure 5.9: Current control scheme

The Voltage transfer function for the system described by figure is:

$$\frac{v_{sa}}{v_{ta}}(s) = \frac{1}{LC_f} \frac{1}{s^2 + \frac{R}{L}s + \frac{1}{LC_f}} \quad (5.21)$$

The natural frequency (ω_n) and damping factor (ξ) for the second order transfer function described by (5.21) are $\frac{1}{\sqrt{LC_f}}$ and $\frac{R}{2} \sqrt{\frac{C_f}{L}}$ respectively.

Applying loop rule for the mesh shown in figure yields:

$$v_{ta} - v_{sa} = iR + L \frac{di}{dt} \quad (5.22)$$

The design parameters for the filter considered here with the ripple current to be 10% of the rated current (42A) are listed in Table.

Table 5.4: Filter Design Considerations

Δi	4.2 A
Voltage drop	20 V
ξ	0.4

With the aforementioned design considerations and by using the equation (5.22) and the expression for damping factor (ξ), the filter parameters (R, L, C_f) are obtained and are listed in Table 5.1..

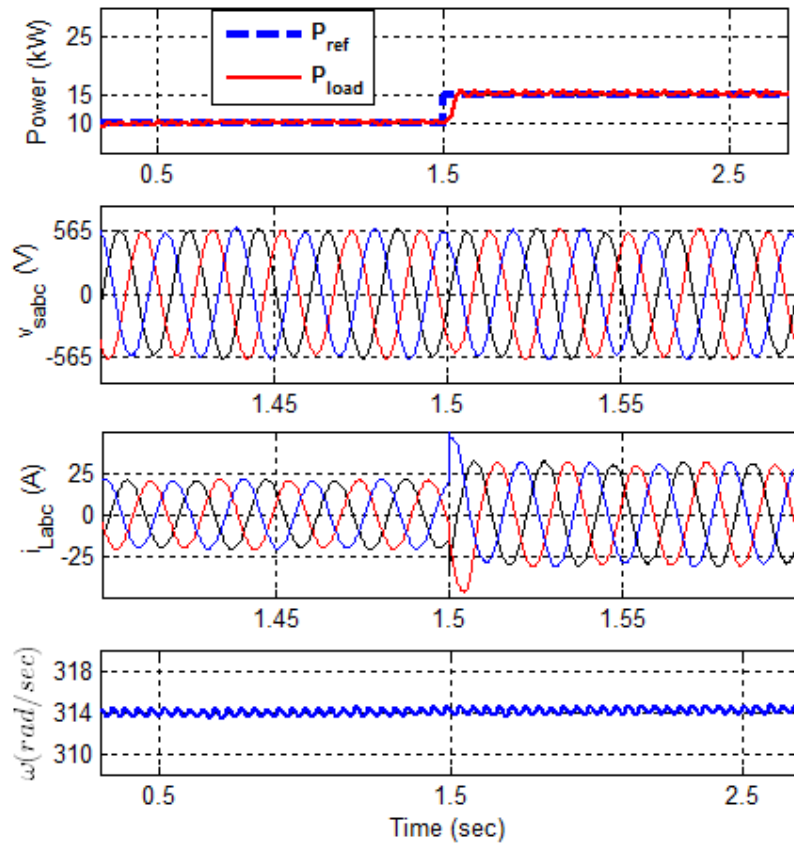
5.2 Simulation and Results

The proposed wind energy conversion system was designed and modelled in MATLAB Simulink using Simpowersystem blocks. To demonstrate effectiveness and applicability of the proposed control strategy, simulations were carried out for various modes of operation. The simulation cases considered here are chosen to demonstrate the usefulness of the control algorithm under varying load demand as well as varying climate conditions

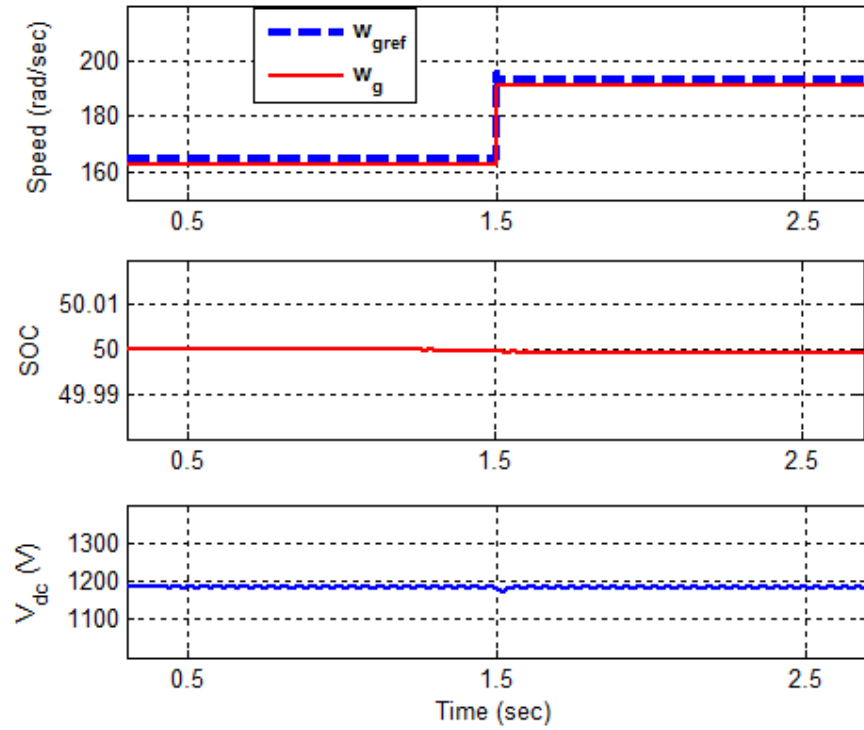
Case 1: Sudden change in load demand

First simulations were carried out for variable load demand during power sufficient mode. Initially the WECS system was operating under steady state condition with

load demand (P_{ref}) of 10 kW when wind speed is 9 m/sec. At this wind speed the WECS can generate a maximum power (P_{max}) of 29 kW, indicating that the proposed control technique will be operating in power sufficient mode. At time $t=1.5$ sec, a step change from 10 kW to 15 kW in P_{ref} is given. Simulation results pertaining to the power delivered to the load (P_{load}) from the wind turbine, V_{dc} dc link voltage, w_{gref} reference speed of generator in rads/sec, w_g actual speed of the generator, and the load current (i_{Labc}) waveforms are shown in Figure 5.10. It can be observed from the waveforms that the proposed controller responds very quickly to the set point changes and hence achieves power balance.



(a)

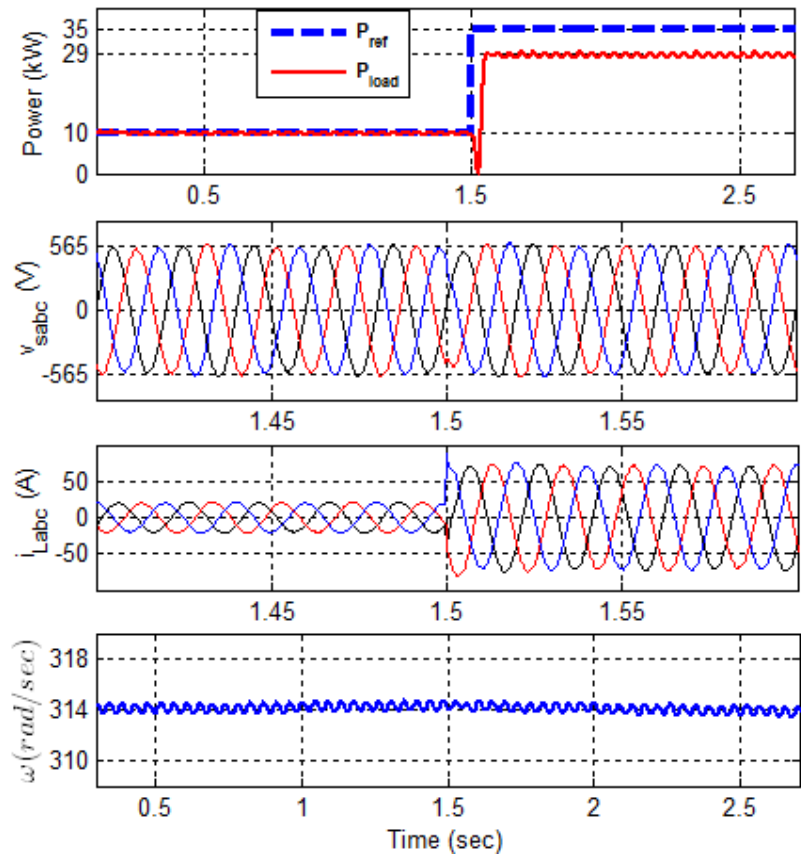


(b)

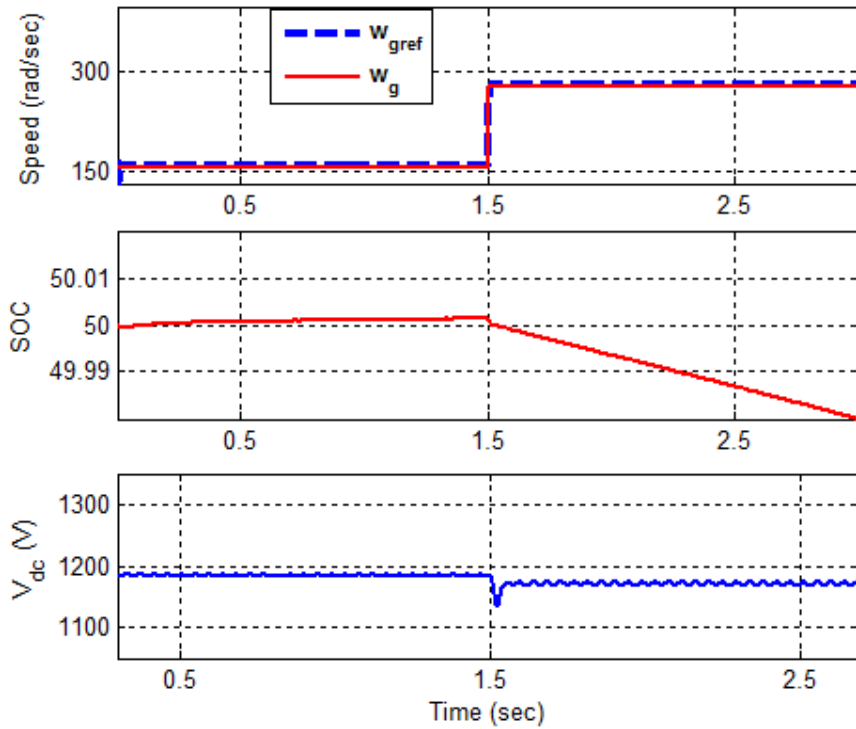
Figure: 5.10 Response to a step change in load demand

Case 2: Operation in MPP mode

The system is assumed to be initially operating under steady state condition with load demand (P_{ref}) of 15 kW when wind speed is 9 m/sec. At 1.5 sec P_{ref} was suddenly changed from 15 kW to 35 kW. As stated earlier, for wind speed of 9 m/sec, P_{max} is 29 kw. Thus the purpose of this simulation case is to demonstrate ability of the controller to move from power sufficient mode to power insufficient mode dynamically. Figure 5.11 shows response of the system to sudden increase in load demand and its effect on Power delivered to the load from the WT (P_{load}), dc-link Voltage (V_{dc}), the generator speed w_g and i_{Labc} which is the net current injection to the load. As can be seen the controller successfully switches from power sufficient mode to power insufficient mode and the system starts operating at MPP. As the power demand is more than the maximum that can be delivered from the turbine, the load network will draw remaining 6 kW from the grid.



(a)

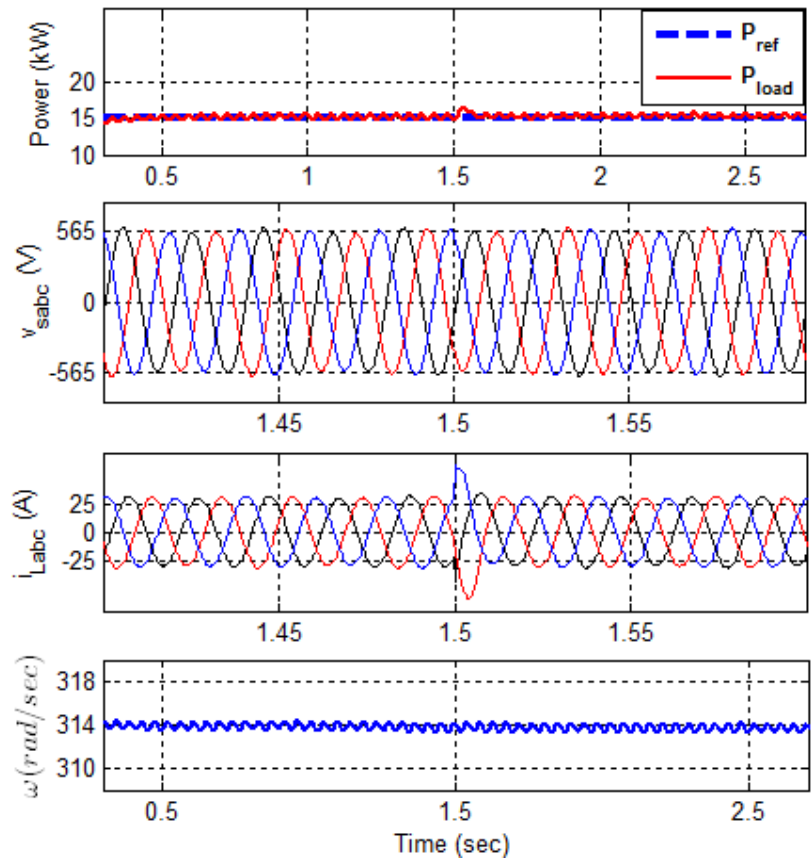


(b)

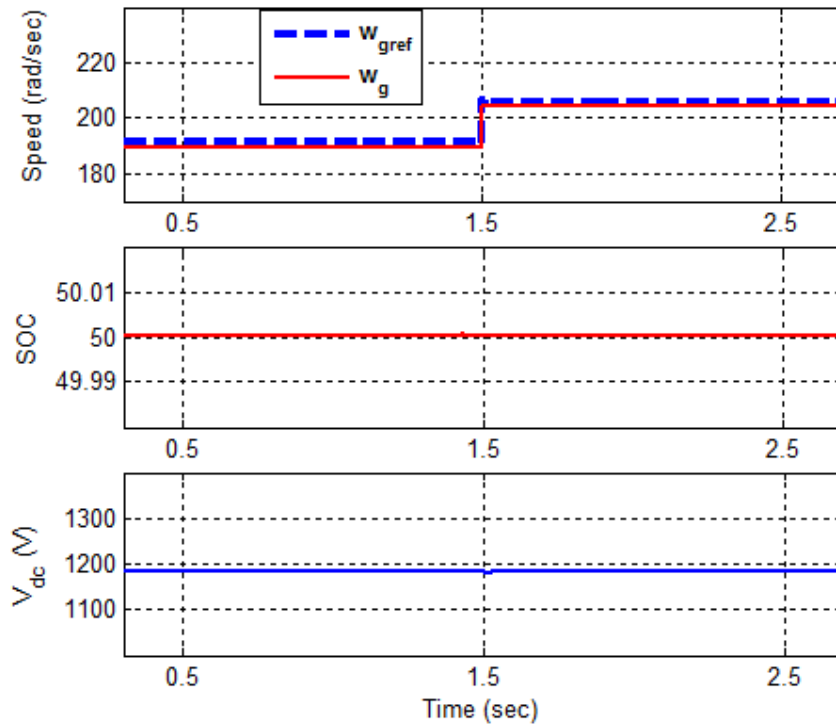
Figure 5.11 : (a,b) Operation under insufficient power condition

Case 3: Sudden change in climatic conditions

WECS systems often encounter sudden climatic changes, which may sometimes lead to system instability. In this case simulations were carried out to study the effects of varying weather conditions by changing wind speed. The system is initially operating at $P_{ref}=15$ kW, with wind speed 9 m/sec. At $t=1.5$ sec the wind speed is changed from 9m/sec to 8 m/sec. As can be seen from Figure 5.12, the controller adjusts the speed reference in such a manner so that even in case of wind speed variation we are able to attain power balance in the system. The settling time for the system was found to be about 6ms.



(a)



(b)

Figure 5.12: (a,b) Operation under sudden climate change condition

5.3 Conclusion

A power balancing control strategy for islanded mode operation of WECS is proposed which takes care of maintaining the voltage and frequency at the load side which is one of the most critical task in isolated operation of DR unit in a microgrid framework. The usage of batteries in the system has been minimized and is been limited for handling transient stability and reliability issues. The proposed limited power point control algorithm can operate the controlled converter in both the modes i.e. at maximum power point (power insufficient) and limited power point (power sufficient). The performance of the proposed control strategy demonstrated its effectiveness and applicability for standalone operation of WECSs under varying load and weather conditions.

Chapter 6

Stability Analysis for Grid Side Converter in grid connected WECS

As clear from the simulation results depicted in Chapter 4 that the grid side system exhibits inverse response characteristics. In this Chapter the finding is validated by performing stability analysis for the grid side system and finding a transfer function which relates voltage at the dc-link to the power delivered to the load.

6.1 Mathematical Analysis

The three phase structure for the connection between inverter terminal end and grid is shown in figure 6.1 [21].

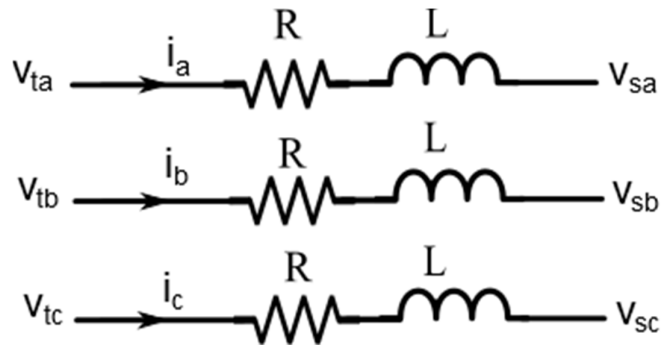


Figure 6.1 Three phase structure for connection between inverter terminal and grid

The dynamics of the dc-link voltage for the system shown in Figure 4.11 is dictated by equation (6.1)

$$\frac{d}{dt} \left(\frac{1}{2} C V_{dc}^2 \right) = P_t - P_{inv} \quad (6.1)$$

where, P_t is the power extracted from the turbine, P_{inv} is the power at the inverter output terminal and V_{dc} is the dc-link Voltage.

The dynamics of inductor current from Figure 6.1 in abc variables is given by equations (6.2), (6.3) and (6.4):

$$L \frac{di_a}{dt} = -Ri_a + v_{ta} - v_{sa} \quad (6.2)$$

$$L \frac{di_b}{dt} = -Ri_b + v_{tb} - v_{sb} \quad (6.3)$$

$$L \frac{di_c}{dt} = -Ri_c + v_{tc} - v_{sc} \quad (6.4)$$

Consider a balanced sinusoidal three phase function represented by equations,(6.5) (6.6) and (6.7)

$$f_a(t) = f_o \cos(\omega t + \theta_o) \quad (6.5)$$

$$f_b(t) = f_o \cos\left(\omega t + \theta_o - \frac{2\pi}{3}\right) \quad (6.6)$$

$$f_c(t) = f_o \cos\left(\omega t + \theta_o - \frac{4\pi}{3}\right) \quad (6.7)$$

where f_o , θ_o and ω are the amplitude, initial phase angle and the angular frequency of the function respectively. Equivalent space phasor representation of the three phase sinusoidal signal as given by (6.5), (6.6) and (6.7) is given by equation (6.8) :

$$\vec{f}(t) = \frac{2}{3} \left(e^{j0} f_a(t) + e^{j\frac{2\pi}{3}} f_b(t) + e^{j\frac{4\pi}{3}} f_c(t) \right) \quad (6.8)$$

Using the relation $e^{j0} + e^{j\frac{2\pi}{3}} + e^{j\frac{4\pi}{3}} = 0$ and the space phasor representation of 3 phase quantities given by (6.8), equations (6.2), (6.3) and (6.4) can be equivalently represented by the space phasor equation (6.9).

$$L \frac{d\vec{i}}{dt} = -R\vec{i} + \vec{v}_t - \vec{v}_s \quad (6.9)$$

$$\frac{3L}{2} \operatorname{Re} \left\{ \frac{d\vec{i}}{dt} \vec{i}^* \right\} = -\frac{3}{2} R \hat{i}^2 + \operatorname{Re} \left\{ \frac{3}{2} \vec{v}_t \vec{i}^* \right\} - \operatorname{Re} \left\{ \frac{3}{2} \vec{v}_s \vec{i}^* \right\} \quad (6.10)$$

$\operatorname{Re} \left\{ \frac{3}{2} \vec{v}_t \vec{i}^* \right\}$ is nothing but the power at inverter's terminal end (P_{inv}) while

$\operatorname{Re} \left\{ \frac{3}{2} \vec{v}_s \vec{i}^* \right\}$ is the power at PCC (P_s). Substituting these values in the above equation

we get (6.11)

$$\frac{3L}{2} \operatorname{Re} \left\{ \frac{d\vec{i}}{dt} \vec{i}^* \right\} = -\frac{3}{2} R \hat{i}^2 + P_{inv} - P_s \quad (6.11)$$

Equation (6.11) can be further simplified to (6.12)

$$P_{inv} = \frac{3L}{2} \operatorname{Re} \left\{ \frac{d\vec{i}}{dt} \vec{i}^* \right\} + \frac{3}{2} R \hat{i}^2 + P_s \quad (6.12)$$

Also,

$$\frac{3L}{2} \operatorname{Re} \left\{ \frac{d\vec{i}}{dt} \vec{i}^* \right\} = \frac{3L}{4} \frac{d\hat{i}^2}{dt} \quad (6.13)$$

The expression for instantaneous complex power is given as:

$$P_s + jQ_s = \frac{3}{2} \vec{v}_s \vec{i}^* \quad (6.14)$$

Applying complex conjugate operator to (6.14) and multiplying by (6.14) we get (6.15)

$$P_s^2 + Q_s^2 = \frac{9}{4} \hat{v}_s^2 \hat{i}^2 \quad (6.15)$$

Substituting for $\hat{i}^2 = \frac{4}{9\hat{v}_s^2} (P_s^2 + Q_s^2)$ from (6.15) in equation (6.13) we deduce:

$$\frac{3L}{2} \operatorname{Re} \left\{ \frac{d\vec{i}}{dt} \vec{i}^* \right\} = \frac{L}{3\hat{v}_s^2} \frac{dP_s^2}{dt} + \frac{L}{3\hat{v}_s^2} \frac{dQ_s^2}{dt} \quad (6.16)$$

Substituting for $\frac{3L}{2} \text{Re} \left\{ \frac{d\vec{i}}{dt} \vec{i}^* \right\}$ from(6.16) in(6.12) and neglecting the drop $\frac{3}{2} R\hat{i}^2$ as

it is very small in comparison to P_t and P_s we get:

$$P_{inv} = P_s + \left(\frac{2L}{3\hat{v}_s^2} \right) P_s \frac{dP_s}{dt} + \left(\frac{2L}{3\hat{v}_s^2} \right) Q_s \frac{dQ_s}{dt} \quad (6.17)$$

Substituting the value of P_{inv} from (6.17)in (6.1) we deduce:

$$\frac{dV_{dc}^2}{dt} = \frac{2}{C} P_{nur} - \frac{2}{C} \left[P_s + \left(\frac{2LP_s}{3\hat{v}_s^2} \right) \frac{dP_s}{dt} \right] + \frac{2}{C} \left[\left(\frac{2LQ_s}{3\hat{v}_s^2} \right) \frac{dQ_s}{dt} \right] \quad (6.18)$$

Equation (6.18) which dictates the dynamics of dc-link voltage is non-linear. Therefore, in order to design a compensator the plant is linearized about steady-state operating point. The system representing the small signal perturbations about the operating point is given by (6.19)

$$\frac{d\tilde{V}_{dc}^2}{dt} = \frac{2}{C} \tilde{P}_t - \frac{2}{C} \left[\tilde{P}_s + \left(\frac{2LP_{so}}{3\hat{v}_s^2} \right) \frac{d\tilde{P}_s}{dt} \right] + \frac{2}{C} \left[\left(\frac{2LQ_{so}}{3\hat{v}_s^2} \right) \frac{d\tilde{Q}_s}{dt} \right] \quad (6.19)$$

Applying Laplace Transform to(6.19) so as to find the transfer function between \tilde{V}_{dc}^2 and \tilde{P}_s we get equation

$$\frac{\tilde{V}_{dc}^2}{\tilde{P}_s}(s) = - \left(\frac{2}{C} \right) \frac{\tau s + 1}{s} \quad (6.20)$$

where, the time constant τ is given by the following equation:

$$\tau = \frac{2LP_{so}}{3\hat{v}_s^2} = \frac{2LP_{to}}{3\hat{v}_s^2} \quad (6.21)$$

As can be seen from(6.20), that the plant has a zero at $s = \frac{-1}{\tau}$. From (6.21), it is clear that τ is directly proportional to the steady state power flow P_{to} . As far as the system is operating in inverting mode P_{to} is positive and hence τ is positive thereby making the zero to lie in left half of s plane and hence the system exhibits minimum phase characteristics. But if at some point of time P_{to} gets negative and the system starts operating in rectifying mode then τ will attain a negative value which indicates a zero in right half of s plane and therefore the system starts exhibiting non-minimum phase characteristics.

6.1 Conclusion

A Transfer function was derived relating the dc-link voltage and the power delivered to the PCC but it turned out to be non-linear. Hence the system was linearized about a steady state operating point and based on the transfer function which turned out finally relating small signal perturbations of dc-link voltage and the power delivered to PCC it is concluded that the system exhibits inverse response.

Chapter 6

Main Conclusions and Suggestions for further work

Main Conclusions:

The major focus of this thesis has been to evolve control strategies for grid connected as well as standalone WECSs wherein the main control objective was to design a flexible controller which can track limited as well as maximum power from WECS while eliminating the use of battery in grid connected mode and minimizing its usage in autonomous mode in face of climatic change conditions. The analysis and design exercise was carried out in SRRF (dq frame) so that simply with linear PI controllers we can get desired tracking of dc signals which otherwise would have been sinusoidal TV quantities.

A grid-interfaced WECS using Permanent Magnet Synchronous Generator was designed, modelled and simulated. A two-converter power electronic system was used to control the speed of PMSG and to interface it with the grid. Hysteresis current control was used to obtain pulses for the two converters. The outer control loop of the PMSG was a speed control loop. The speed reference for the machine was obtained using a limited power point tracking control algorithm. In order to control the power output from the wind turbine the speed of the generator was controlled. Mathematical model of the wind energy conversion system was developed and the linearized model was used for controller design. In the absence of battery, regulation of dc-link voltage is must for effective operation of grid side converter (inverter). Hence, a PI controller was used to regulate the dc-link voltage and the PWM signals for the switches was produced by hysteresis control scheme. The simulated performance of the system was verified for different operating conditions including Limited Power Point Tracking, Maximum Power Point Tracking and operation under climatic change condition and the results were found to be satisfactory. Results

verified the proper operation of both machine side control as well as grid side control scheme.

A standalone WECS using Permanent Magnet Synchronous Generator was designed, modelled and simulated. A two-converter power electronic system was used to control the PMSG and to interface it with the load. Hysteresis current control was used to obtain pulses for the machine side converter while sinusoidal PWM technique was used to generate pulses for the load side converter. While the machine side control for the standalone system was entirely same as that for grid connected WECS and was dedicated for extracting desired power from the turbine by controlling the speed of PMSG, the load side control is entirely different and follows a much complex control structure as compared to the grid side control. Here also the main objective was to extract desired power from the turbine in face of wind speed variations while minimizing the usage of batteries in the system. The purpose for using battery in the system is just to facilitate transient stability and ensure system reliability which are some of the major requirements in standalone WECSs. Unlike the grid-connected mode, wherein most of the system level dynamics were governed by the grid due to relatively small size of micro source, in standalone mode the system dynamics are dictated by micro source themselves, their power regulation control and, to an unusual degree, by the network itself. Therefore, the control of load voltage magnitude and frequency which were one of the most important control requirements were addressed properly by using proper feed forward and decoupling control techniques. The simulated performance of the system was verified for different operating conditions including Limited Power Point Tracking, Maximum Power Point Tracking and operation under climatic change condition and the results were found to be satisfactory. Results verified the proper operation of both machine side control as well as the load side control scheme.

Future Work:

- Putting WECS with other DG units like Solar Photovoltaic Energy Conversion System, fuel cells, diesel generators, etc in a microgrid framework and implementing MPC as a master controller which will supervise the power commands to each system based on optimality

considerations while respecting various constraints which are to be met during the operation.

- Stability analysis for the entire WECS for grid connected as well as islanded mode.
- Switching the system from grid-connected to islanded mode at run time.
- Implementing the proposed control strategy for multi wind farms and evolving various possible scenarios.

References

- [1] Shubham Khandelwal, Nikhil Bhugra, Ketan P Detroja, Controlled Power Point Tracking for Power Balancing in PMSG based Wind Energy Conversion System, presented at Advanced Control of Industrial Process (ADCONIP 2014), Hiroshima, Japan
- [2] E. Ela, V. Gevorgian, P.Fleming, Y.C. Zhang, M. Singh, E. Muljadi, A. Scholbrook, J. Aho, A. Buckspan, L. Pao, V. Singhvi, A. Tuohy, P. Pourbeik, D. Brooks and N. Bhatt. Active Power Controls from Wind Power: Bridging the gaps. Technical report from National Renewable Energy Laboratory, Jan 2014.
- [3]Thongman Jogendra Singh and Ouhrouche Mohand. MPPT Control Methods in wind energy conversion systems. Fundamental and Advanced topics in wind power.B.Kirby,(2003). Spinning Reserve for Responsive Loads, ORNL/TM-2003/19, Oak Ridge Nat. Lab., Oak Ridge, T.N, Tech Rep.
- [4] Orlando N.A., Liserre M., Aquila A.Dell'. "Management of power excess in wind turbine system". European Conference on Power Electronics Applications (EPE-2009), Barcelona.
- [5] E. Ela, V. Gevorgian, P.Fleming, Y.C. Zhang, M. Singh, E. Muljadi, A. Scholbrook, J. Aho, A. Buckspan, L. Pao, V. Singhvi, A. Tuohy, P. Pourbeik, D. Brooks and N. Bhatt. Active Power Controls from Wind Power: Bridging the gaps. Technical report from National Renewable Energy Laboratory, Jan 2014.
- [6] Nikhil Bhugra, Model Predictive Control Based Wind-Solar Hybrid Energy Conversion System, A dissertation submitted to Indian Institue of Technology Hyderabad, June 2013.

- [7] [Online] MIT Technology Review. GE grabs Gearless Wind Turbines. Available at: <http://www.technologyreview.com/news/415425/ge-grabs-gearless-wind-turbines/>.
- [8] Omid Alizadeh, Amirnaser Yazdani. (2013) A Strategy for Real Power Control in a Direct-Drive PMSG-based Wind Energy Conversion System, IEEE Transactions on Power Delivery, 28 (3), 1297 – 1305.
- [9] Libo W., Zhengming Z., and Jianzheng L., "A single-stage three-phase grid-connected photovoltaic system with modified MPPT method and reactive power compensation," IEEE Transactions on Energy Conversion, vol. 22, pp. 881-886, 2007.
- [10] Qi Wei, Litu Jingfong, and Christofides Panagiotis D., "Distributed supervisory predictive control of distributed wind and solar energy systems," IEEE Transactions on Control Systems Technology, 21(2), 504-512.
- [11] Qung Huyuh, Fredric Nollet, Najib Essounboulli, Abdelaziz Hamzaoui, "Control of permanent magnet synchronous generator wind turbine for stand-alone system using fuzzy logic". EUSFLAT-LFA July 2011.
- [12] Nikhil Bhugra and Ketan P Detroja, Sliding Mode Control based Power Balancing for Grid Connected PV System, presented at IEEE Multi Conference on Systems and Control (IEEE MSC 2013), Hyderabad, India.
- [13] Wei Qi, Jifeng Liu, Xianzhong Chen, and Panagiotis D. Christofides. Supervisory predictive control of standalone wind/solar energy generation systems. IEEE transaction on control system technology, Vol. 19, No. 1, 2011
- [14] [Online]. Wind Turbine Control Methods, 2008. Available@www.ni.com.

- [15] L.Umanand. CEDT, Indian Institute of Science, Bangalore, 2007.
- [16][Online].Available@:<http://www.science.howstuffworks.com/environmental/green-science/wind-power2.htm>
- [17][Online].Available@http://www.crosswindpower.com/index.php?option=com_content&view=article&id=19&Itemid=13.
- [18] Mohit Singh and Surya Santoso. National Renewable Energy Laboratory (NREL October 2011)
- [19] Martin O.L.Hansen. Aerodynamics of Wind Turbines. Second Edition, Eartscan, 2008.
- [20] Representing Wind Turbine Electrical Generating Systems in Fundamental Frequency Simulations. IEEE Transactions on Energy Conversion, 18(4), 2003.
- [21] Amirnaser Yazdani and Reza Iravani. Voltage-Sourced Converters in Power Systems, Modelling Control and Applications. IEEE Press, 2010.
- [22] Savita Nema, R.K NemaMatlab/Simulink based study of photovoltaic cells/modules array and their experimental verification. International Journal of Energy and Environment. Volume 1, Issue 3, 2010
- [23] Paul C. Krause, Oleg Wasynczuk, Scott D. Sudhoff. Analysis of Electric Machinery and Drive Systems. Wiley Publications.
- [24] Frede Blaabjerg, Remus Teodorescu, Marco Liserre and Adrian V.Timbus. Overview of Control and Grid Synchronization for Distributed Power Generation Systems. IEEE Transactions on Industrial Electronics 53(5), 2006.

- [25] Donald R. Coughanowr. Process System Analysis and Control. Mc Graw Hill Publications.
- [26] M.Gopal. Control System Principles and Design. Mc Graw Hill Publications.
- [27] Prashant Patel, Modeling, Stability Analysis and Control of Renewable Driven Islanded and Grid Connected Microgrids. A dissertation submitted to Indian Institute of Technology Hyderabad, June 2013.
- [28] M. Gopal . Modern Control System Theory. New Age International Publishers.
- [29] Salvador Alepuz, Sergio busquets-Monge. Control Strategies based on symmetrical components for Grid-connected converters under voltage dips. IEEE transactions on Industrial electronics, Vol. 56, No. 6, June 2009
- [30] Sachin C. Patwardhan. Linear Quadratic Optimal Control and MPC. Class Notes.
- [31] G.E. Garcia, D.M. Prett and M.Morrari, "Model Predictive Control: Theory and Practice- A Survey", Automatica, vol 25, pp.335-348, 1989
- [32] Camacho and Bordons. Model Predictive Control. Springer
- [33] Robert Lasseter, Abbas Akhil, Chris Marnay, John Stephens, Jeff Dagle, Ross Guttromson, A. Sakis Meliopoulos, Robert Yinger and Joe Eto. White Paper on Integration of DERs ,April 2002.
- [34] Farid Katiraei, Reza Iravani, Nikos Hatziargyriou, and Aris Dimeas, Controls and Operation Aspects of Microgrid. IEEE power and energy magazine 2008.
- [35] Nikos Hatziargyriou, Hiroshi Asano, Reza Iravani, Chris Marnay. An Overview of ongoing Research, Development and Demonstration Projects. IEEE power and energy magazine 2008.

[36] Robert H. Lasseter, Paolo Piagi. Microgrid: A Conceptual Solution. PESC' 04 Aachen, Germany 20-25 June 2004.

[37] A.B. Raju, B.G. Fernandes, K. Chatterjee. A UPF Power Conditioner with Maximum Power Point Tracker for Grid Connected Variable Speed Wind Energy Conversion System. Proceedings of 1st International Conference on Power Electronics Systems and Applications (PESA 2004), Bombay, India.

[38] Jogendra Singh Thongman and Mohand Ouhrouche. MPPT Control Methods in wind energy conversion systems, Fundamental and Advanced topics in wind power, Dr. Rupp Carriveau (Ed.), ISBN:978-953-307-508—2, In Tech available from <http://www.intechopen.com/books/fundamental-and-advanced-topics-in-wind-power/mppt-control-methods-in-wind-energy-conversion-systems>.

[39] Ying Zhu, Ming Cheng, Wei Hua and Wei Wang. A Novel Maximum Power Point Tracking Control for Permanent Magnet Direct Drive Wind Energy Conversion Systems. *Energies* 2012, 5, 1398-1412.

[40] C.N. Bhende. S. Mishra and Siva Ganesh Malla. Permanent Magnet Synchronous Generator-Based Standalone Wind Energy Supply System. *IEEE Transaction on Sustainable Energy*, VOL. 2, NO.4, October 2011.

[41] J.S. Thongam, R.Beguenane, A.F.Okou, M.Tarbouchi, A.Merabet and Pierre Bouchard. A Method of Tracking Maximum Power Points in Variable Speed Wind Energy Conversion Systems. *International Symposium on Power Electronics, Electric Drives, Automation and Motion* 2012.

[42] Yun-Su Kim, Il-Yop Chung and Seung-Il Moon. An Analysis of Variable Speed Wind Turbine Power-Control Methods with Fluctuating Wind Speed. *Energies* 2013.

[43] M. Matsui, D. Xu, L. Kang and Z. Yang. Limit Cycle Based Simple MPPT Control Scheme for a Small Sized Wind Turbine Generator System. *Proc. Of 4th International Power Electronics and Motion Control Conference*, Xian 2004.

- [44] M.G.Molina and P.E.Mircado. A New Control Strategy of Variable Speed Wind Turbine Generator for Three-Phase Grid Connected Applications. Proc. of IEEE/PES Transmission and Distribution Conference and Exposition: Latin America 2008, Bogota, pp 1-8.
- [45] A.Mesemanolis, C.Mademlis and I.Kioskeridis. A Fuzzy Logic Based Control Strategy for Maximum Efficiency of a Wind Energy Conversion System. International Symposium on Power Electronics, Electric Drives, Automation and Motion 2012.
- [46] J.Yaoqin, Y.Zhongqing and C.Binggagng. A new maximum power point tracking scheme for wind generation. Proc. of International Conference on Power System Technology 2002 (Powercon 2002), pp 144-148.
- [47] F.D.Kanellos and N.D.Hatziargyriou. Control of Variable Speed Wind Turbines equipped with synchronous or doubly fed induction generators supplying islanded power systems. Renewable Power Generation IET 3(1), 2009, pp 96-108.
- [48] Carlos J. Ramos, Antonio P. Martins, Armando S. Araujo, Adriano S. Carvalho. Current Control in the Grid Connection of the Double-Output Induction Generator Linked to a Variable Speed Wind Turbine. IECON 02 [Industrial Electronics Society, IEEE 2002 28th annual Conference of the].
- [49] Denis Candusso, Lanko Valero, Aurelin Walter, Seddik Bacha, Elisabeth Rulliere, Bertrand Raison. Modelling, Control and Simulation of a Fuel Cell based Power Supply System with Energy Management. IECON 02 [Industrial Electronics Society, IEEE 2002 28th annual Conference of the].

- [50] Nikos Hatziargyriou, Hiroshi Asano, Reza Iravani, Chris Marnay. An Overview of ongoing Research, Development and Demonstration Projects. IEEE power and energy magazine 2008.
- [51] Erika Twining and Donald Grahame Holmes. Grid Current Regulation of Three Phase Voltage Source Inverter With an LCL Input Filter. IEEE Transaction on Power Electronics 18(3) 2003.
- [52] D.N. Zmood, D.G. Holmes and G. Bode. Frequency Domain Analysis of Three Phase Linear Current Regulators. Industry Applications Conference, 1999. Thirty Fourth IAS annual meeting.
- [53] R. Teodorescu, F. Blaabjerg, M. Liserre and P.C. Loh. Proportional-resonant controllers and filters for grid-connected voltage-source converters. Electric Power Applications. IEE Proceedings 153(5) 2006.
- [54] Shoji Fukuda and Takehito Yoda. A novel Current-Tracking Method for Active Filters Based on a Sinusoidal Internal Model. IEEE Transactions on Industry Applications 37(3) May/June 2001.
- [55] R. Krishnan. Electric Motor Drives Modelling, Analysis and Control. Pearson Education.
- [56] K.H. Ang, G. Chong, and Y. Li. PID control system analysis, design and technology. IEEE Trans. Control Syst. Technol., vol 13, no.4, pp.559-576, Jul. 2005.
- [57] R. Ortega and R. Kelly. PID self tuners: Some theoretical and practical aspects. IEEE Trans. Ind. Electron., volIE31, no.4 ,pp 332-338, Nov 1984
- [58] Mahesh K. Mishra and K. Karthikeyan. A Fast-Acting DC-Link Voltage Controller for Three-Phase DSTATCOM to Compensate AC and DC Loads. IEEE Transactions on Power Delivery, VOL. 24, NO. 4, October 2009.
- [59] Nagaraju Pokagu, Student member IEEE, Milan Prodanovic, Member IEEE and Timothy C. Green, Senior member IEEE, Modelling, Anaysis and Testing of

Autonomous Operation of an Inverter-based Microgrid. IEEE Transactions on Power Electronics, 22(2), 2007.

[60] Jong Yul Kim, Jin-Hong Jeon, Seul-Ki Kim, Changhee Cho, June Ho Park, Hak-Man Kim and Kee- Young Nam Coperative Control Strategy of Energy Storage Systems and Microsources for Stabilizing the Microgrid during Islanded Operation. IEEE Transaction on Power Electronics 25(12), 2012.

[61] Mohammad B.Delghavi and Amirnaser Yazdani. A Control Strategy for Islanded Operation of a Distributed Resource (DR) Unit. Proc. IEEE Power Energy Soc. Gen. Meeting , Jul. 2009, pp. 1–8.

[62] Mohammad B.Delghavi and Amirnaser Yazdani. An Adaptive Feedforward Compensation for Stability Enhancement in Droop-Controlled Inverter-Based Microgrids. IEEE Transactions on Power Delivery 26(3), 2011.

[63] Mohammad B.Delghavi and Amirnaser Yazdani. A Unified Control Strategy for Electronically Interfaced Distributed Energy Resources. IEEE Transactions on Power Delivery 27(2), 2012.

[64] Mohammad B.Delghavi. Advanced Islanded Mode Control of Microgrids. Thesis submitted at University of Western Ontario, Canada, 2011.

[65] Behrooz Bahrani, Stephan Kenzelmann and Alfred Rufer. Multivariable-PI Based dq Current Control of Voltage Source Converters With Superior Axis Decoupling Capability. IEEE Transaction on Industrial Electronics, 58(7), 2011.

[66] Ludbrook, Allan. Power Engineering Society Summer Meeting, 2001. Vol.2, pp 797-800, 2001

[67] Shahil Shah. Design and Implementation of Parallel Operation of inverters with Instantaneous Current Sharing Scheme using Multiloop Control Strategy on FPGA Platform. Indian Institute of Technology Kanpur July 2008.

- [68] K.H. Ahmed, S.J. Finney and B.W. Williams. Passive Filter Design for Three-Phase Interfacing in Distributed Generation. *Compatibility in Power Electronics (CPE)* 2007.
- [69] Robert E. Wilson, Peter B.S.Lissaman and Stel N. Walker. National Renewable Energy Laboratory, 1976.
- [70] Shuhui Li, Timothy A.Haskew and Ling Xu. Conventional and novel control designs for direct driven PMSG wind turbines. *Electric Power System Research* 80(2010) 328-338.
- [71] Ali H.Kasem Alaboudy, Ahmed A.Daoud, Sobhy S.Desouky and Ahmed A.Salem. Converter controls and flicker study of PMSG-based grid connected wind turbines. *Ain Shams Engineering Journal* (2013)4, 75-91.
- [72] Optimal Power Control Model of Direct Driven PMSG. *SciVerse ScienceDirect, Energy Procedia* 12(2011) 844-848
- [73] Cristian Busca, Ana-Irina Stan, Tiberiu Stanciu and Daniel Ioan Stroe. Control of Permanent Magnet Synchronous Generator for Large Wind Turbines. *IEEE International Symposium on Industrial Electronics (ISIE)* 2010.
- [74] Chunxue Wen, Guojie Lu, Peng Wang, Zhengxi Li, Xiongwei Liu and Zaiming Fan. Vector Control Strategy for small-scale grid-connected PMSG wind turbine converter. *2nd IEEE PES International Conference and Exhibition on Innovative Smart Grid Technologies (ISGT Europe)* 2011
- [75] Y.Errami, M.Maaroufi, M.Ouassaid. Modelling and Control strategy of PMSG based variable speed wind energy conversion system. *International Conference on Multimedia Computing and Systems (ICMCS – 2011)*, Ouarzazate, Morocco.

